國立臺灣大學生命科學院植物科學研究所

博士論文

Institute of Plant Biology
College of Life Science
National Taiwan University

Doctoral Dissertation

*Ib*Pep1 激活 *Ib*LRR-RK1 所調控之甘藷防禦反應

*Ib*Pep1-mediated Activation of *Ib*LRR-RK1 Receptor Regulates Defense Responses in Sweet Potato

呂學翰

Hsueh-Han Lu

指導教授: 葉開溫 博士

Advisor: Dr. Kai-Wun Yeh

共同指導教授: Axel Mithöfer 博士

Co-Advisor: Dr. Axel Mithöfer

共同指導教授: 鄭秋萍 博士

Co-Advisor: Dr. Chiu-Ping Cheng

中華民國 112 年 7 月

July 2023

doi:10.6342/NTU202302113

國立臺灣大學博士學位論文

口試委員會審定書

DOCTORAL THESIS ACCEPTANCE CERTIFICATE

NATIONAL TAIWAN UNIVERSITY

*Ib*Pep1 激活 *Ib*LRR-RK1 所調控之甘藷防禦反應
*Ib*Pep1-mediated Activation of *Ib*LRR-RK1 Receptor Regulates Defense Responses in Sweet Potato

本論文係呂學翰君（學號 D05B42003）在國立臺灣大學植物科學研究所完成之博士學位論文，於 2023 年 7 月 7 日承下列考試委員審查通過及口試及格，特此證明

The undersigned, appointed by the Institute of Plant Biology on September 7, 2023, have examined a Doctoral thesis entitled above presented by Hsueh-Han Lu (D05B42003) candidate and hereby certify that it is worthy of acceptance.

口試委員 Oral examination committee：

臺灣大學植物科學研究所
鄭秋萍 教授 (指導教授 Advisor)

Max Planck Institute for Chemical Ecology
Axel Mithöfer Professor (共同指導教授 Co-Advisor)

臺灣大學植物科學研究所
謝旭亮 教授

臺灣大學生命科學系/植物科學研究所
鄭貽生 教授

中研院農業生物科技研究中心
葉國楨 研究員

臺灣大學植物科學研究所
陳賢明 助理教授

成功大學生物科技與產業科學系
陳盈嵐 助理教授

中國文化大學園藝暨生物技術學系
陳仕朋 助理教授

謝辭

在我的博士生的旅程，以及本論文之完成，首要感謝我的指導教授葉開溫老師，從大學、碩士、一路走到博士，是葉開溫老師帶領我進入植物科學的學術領域，培養了我的研究能力，從背後不斷支持與督促著我的前進，提供良好的實驗環境讓我能專心在學術研究不用擔心後勤支援，並且對於我個人和專業發展上提供了相當寶貴的指導和支持，我心存無限感激和敬佩。相當遺憾在我博士生的學術旅程完成之前，葉開溫老師不幸辭世，但他對專業知識的熱情、對卓越的不懈追求、對學術的嚴謹態度將永遠被我銘記，並成為我持續進取的動力。感謝您選擇了我成為您的關門弟子，葉開溫老師。

相當感謝我的共同指導教授鄭秋萍導師、以及 Axel Mithöfer 教授。在我的博士班生涯中無論在學術或是為人處事上，兩位老師不吝於提供專業的見解與指導，讓我能成為更好的學者與更好的人。並在葉老師辭世後，協助我走完期刊的發表以及博士論文的完成與修訂，讓我能順利的通過博士口試並走向下一段旅程。同時也感謝謝旭亮、葉國楨、鄭貽生、陳賢明、陳盈嵐、陳仕朋老師們撥冗擔任口試委員，並提供寶貴的建議及對論文的審閱與修正，幫助我完善了論文。

再來感謝實驗室的夥伴們，感謝仕朋學長對於實驗的建議以及對我學術研究上的幫助，耀中學長安心的後勤支援，朝瑋學長一起努力畢業，又云的陪伴，以及其他 R920 的夥伴，是你們讓我在求學旅途的記憶中充滿歡笑。

最後要感謝家人給予無限的支持，無論是經濟上還是心理上都讓我能夠毫無顧忌地往前進，因為你們的支持才有現在的我，僅以本論文獻給最愛的你們。

呂學翰 2023/7/19

doi:10.6342/NTU202302113

摘要

甘藷（*Ipomoea batatas*）是重要的塊根作物，卻時常受到各種蟲害的威脅，而甘藷塊根富含高量具有胰蛋白酶抑制活性之儲藏蛋白 SPORAMIN，為其重要抗蟲機制之一，且在甘藷葉片中 *SPORAMIN* 基因表現會被機械性損傷、昆蟲取食或防禦相關揮發物誘導而快速表現，進而藉由抑制昆蟲腸道之消化力以增強植物對昆蟲之抵抗能力。不過，儘管目前對於受傷誘導 *SPORAMIN* 表現的信號傳導途徑已有一些了解，但關於其受體如何辨識逆境訊號卻仍無相關報導。本研究發現一個在甘藷葉中能被受傷/蟲咬誘導而表現之受體激酶 *Ib*LRR-RK1 (leucine-rich repeat receptor kinase1)，此受體蛋白質富含亮胺酸重複（leucine-rich repeat），親源分析顯示其屬於相近於番茄 *Sl*PEPR1 以及阿拉伯芥 *At*PEPR1/2 之 peptide-elicitor receptors (PEPRs) 受體蛋白質家族。功能性研究發現激活此 *Ib*LRR-RK1 受體能誘導許多典型的植物受傷天然免疫 (Damage-Associated Molecular Pattern (DAMP)-triggered immunity，簡稱 DTI) 反應，包括: 過氧化物大量累積以及植物賀爾蒙乙烯之生合成。此外，本研究進一步發現能激活 *Ib*LRR-RK1 之胜肽配體 *Ib*Pep1 與其前體蛋白 *Ib*PROPEP1；利用人工合成的 *Ib*Pep1 與其衍伸胜肽進行試驗證實甘藷 *Ib*Pep1/*Ib*LRR-RK1 為新的配體/受體系統並近似於其他植物典型的 Pep/PEPRs 系統。更重要的是，*Ib*Pep1 可能與另一參與 DTI 之胜肽 *Ib*HypSys 協力或並行地傳遞訊號，以調控並增強甘藷抵抗昆蟲的能力。此外本研究也發現 *Ib*LRR-RK1 與 *Sl*PEPR1 能交叉識別其各自之配體 *Ib*Pep1 與 *Sl*Pep6，第一次揭示了旋花科與茄科 Pep/PEPR 系統之間的家族相容性。綜上所述，本研究以分子生物的方式更深入的揭示了甘藷在面對傷害和食草動物攻擊時的綜合防禦機制。

關鍵字：損傷相關分子模式、甘藷、植物防禦、蟲害、胜肽配體、植物受體

doi:10.6342/NTU202302113

Abstract

Sweet potato (*Ipomoea batatas*) is an important crop with tuberous roots that is vulnerable to various insect pests. To defense off herbivores, the tuberous roots of sweet potato contain a storage protein called sporamin, which exhibits inherent trypsin inhibitory activity. Transcription of *SPORAMIN* in sweet potato leaves can be rapidly induced by herbivore attack, wounding, or defense-related volatiles, leading to enhanced resistance against insects by suppressing their digestion. The signaling transduction network regulating *SPORAMIN* expression in wounding response to stress has been partially elucidated; however, the perception of stress-related signals by receptors in sweet potato remains unknown. In this study, a wound/herbivory-inducible pattern recognition receptor (PRR), namely *Ib*LRR-RK1 (leucine-rich repeat receptor kinase1), was identified. Phylogenetic analysis revealed that *Ib*LRR-RK1 belongs to the peptide-elicitor receptors (PEPRs), and is related to the receptors *At*PEPR1/2 in Arabidopsis and *Sl*PEPR1 in tomato. Functional assays demonstrated the activation of *Ib*LRR-RK1 triggered typical Damage-Associated Molecular Pattern (DAMP)-triggered immunity (DTI) defense responses such as the oxidative burst or the synthesis of the phytohormone ethylene. Furthermore, a precursor protein, namely *Ib*PROPEP1, was discovered, and this protein contains a peptide ligand named *Ib*Pep1 that can activate *Ib*LRR-RK1. Experiments utilizing synthetic *Ib*Pep1 and its derivatives provided evidence for a novel ligand/receptor pair in sweet potato that is related to canonical Pep/PEPRs in other plant species. *Ib*Pep1 serves as a distinct signaling peptide in sweet potato and may function in conjunction with, or in parallel to, the previously identified HypSys peptides to enhance resistance against insects. Interestingly, *Ib*LRR-RK1 and *Sl*PEPR1 exhibit cross-recognition of their respective ligands, *Ib*Pep1 and *Sl*Pep6, revealing inter-family compatibility of the Pep/PEPR systems within the Convolvulaceae and Solanaceae families for the first time. In summary, this research provides insights into the

doi:10.6342/NTU202302113

comprehensive defense mechanisms of sweet potato in the face of injury and herbivore attack, shedding light on the molecular processes involved in these responses.

Keywords: DAMP, sweet potato, plant DTI, herbivore, peptide ligand, plant receptor

doi:10.6342/NTU202302113

Index

doi:10.6342/NTU202302113

doi:10.6342/NTU202302113

Index of tables

Index of figures

doi:10.6342/NTU202302113

doi:10.6342/NTU202302113

Index of supplementary figures

doi:10.6342/NTU202302113

Introduction

Pattern recognition receptors (PRRs) in plants

Throughout the course of evolution, plants have developed various mechanisms to perceive and respond to diverse biotic and abiotic stresses. In response to stressors such as insect herbivory, pathogen infection, and mechanical damage, receptor-like proteins (RLPs) or receptor kinases (RKs) located at the cell membrane to detect specific stress-related patterns. These patterns can arise from various sources, including herbivore-associated molecular patterns (HAMPs) and microbe-associated molecular patterns (MAMPs), which are derived from invaders, or from disruptions in cellular integrity known as damage- or danger-associated molecular patterns (DAMPs). After recognizing the specific patterns, pattern recognition receptors (PRRs) in plants initiate signal transduction pathways that trigger appropriate immune responses, leading to the activation of pattern-triggered immunity (PTI) (Boller and Felix, 2009). PTI serves as an effective defense mechanism, enhancing plant resistance and minimizing the detrimental effects caused by various insects and pathogens (Boehm et al., 2014).

Pattern recognition receptors are commonly characterized by their structural composition, which normally composed of extracellular domain, transmembrane domain, and intracellular domain. The classification of PRRs is primarily based on the distinctive features of their extracellular domains. As an example, a distinct subgroup of PRRs

doi:10.6342/NTU202302113

known as leucine-rich repeat receptor kinases (LRR-RKs) have garnered significant attention. LRR-RKs exhibit a characteristic structural arrangement, comprising an extracellular leucine-rich repeat domain, a transmembrane domain that spans the cellular membrane once, and an intracellular protein kinase domain. LRR-RKs and LRR-RLPs (leucine-rich repeat receptor like proteins) serve as vital sensors for proteinaceous immunogenic ligands. These ligands encompass a range of molecules, including small proteins and peptides (Boehm et al., 2014). For instance, the EFR receptor recognizes a conserved N-terminal fragment found in bacterial elongation factor Tu (Zipfel et al., 2006). The *Sl*Eix1 and *Sl*Eix2 receptors have been identified to bind to trichoderma cell wall-derived xylanase (Ron and Avni, 2004). Furthermore, specific receptors like FLS2 have the ability to detect a conserved 22-amino acid epitope called flg22, which is present in bacterial flagellins (Chinchilla et al., 2006).

In addition to PRRs receptors with LRR extracellular structures, there are also many reports on other subgroups of PRRs with other extracellular structures, such as those with Lysine-motif domain (LysM domain). These receptor proteins can be further divided into LysM-RKs and LysM-RPs based on whether they have kinase activity or not. This type of receptor has been reported to bind to carbohydrate ligands containing acetylglucosamine (GlcNAc), such as bacterial peptidoglycan (PGN), nodulation factors (NF), and fungal chitin, and induce plant symbiosis or immune responses, such as

doi:10.6342/NTU202302113

*At*CERK1 in Arabidopsis thaliana (Iizasa et al., 2010), *Os*CERK1 and *Os*CEBiP in rice (Shimizu et al., 2010). In addition, lectin-type PRRs (Lectin-RK) have been reported to bind extracellular ATP or bacterial lipopolysaccharide (LPS) (Choi et al., 2014), while PRRs with extracellular structures containing epidermal growth factor (EGF)-like domains (EGF-RK) have been reported to recognize derivatives of plant cell walls such as oligogalacturonides (Brutus et al., 2010).

The production and function of plant endogenous peptide ligands

Peptides, usually defined as proteins consisting of 2-100 amino acids. Endogenous peptides in plants play important roles in various physiological functions. Numerous peptides have been reported to participate in regulating plant development and growth. These peptides assist in the regulation of seed germination, root growth, lateral root development, flower and seed formation, and fruit development. Well-studied peptides involved in these functions include RAPID ALKALINIZATION FACTORS (RALFs), INFLORESCENCE DEFICIENT IN ABSCISSION (IDA), CLAVATA3 (CLV3)/EMBRYO SURROUNDING REGION-related (CLE) family, and EMBRYO SURROUNDING FACTORS (ESFs), among others (Costa et al., 2014; Grienenberger et al., 2015; Murphy et al., 2014; Yamaguchi et al., 2016). Endogenous peptides in plants have also been shown to participate in various stress responses. Regarding abiotic stress,

doi:10.6342/NTU202302113

peptides such as *At*Pep3, RAPID ALKALINIZATION FACTORS (RALFs), and CAP-Derived peptide 1 (CAPE1) assist plants in salt tolerance and growth under salinity stress (Chien et al., 2015; Kim et al., 2021; Zhao et al., 2018). Peptides including Phytosulfokines (PSK), INFLORESCENCE DEFICIENT IN ABSCISSION (IDA), CLAVATA3 (CLV3)/EMBRYO SURROUNDING REGION-related (CLE) help plants combat water deficiency/drought stress (Patharkar and Walker, 2016; Takahashi et al., 2018; Xie et al., 2022). CLE45 aids Arabidopsis in maintaining proper seed production under heat stress (Xie et al., 2022). Peptides such as RGFs, CLEs, and CEPs have been identified to regulate nutrient acquisition and growth responses under nutrient deficiency stress (Cederholm and Benfey, 2015; Ma et al., 2020; Tabata et al., 2014). In terms of biotic stress, certain plant-derived defensins such as *Vr*D1 (defensin from *Vigna radiate*), *Na*D1 (defensin from *Nicotiana alata*), and *Alf*AFP (antifungal protein from alfalfa) can disrupt cell membrane integrity, leading to cell lysis, or induce the production of reactive oxygen species and program cell death (PCD) in pathogens. These peptides directly combat pathogenic microorganisms by exerting their properties (Sher Khan et al., 2019). Many other peptides utilize pattern recognition receptors localized on the plasma membrane of plant cells to initiate plant defense responses. This aspect will be further discussed in detail in subsequent sections.

Peptides derived from nonfunctional precursor proteins such as antimicrobial peptides

doi:10.6342/NTU202302113

(AMPs) and secreted small signaling peptides have mainly been reported. Many of these nonfunctional precursor proteins contain a N-terminal signal sequence (NSS), which leads the precursor to the secretory pathway through endoplasmic reticulum (ER). Subsequently, the precursor protein undergoes enzymatic cleavage or modification, resulting in the removal of NSS and generation of mature peptides (Chen et al., 2020; Tavormina et al., 2015). In addition to the peptides derived from nonfunctional precursors, there are reports reveal the existence of peptides derived from functional proteins but with distinct activities from their precursors such as tomato CAPE1, peptide derived from C-terminal of PR-1b, and INCEPTIN, fragments of ATP synthase (Chen et al., 2014; Schmelz et al., 2006). Furthermore, recent researches indicate the existence of peptides which are not derived from precursor proteins. The sources of these peptides are quite diverse, such as (1) peptides translated from 5' leader region of mRNA, (2) in transcripts encoding short open reading frames (sORFs) (less than 100 amino acids), and (3) in transcripts of pri-microRNAs (miRNAs) (Tavormina et al., 2015). These examples highlight the diversity of plant endogenous peptide sources, suggesting that there may be many more functional endogenous peptides that have yet to be discovered.

Plant endogenous peptide ligands involved in defense responses

Peptide ligands are crucial in regulating signal transduction pathways involved in

doi:10.6342/NTU202302113

wound defense responses and insect resistance (Bartels and Boller, 2015; Huffaker, 2015). A set of eight plant elicitor peptides (*At*Pep1-*At*Pep8) are involved in defense responses triggered by damage in *Arabidopsis thaliana*, which occurs upon recognition by a pair of LRR-RKs, known as the *At*PEPR1 and *At*PEPR2 (Krol et al., 2010; Yamaguchi et al., 2010). These *At*Peps are derived from the carboxyl terminus of their precursor proteins *At*PROPEPs (Bartels et al., 2013; Huffaker et al., 2006), although the specific mechanism of peptide cleavage remains largely unknown. However, recent studies have described a METACASPASE4 (MC4)-dependent maturation of *At*Pep1. Upon damage, high levels of cytoplasmic [Ca^{2+}] bind to MC4, which then cleaves *At*PROPEP1 and releases active *At*Pep1 (Chen et al., 2020; Hander et al., 2019). Upon herbivore attack, Arabidopsis plants activate the expression of the receptor genes *AtPEPR1/2* and ligand precursor genes *AtPROPEP2/3*. This induction plays a crucial role in plant defense, as demonstrated by reduced resistance to *Spodoptera littoralis* larvae in *pepr1 pepr2* double mutant Arabidopsis (Huffaker, 2015; Klauser et al., 2015; Ross et al., 2014). In *Zea mays*, the presence of insect oral secretions and herbivore-associated molecular patterns (HAMPs) can induce the expression of the precursor protein of an ortholog of *At*Pep called *Zm*Pep3. Upon the application of *Zm*Pep3, the plant exhibits various defense responses. This includes activation of transcripts indirectly involved in defense against herbivores, the synthesis and accumulation of phytohormones, and the release of volatile organic

doi:10.6342/NTU202302113

compounds (VOCs) associated with insect herbivory. Additionally, *Zm*Pep3 stimulates the accumulation of proteinase inhibitors, which contribute to the resistance against lepidopteran insects in *Zea mays* (Huffaker et al., 2013).

Systemin, the first identified peptide with signaling capacities in plants, has been shown to be induced by injury and cause defense responses against insects in *Solanum lycopersicum* (tomato) (Orozcocardenas et al., 1993; Pearce et al., 1991). The endogenous systemin peptide ligand consists of 18 amino acids and is generated through the phytaspase-dependent cleavage of a precursor protein at two specific aspartate residues (Beloshistov et al., 2018). The application of systemin stimulates the activation of phospholipase A2, resulting in the liberation of jasmonic acid precursors from the cell membrane and the induction of proteinase inhibitors. Subsequently, the jasmonic acid signaling pathways activate defense genes associated with insect resistance, thereby enhancing the plant's ability to withstand herbivory (Pearce et al., 1991). The LRR-RK receptor *Sl*SYR1 can recognize systemin and serves as a mediator for this process, although it is not necessary for wound responses in tomato (Wang et al., 2018).

Hydroxyproline-rich systemins (HypSys) are endogenous peptide ligands with systemin-like properties that are present in Solanaceae plants. The HypSys precursor protein, preproHypSys, contains a conserved hydroxyproline-rich sequence and an N-terminal secretion sequence, distinguishing it from systemin and Peps precursor proteins.

doi:10.6342/NTU202302113

Resembling to systemin, HypSys is capable of triggering the production of jasmonates and the activation of defense gene expression, such as immune gene defensin1 in petunia (Pearce et al., 2007; Pearce, 2011). The accumulation of tomato *Sl*HypSys I, II, and III precursor proteins take place within the cell wall matrix of phloem parenchyma cells in response to signaling such as methyl jasmonate, wounding, and systemin (Narvaez-Vasquez et al., 2005). Likewise, upon injury, the expression of the precursor gene *Ib*preproHypSys is elevated in sweet potato. When *Ib*HypSys is applied to sweet potato, it triggers the activation of downstream insect-resistance genes, including *IPOMOELIN* and *SPORAMIN*, and promotes the biosynthesis of lignin to augment insect repellence (Chen et al., 2008; Li et al., 2016). However, the precise mechanisms through which HypSys interacts with receptors and orchestrates defense responses in plants are still largely unexplored.

Insect resistance of sweet potato

Sweet potato (*Ipomoea batatas*) is a globally significant food crop that ranks fifth in terms of production and possesses substantial nutritional and economic value. Notably, certain sweet potato cultivars exhibit enhanced resistance to insect pests compared to others. One such cultivar is Tainong 57, which is widely cultivated in Taiwan and displays strong insect resistance. This cultivar serves as an excellent model crop for investigating

doi:10.6342/NTU202302113

the underlying mechanisms involved in insect resistance. The insect-resistant genes, *IPOMOELIN and SPORAMIN*, can be activated in sweet potato in response to injury (Imanishi et al., 1997; Yeh et al., 1997b). Initially, SPORAMIN was considered a unique storage protein found in the tuberous roots of sweet potato. However, subsequent studies revealed that *SPORAMIN* can be rapidly induced in sweet potato leaves following injuries, exposure to jasmonic acid, herbivore attack, and treatment with the homoterpene (E)-4,8-dimethyl-1,3,7-nonatriene (DMNT) (Meents et al., 2019; Rajendran et al., 2014). Functional studies have elucidated that SPORAMIN functions as a serine-type trypsin inhibitor, exerting its effects primarily in the insect intestine and impeding insect growth and development (Imanishi et al., 1997; Yeh et al., 1997a). Remarkably, transgenic plants of *Brassica rapa* subsp. *chinensis* and *Nicotiana benthamiana* that overexpress *SPORAMIN* have demonstrated robust resistance against pests (Chen et al., 2006; Yeh et al., 1997b). Given its distinctive role as an insect-resistant protein in *Ipomoea* plants, understanding the mechanisms underlying its injury-induced expression holds significant importance.

In sweet potato leaves, the *IbNAC1* transcription factor exhibits rapid induction in parallel with *SPORAMIN* in response to injury and jasmonic acid. *Ib*NAC1 is a transcription factor that functions by recognizing and binding to a specific region in the *SPORAMIN* promoter called the *SPORAMIN wounding response element* (*SWRE*). This

doi:10.6342/NTU202302113

interaction plays a crucial role in regulating the induction of *SPORAMIN* and is associated with the wound response. Transgenic sweet potato plants expressing *IbNAC1* show strong insect resistance. *Ib*NAC1 also participates in ROS signaling and jasmonic acid response (Chen et al., 2016a). Subsequently, *IbNAC1* is found to be regulated by the transcription factors *Ib*bHLH3, which belongs to the basic helix–loop–helix transcription factors family. *Ib*bHLH3 acts as an ortholog of MYC2 and operates downstream of jasmonates. During the early stage of the wound response, *Ib*bHLH3 plays a pivotal role in initiating the activation of *IbNAC1*, thereby triggering the expression of downstream insect resistance genes, including *SPORAMIN*. When the injury is advanced, the transcriptional repressor *Ib*bHLH4 will block the expression of *IbNAC1* to stop the wound response by forming protein complex with *Ib*bHLH3 or competing for the *Ib*bHLH3 binding site of the *IbNAC1* promoter. The expression of *IbNAC1* is also under the regulation of multiple factors, including *Ib*JAZ2 (jasmonate-ZIM domain protein, which acts as a repressor of MYC2), *Ib*WIPK1 (wound-induced protein kinase), and *Ib*EIL1 (ethylene-insensitive-like transcription factor). These regulatory elements exert their influence on *IbNAC1* expression in response to injury (Chen et al., 2016b). By treating with PD98059 (ERK1/2 signaling inhibitor), induction of *SPORAMIN* and *IbNAC1* by injury can be greatly reduced. This investigation conducted by Lo et al. (unpublished data) shed light on the involvement of the MAPK pathway in the transmission of signals from wounding

doi:10.6342/NTU202302113

stress to the expression of *SPORAMIN*. Nonetheless, the precise molecular mechanisms that connect the perception of danger, including the involvement of ligands and receptors, to the activation of downstream defense responses, still remain enigmatic.

Objective of this study

Sweet potato (*Ipomoea batatas* cv. Tainong 57) has strong resistance against insect feeding. Our previous studies demonstrated that *IbWIPK*, one of the member in MAPK cascades, can be rapidly induced by wound treatment in sweet potato. *Ib*WIPK can be phosphorylated and binds to downstream bHLH transcription factor family proteins *Ib*bHLH3/4 and co-regulate the expression of *IbNAC1* after injury. The expression of the insect-resistant gene *SPORAMIN* can be induced by the wound-induced *Ib*NAC1 transcription factor. Finally, the trypsin-inhibitory activity of SPORAMIN helps sweet potato to achieve the purpose of resistance to insects. However, it is still unclear how sweet potato senses the wounding or herbivory attack to activate the wound signal transduction. In order to elucidate the key components in the intracellular signaling cascade that triggers induced resistance against herbivores, we will employ a bioinformatics approach to identify potential receptor that can recognize DAMP signals in sweet potato. By validating its gene expression levels during injury and herbivory attack, we aim to determine whether this receptor is capable of recognizing the

doi:10.6342/NTU202302113

endogenous peptide ligand *Ib*HypSysIV, which has been previously reported in sweet potato, and subsequently initiating various downstream defense responses. Additionally, we will explore other peptide ligands that can be recognized by this receptor in sweet potato. Ultimately, our goal is to establish a comprehensive hypothesis that encompasses the entire cascade from injury signal perception to the induction of defense responses, including SPORAMIN- dependent insect resistance genes in sweet potato.

doi:10.6342/NTU202302113

Materials and methods

Plant material and growth conditions

Sweet potato scions (*Ipomoea batatas* Lam. cultivar Tainong 57) were grown in Phyto chambers under controlled conditions. The plants were subjected to long-day conditions (16 h photoperiod) at a temperature range of 28°C/25°C (day/night), with a relative humidity of 70%. The plants were allowed to grow for a period of 3-4 weeks before they were used for experiments. *Nicotiana benthamiana* plants were grown in a greenhouse with a 16 h photoperiod and a temperature range of 25°C/20°C (day/night) after 4-5 weeks of growth before they were used for experiments. *Arabidopsis thaliana* ecotype Columbia-0 (Col-0) was grown in growth chambers at a temperature of 22°C and an 8 h photoperiod for 4-5 weeks before they were used for experiments. All the plants were grown in soil mixtures that contained a blend of peat, perlite, and vermiculite. The soil was kept moist, and fertilizers were applied as needed. The plants were regularly monitored for signs of stress or disease and were treated accordingly.

Peptides

Peptides were synthesized by GenScript Biotech (Leiden, Netherlands) and were dissolved in BSA/NaCl (10 mg/ml, 0.1 M) solution before each experiment. The detailed sequences of the peptides used in this study are listed in Table 1. The purity of the peptides

doi:10.6342/NTU202302113

was verified by high-performance liquid chromatography (HPLC) and mass spectrometry analysis.

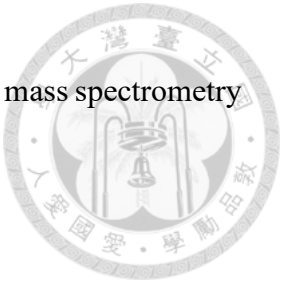

RNA extraction and qRT-PCR analyses

RNA extraction was performed according to the protocol described by Meents et al. (2019). Briefly, harvested sweet potato leaves were ground to a fine powder in liquid nitrogen, and total RNA was extracted using TRIzol reagent (Thermo Fisher Scientific). RNA quality and quantity were assessed using an Infinite M200 PRO plate reader, (TECAN).

For qRT-PCR analysis, cDNA was synthesized from 1 μg of total RNA using a RevertAid First Strand cDNA Synthesis Kit (Thermo Fisher Scientific). Quantitative real-time PCR was performed using a Bio-Rad CFX96 Real-Time PCR Detection System (Bio-Rad Laboratories) with gene-specific primers (Table 2). The PCR reaction mixture contained SYBR Green PCR Master Mix (Bio-Rad Laboratories), cDNA template, and gene-specific primers. The thermal cycling conditions were as follows: 95°C for 3 min, followed by 45 cycles of 95°C for 10 s and 60°C for 30 s. The expression levels of target genes were normalized to the expression of the sweet potato housekeeping gene *IbActin1*. The relative expression levels were calculated using the 2^−ΔΔCT method (Livak and Schmittgen, 2001).

doi:10.6342/NTU202302113

RNA-Seq analysis and processing

RNA from single 3rd leaves treated for 1 h with *Ib*HypSysIV, *Ib*Pep1, and water (control) was extracted according to Meents et al. (2019) using TRIzol Reagent (Invitrogen). Four biological replicates per treatment were used for RNA-Seq experiments conducted by Novogene Europe (Cambridge). RNA quality was monitored using NanoPhotometer® spectrophotometer (IMPLEN) and RNA Nano 6000 Assay Kit of the Bioanalyzer 2100 system (Agilent Technologies). 1 μg of RNA per sample was used as template material for further sample preparations. Sequencing libraries were generated *via* NEBNext® UltraTM RNA Library Prep Kit for Illumina® (NEB) following manufacturer's instructions. 20 M paired end reads of 150 bp per sample were generated, sequenced on an Illumina NovaSeq 6000 instrument (San Diego). Raw reads were trimmed by in-house scripts. The clean reads were mapped onto *Ipomoea trifida* reference genome (http://sweetpotato.uga.edu/), using HISAT2 V2.0.5 with default parameter. HTSeq V0.6.1 software was used with the union mode to count read numbers mapped of genes for each sample.

R package from Bioconductor, DESeq2 V1.22.2 was used to estimate gene abundance and detect differentially expressed genes (DEGs) among the sample groups. A model based on the negative binomial distribution was carried out to determinate DEGs with an

doi:10.6342/NTU202302113

adjusted p-value cutoff of 0.05 using the Benjamini-Hochberg correction. Genes with a log2-fold change >=1 and padj <0.05 were considered as significantly DEGs. Gene ontology (GO) and Kyoto Encyclopedia of Genes and Genomes (KEGG) pathway enrichment analyses of DEGs were implemented by the GOseq V1.34.1 R package and KOBAS V3.0 software.

Wounding, insect feeding, and peptide spray treatments

To investigate the effect of peptide solutions on sweet potato plants, experiments were conducted on six to eight fully developed leaf plants of *I. batatas* and *N. benthamiana*. To induce wound stress, the third or fourth fully expanded leaves of the plants were mechanically wounded using tweezers, and the leaves were sampled at different time points to monitor the wound response. For insect feeding treatment, second instar *Spodoptera litura* larvae were placed on the third or fourth fully expanded leaves, and the treated leaves were sampled at intervals to study the insect feeding responses.

To examine the local effects of peptide solutions on DMNT emission and gene expression, whole sweet potato plants were sprayed with peptide solution or double-distilled water (control) until all leaves were fully covered. The plants were incubated for 1 h, after which single plants were placed for 24 h in 2.4 L glass desiccators (VWR international) for headspace volatile collection. For RNA-Seq, qRT-PCR, and

doi:10.6342/NTU202302113

phytohormone analyses, the third fully expanded leaf was locally sprayed with peptide solution or double-distilled water (control), and the adjacent fourth leaf (systemic) were harvested after the indicated time points.

VOC collection and quantification

The closed-loop stripping technique was used to collect volatiles from sweet potato plants treated with peptides or double-distilled water (control) for 24 h. The plants were enclosed in 2.4 L desiccators and connected to an air circulation pump (Fürgut GmbH) containing a charcoal trap with 1.5 mg absorption material (CLSA filter, 6 cm long, 0.5 cm diameter, Gränicher & Quartero). The volatiles were then eluted with 2 x 20 µl of dichloromethane containing 10 µg ml^{-1} *n*-bromodecane as internal standard used for further relative quantification. This method was adapted from previous studies with minor modifications (Kunert et al., 2009; Meents et al., 2019).

Cloning of receptor and propeptide gene candidates

*Ib*LRR-RK1 (MT210638) and *Ib*PROPEP1 (OP311829) genes were identified using blastn as well as tblastn on various databases using the receptor and propeptide sequences for Solanaceae plants from Lori et al. (2015). The databases used to find the genes included Sweet Potato Genomic Resource database

doi:10.6342/NTU202302113

(http://sweetpotato.plantbiology.msu.edu/index.shtml), *I. batatas* cv. TN57 transcriptome database (Rajendran et al., 2014), *I. batatas* database: Ipomoea Genome Hub (https://ipomoea-genome.org/), and NCBI (https://www.ncbi.nlm.nih.gov/). The *Ib*LRR-RK1 and *Ib*PROPEP1 coding sequences were amplified from sweet potato leaf cDNA using gene-specific primers (*Ib*LRR-RLK1_FL_F, *Ib*LRR-RLK1_FL_R, *Ib*PROPEP1_FL_F, *Ib*PROPEP1_FL_R, as shown in Table 2) in a PCR reaction with Q5 High-Fidelity DNA Polymerase (NEB), respectively. The coding sequence encoding the tomato *Sl*PEPR1 (XP_004235511) was amplified using the primers *Sl*PEPR1_FL_F and *Sl*PEPR1_FL_R (Table 2). All full-length coding sequences were cloned into the pCR8/GW/TOPO vector (Invitrogen). LR clonase (Invitrogen) was used to transfer these coding sequences from PCR8 to pMDC83 vectors (Curtis and Grossniklaus, 2003), generating C-terminal fusions with GFP.

Generation of chimeric receptors

In order to create chimeric receptors, gene-specific level I modules for the SYR1 (Wang et al., 2018) and *Ib*LRR-RK1 (see above) genes were first generated through proofreading PCR using the Phusion High Fidelity DNA Polymerase (ThermoFisher Scientific) from existing templates. The oligonucleotide primers used in the PCR reaction were listed in Table 2. After subcloning, the accuracy of the gene-specific level I modules

doi:10.6342/NTU202302113

was verified by sequencing. To assemble the receptor expression constructs, GoldenGate cloning was employed using general level I modules, including A-B p35S (G005), D-E GFP (G011), E-F nos-T (G006), and dy F-G (BB09) (Supplementary Figure S1). These general level I modules were integrated into the vector backbone LIIα F 1-2 (BB10), which was previously described (Binder et al. in 2014).

Transient expression of receptor constructs

For transient expression of chimeric proteins in *Nicotiana benthamiana* leaves, *Agrobacterium tumefaciens* GV3101 strains carrying the receptor constructs were grown at 28°C for 16 h in liquid LB medium supplemented with appropriate antibiotics (50 mg/L). Cultures were centrifuged at 5000g for 5 min, removed supernatants, and re-suspended in a solution containing 10 mM MES (pH 5.6), 10 mM $MgCl_2$, and 150 μM acetosyringone to reach OD600 = 0.1. Allow the re-suspended agrobacteria solutions to incubate for a minimum of 2 h, followed by infiltration of the solution into 4-week-old *Nicotiana benthamiana* leaves using a needleless syringe. Infiltrated leaf areas were harvested 24 h after infiltration, floated on the water, and used for oxidative burst, ethylene production, and subcellular localization experiments upon peptide treatment on the following day. For transient expression of chimeric proteins in *Arabidopsis thaliana* mesophyll protoplast, polyethylene glycol (PEG) transformation method refers to Yoo et

doi:10.6342/NTU202302113

al. (2007) was used to transfer the vectors into *Arabidopsis thaliana* mesophyll protoplast. The Arabidopsis mesophyll protoplasts transfer with different vectors were used for subcellular localization or transient activation assay.

Oxidative burst and ethylene production measurement

Oxidative burst and ethylene production were done referring to ethylene and oxidative burst measurement methods (Albert et al., 2010), except for the substrate solution in the oxidative burst assay and instruments that detected luminescence. The oxidative burst was measured per min for 1 h with leaf pieces floating on 100 µl water containing 20 µM L-012 (Wako) and 2 µg/ml horseradish peroxidase (Applichem), after addition of peptides, *Nicotiana benthamiana* leaf discs transiently expressed with different chimeric receptor proteins, with a luminescence plate reader (Mithras LB 940, Berthold, or Infinite M200 PRO plant reader, TECAN). The amount of ethylene was measured by gas chromatography (GC) in the headspace of 4 leaf pieces floating on 500 µl water, treated for 4 h with the peptides or controls.

Transient activation assay

Transient co-expression of the *pFRK1*:Luciferase reporter (Yoo et al., 2007) with the receptor expression constructs in mesophyll protoplasts of *A. thaliana* Col-0 wild-type

doi:10.6342/NTU202302113

was performed as described (Wang et al., 2016). The mesophyll protoplasts were isolated from 4-week-old *A. thaliana* Col-0 wild-type plants, and the receptor expression constructs and the *pFRK1*:Luciferase reporter were co-transfected into the protoplasts using polyethylene glycol (PEG)-mediated transformation. Luminescence was recorded for up to 6 h in W5-medium containing 200 μM firefly luciferin (Synchem UG) after overnight incubation for 14 h and subsequent treatment with peptides or control solution, with a luminescence plate reader (Mithras LB 940, Berthold, or Infinite M200 PRO plant reader, TECAN).

Subcellular localization

Subcellular localization of the *Ib*LRR-RK1-GFP and *Ib*PROPEP1-GFP fusion proteins was determined in *N. benthamiana* leaves and *A. thaliana* mesophyll protoplasts using transient expression as described above. The γ-Tip-mCherry fusion protein (Nelson et al., 2007) was used as a tonoplast localization marker, while PIP2A-mCherry was used as a plasma membrane marker. To induce plasmolysis, 1.0 M mannitol was infiltrated to *N. benthamiana* leaves before fluorescence images were taken. Confocal microscopy was performed using a TCS SP5 Confocal microscope (Leica) and analyzed with LAS AF Lite application software (Leica) or a Zeiss Axio Zoom.V16. The subcellular localization of the fusion proteins was determined by overlaying GFP or mCherry fluorescence signals

doi:10.6342/NTU202302113

with differential interference contrast images. The localization patterns of the fusion proteins were confirmed by co-localization studies with the tonoplast and plasma membrane markers.

Immunoblotting

To perform immunoblotting, wounded leaves of *N. benthamiana* transiently expressing *Ib*PROPEP1-GFP were first ground into a fine powder using liquid nitrogen. Then, 100 µl of 2× SDS sample buffer solution (Nacalai Tesque Inc.) was added to the powder immediately, which was then heated to 95°C for 5 min. After centrifugation at 16,000 x g for 10 min to remove cellular debris, 10 µg of extracted proteins were loaded into 15% SDS polyacrylamide gels for separation of *Ib*PROPEP1-GFP and *Ib*Pep1-GFP. The separated proteins were then transferred to PVDF membranes (MILLIPORE) using semi-dry Western blotting (Wealtec). The membranes were then incubated with anti-GFP antibodies (rabbit, 1:2000; Abcam) overnight, followed by a second incubation with Goat-anti-Rabbit IgG labeled with horseradish peroxidase enzyme (1:20000; Jackson). Detection of luminescence was achieved using chemiluminescent substrates (Chemi-Lumi One Super; Nacalai Tesque Inc.). The luminescent images were captured and analyzed using a KETA CLX Chemiluminescence Imaging System (Wealtec).

doi:10.6342/NTU202302113

Crude endogenous ligand extraction

In this study, crude endogenous ligands were extracted from sweet potato leaves using a modified protocol based on (Chien et al., 2015). Briefly, 10 g of both injured and non-injured leaves were harvested and homogenized using 1% cold trifluoroacetic acid (TFA) in a blender for 2 min. The resulting extracts were filtered through 4 layers of Miracloth to remove any plant debris, followed by centrifugation at 8,500 rpm for 20 min at 4°C. The supernatant was then slowly pressed through a custom-made Sep-Pak C18 solid phase extraction cartridge (Waters) and eluted with 60% (v/v) methanol/0.1% (v/v) TFA. The eluate containing peptides was dried using a speed vac and re-suspended in 200 μl of double-distilled water.

Phytohormone extraction and quantification

Plant hormone extraction and quantification were performed as previously described (Meents et al., 2019). Briefly, local and systemic leaves were collected 1 h after peptide treatment, and extracted with a mixture of methanol and water containing 0.1% formic acid. The extract was then purified by solid-phase extraction using Oasis HLB cartridges (Waters), and analyzed by high-performance liquid chromatography (HPLC) using an Agilent 1200 system (Agilent, USA). Hormones were quantified by tandem mass

doi:10.6342/NTU202302113

spectrometry (MS/MS) using an API 5000 mass spectrometer (Applied Biosystems, USA) equipped with a Turbo spray ion source operating in negative ionization mode. The data were analyzed using Analyst software (Applied Biosystems, USA). The concentrations of phytohormones in the samples were determined by comparison with standard curves generated with authentic standards of each hormone.

Agrobacterium-mediated transformation in sweet potato

The LBA4404 strain *A. tumefaciens* with vectors was cultured in LB medium containing appropriate antibiotics at 28°C for transgene. Sweet potato callus suspension culture was established by isolating healthy callus tissue and crushing it into conical flasks. The callus was infected by immersing in the Agrobacterium solution. After incubation and separation, the infected callus was washed with ddH_2O and placed on an appropriate medium with antibodies to remove residual Agrobacterium. Subsequently, the culture is followed by a medium containing the appropriate phytohormones for the shoot and root development. The regenerated plantlets were transferred to soil and maintained through regular subculturing. Genomic DNA was extracted from transgenic sweet potato leaves and PCR amplification and gel electrophoresis were performed to confirm the presence of the introduced gene.

doi:10.6342/NTU202302113

Statistical analysis

The data generated by qRT-PCR was analyzed according to the methods described in (Meents et al., 2019) and followed by a Shapiro-Wilk normality test. The data distribution determined whether a t-test or Mann-Whitney rank sum test was used for statistical analysis. The phytohormone levels were analyzed using a two-way ANOVA with an initial Shapiro-Wilk normality and equal variance test. For all analyses, phytohormone content was set as the dependent variable with treatment and leaf type as independent variables. For identification of significant differences between groups, pairwise multiple comparison procedure via the Holm-Sidak method was implemented with a significance level of $p < 0.05$. All statistical analyses were conducted in SigmaPlot (V 11.0).

doi:10.6342/NTU202302113

Results

Comparison of the putative DAMP receptors in sweet potato

In our study, we aimed to identify potential receptors in sweet potato that are involved in the response to herbivore attack and wounding. To guide our search, we referred to the reported sequences of damage-associated molecular pattern (DAMP)-related receptors in other plant species, such as *At*PEPR1/2 (AT1G73080/AT1G17750) in Arabidopsis and *Sl*SYR1/2 (Solyc03g082470/Solyc03g082450.2.1), *Sl*PEPR1 (XP_004235511) in tomato. Utilizing the "Sweet potato Genomic Resource database" (http://sweetpotato.plantbiology.msu.edu/index.shtml) from *Ipomoea trifida*, we successfully identified several receptor genes that are closely related to DAMP-related receptors. These identified receptors have been designated as *It*LRR-RK1 to *It*LRR-RK13 (Figure 1). To further investigate potential LRR-RK genes with sequence similarity to *It*LRR-RKs in sweet potato (*Ipomoea batatas*), we utilized two transcriptomic databases: the "Ipomoea Genome Hub" (https://ipomoea-genome.org/) and the transcriptome database of *I. batatas* cv. Tainong 57 (Rajendran et al., 2014). Through this analysis, we successfully identified five putative receptor kinase genes in *I. batatas*, which have been designated as *Ib*LRR-RK1 to *Ib*LRR-RK5.

To validate their expression patterns, we performed RT-PCR and qRT-PCR experiments. Interestingly, we found that among these genes, only *IbLRR-RK1*

doi:10.6342/NTU202302113

(MT210638) exhibited rapid upregulation upon wounding treatment, while *IbLRR-RK2* to *IbLRR-RK5* did not show significant changes in expression levels (Figure 2A, B). After treatment by wounding along with oral secretions from Spodoptera larvae, the relative expression level of *IbLRR-RK1* exhibited a significant increase, reaching peaking at nearly 30-fold after 15 min of treatment, followed by a 12-fold increase after 30 min, and returning to baseline after 60 min. Similarly, herbivory feeding resulted in a 5.4-fold increase in *IbLRR-RK1* expression after 15 min of treatment, and a 1.7-fold increase after 30 min (Figure 3A, B). The results provide strong evidence that both insect herbivory and mechanical wounding are potent inducers of the receptor-like kinase gene *IbLRR-RK1* in sweet potato leaves. These findings strongly suggest that *Ib*LRR-RK1 is involved in the perception of a signal associated with tissue damage and may play a role in the wound-related signals transduction in sweet potato.

The putative *Ib*LRR-RK1 receptor is related to PEPRs

The sweet potato gene *IbLRR-RK1*, originating from the cultivar Tainong 57 (*I. batatas*), exhibits the characteristic features commonly found in members of the PEPR (Plant Elicitor Peptide Receptor) family. The *IbLRR-RK1* gene encodes a protein with a complex structure consisting of various domains. The protein includes an ectodomain that comprises a signal peptide, an N-terminal cap region commonly observed in plant LRR-

doi:10.6342/NTU202302113

RKs, 26 repeats of the extracellular LRR (Leucine-Rich Repeat) motif, an outer juxtamembrane region, a transmembrane domain, and a cytosolic region containing the inner juxtamembrane domain. The cytosolic region is followed by a serine/threonine kinase domain, which suggest to be responsible for enzymatic activity and signal transduction within the cell (Figure 4). The localization of the *Ib*LRR-RK1 protein was investigated by transiently expressing a fusion protein containing green fluorescent protein (GFP) in *N. benthamiana* leaves and *A. thaliana* protoplasts. The GFP-tagged *Ib*LRR-RK1 protein was observed to localize predominantly at the plasma membrane, consistent with the expected localization pattern of other plant LRR receptors such as *At*EFR-GFP and *Sl*SYR1-GFP, which were used as positive controls for the experiment (Figure 5A, B).

*Ib*LRR-RK1 exhibits high similarity to PEPRs found in Arabidopsis (*At*PEPR1 /*At*PEPR2; At1g73080/At1g17750) and tomato (*Sl*PEPR1, XP_004235511) (Figure 6). *Ib*LRR-RK1 shares 97% identity in amino acid residues with *It*LRR-RK1 and displays 50% and 65% identity with *At*PEPR1 and *Sl*PEPR1, respectively. Moreover, it shows 36% identity to *Sl*SYR1 (Table 3), while other putative *Ib*LRR-RKs in this study share no more than 36% identity with any of the mentioned receptors (Data not shown). By conducting a comparative analysis of the extracellular domains of various receptors, it was observed that *Ib*LRR-RK1 shares a remarkably similar ligand-binding surface with *Sl*PEPR1 (60%

doi:10.6342/NTU202302113

identity) and *At*PEPR1 (48% identity). In contrast, *Ib*LRR-RK1 exhibits a lower degree of sequence conservation with tomato *Sl*SYR1, with only 36% of the residues being identical (Table 4). Based on these findings, it can be concluded that *Ib*LRR-RK1 belongs to the plant elicitor peptide receptor (PEPR) group, characterized by its structural similarity to known members of the PEPR family.

Investigating the functionality of the *Ib*LRR-RK1 receptor in defense responses

Validating the functionality of newly identified receptor candidates, particularly in cases for which the ligands are unknown, is challenging. However, these challenges can be overcome by employing approaches such as ectopically expressed the chimeric version receptors in suitable plant systems (Albert et al., 2010; Butenko et al., 2014). To assess the potential of the kinase domain of the putative receptor from sweet potato in activating the immune response pathway, a chimeric receptor was generated by fusing the extracellular domain of the tomato receptor *Sl*SYR1, which is known to bind systemin ligand, with the kinase domain of *Ib*LRR-RK1 from sweet potato (Supplementary Figure S1). This chimeric receptor, referred to as SYR1-*Ib*K, was created to investigate the functionality of the *Ib*LRR-RK1 kinase domain in triggering signal transduction and activation of the immune response pathway. The chimeric receptor SYR1-IbK, as well as the native *Sl*SYR1 and *Ib*LRR-RK1 receptors, were transiently expressed in *N.*

doi:10.6342/NTU202302113

benthamiana leaves. Consistent with expectations, the GFP-tagged SYR1-*Ib*K receptor were observed to localize at the plasma membrane (Figure 5B).

Upon treatment with the systemin ligand specific to *Sl*SYR1, leaf discs expressing SYR1-*Ib*K showed an induction of oxidative burst (Figure 7, 8A), indicating the activation of downstream signaling pathways and validating the functionality of the *Ib*LRR-RK1 kinase domain. To further assess the receptor's response to defense-related peptides in addition to systemin from various plant sources, including *Sl*Pep6, *Sl*HypSysIII, *Ib*HypSysIV, and *At*Pep1 (Table 1). Oxidative burst bioassays were conducted using *N. benthamiana* leaves transiently expressing either the SYR1-*Ib*K or native *Ib*LRR-RK1 treated with mentioned peptides. Remarkably, upon treatment with *Sl*Pep6 peptide ligand, the activation of the defense pathway was observed in the presence of *Ib*LRR-RK1, resulting in the production of reactive oxygen species (ROS) and the accumulation of ethylene (Figure 8B, 9B). To further validate the recognition of *Sl*Pep6 by *Ib*LRR-RK1, we performed experiments in protoplasts derived from mesophyll cells of *A. thaliana* Col-0. We utilized the promoter of *AtFRK1* (flg22-induced receptor-like kinase 1), a well-known early defense marker gene in Arabidopsis (Asai et al., 2002), along with a luciferase reporter gene driven by *AtFRK1* promoter, to assess PAMP (pathogen-associated molecular pattern) activity (Yoo et al., 2007). Transient activation assay showed that co-expression of *Ib*LRR-RK1 with p*FRK1:LUC* triggered the

doi:10.6342/NTU202302113

induction of the luciferase reporter in *Sl*Pep6-dependent manner (Figure 10B), validating the findings from the previous *N. benthamiana* experiments. Notably, the chimeric SYR1-*Ib*K receptor specifically recognized systemin but not *Sl*Pep6 (Figure 8A, 9A, 10A). Collectively, these results demonstrate that the activation of *Ib*LRR-RK1 can elicit plant immune responses such as oxidative burst, production of ethylene, and the expression of defense genes, thereby identifying a heterologous ligand for *Ib*LRR-RK1.

_Ib_LRR-RK1 perceives endogenous ligands from sweet potato leaves

Thus far, the native ligands of *Ib*LRR-RK1 receptor in *I. batatas* leaves are still remain unknown. To investigate the peptide ligands in sweet potato leaves that can activate *Ib*LRR-RK1 receptor. We utilized the extracts purified from leaves of *I. batatas* cv. TN57 by applying to *N. benthamiana* leaves transiently expressing *Ib*LRR-RK1. Leaf discs expressing the receptor exhibited a ROS burst in response to leaf extracts, while control leaves transformed with p19 alone did not show such response (Figure 11). This result indicates that sweet potato leaves indeed contain endogenous ligands that can be specifically recognized by the *Ib*LRR-RK1 receptor and activate downstream signaling pathways. Further investigation is warranted to identify this endogenous ligand.

doi:10.6342/NTU202302113

***Ib*Pep1 peptide ligand activates *Ib*LRR-RK1 receptor**

To identify the native cognate ligand of *Ib*LRR-RK1 in sweet potato, we employed a strategy based on the functional activation of *Ib*LRR-RK1 by *Sl*Pep6. Utilizing the sequence of *Sl*Pep6 and other Peps reported from Solanaceae family plants as probes (Bartels et al., 2013) (Figure 12), we conducted a scanning sequence pattern and tBlastn analysis to search for potential endogenous ligands in sweet potato. This search was performed using the Ipomoea genome hub database and the sweet potato genomic resource database. Two putative Peps and their precursor protein were identified in this experiment. Based on the typical length of Peps as reported by Lori et al. (2015), we selected a 23 amino-acids residue segment from the C-terminal region of the precursor protein *It*PROPEP1 (itf01g30920.t1) was selected and named *It*Pep1 (LSSRPPRPGLGNSGDPQTNDTSS) (Supplementary Figure S2A). Furthermore, we identified *It*Pep2 (RRGRTPPRPENLKLNLRARKHSLEDQ) from the C-terminus of the precursor protein *It*PROPEP2 (itf07g21780.t1), which contained the conserved Peps motif RRGRXP (Supplementary Figure S2B). Both putative peptide ligands, *It*Pep1 and *It*Pep2, were chemically synthesized and examined their ability to activate *Ib*LRR-RK1 receptor. Both synthetic peptides, *It*Pep1 and *It*Pep2, were administered to *N. benthamiana* leaves that were transiently expressing *Ib*LRR-RK1. *It*Pep1 triggered the production of reactive oxygen species (ROS) in an *Ib*LRR-RK1-dependent manner, while

doi:10.6342/NTU202302113

*It*Pep2 did not induce such a response (Figure 13A). Notably, neither *It*Pep1 nor *It*Pep2 elicited a response in leaf discs expressing the chimeric receptor SYR1-*Ib*K or the p19 control (Figure 13B, C).

Based on the activation of *Ib*LRR-RK1 by *It*Pep1, we intended to identify its homologous peptide, *Ib*Pep1, and its precursor protein, *Ib*PROPEP1, in sweet potato (*Ipomoea batatas*). The *Ib*PROPEP1 gene was amplified from *I. batatas* cv. TN57 using reverse transcription PCR (RT-PCR) with oligonucleotides designed based on the sequence of *It*PROPEP1. The coding sequence (CDS) of *Ib*PROPEP1 is composed of 378 base pairs and encodes a deduced protein of 125 amino acid residues. The predicted protein has an isoelectric point (pI) of 4.44a and a calculated molecular weight of 13.25 kDa. The bioactive peptide, *Ib*Pep1, consists of 23 amino acids and is located at the C-terminus of the precursor protein *Ib*PROPEP1. *Ib*Pep1 shows completely identity with the corresponding peptide derived from *It*PROPEP1 (Figure 14). Alignments among the *Ib*Pep1 with other Peps from Solanales plants and Arabidopsis showed that *Ib*PepI shares ~42% identity to *Nb*Pep6, *Ns*Pep6, *Nt*Pep6, and ~37% identity to *Sl*Pep6, *St*Pep6, *Sm*Pep6, while other Peps sequences from Arabidopsis share less than 32% identity with *Ib*Pep1 (Table 5). Phylogenetic analyses of *Ib*PROPEP1 with several PROPEPs from Solanales plants and Arabidopsis were also conducted (Figure 15). Consistent with expectations, the amino acid sequences of *Ib*PROPEP and *Ib*Pep exhibit closer similarity to solanaceous

doi:10.6342/NTU202302113

plants than to Arabidopsis.

_Ib_LRR-RK1 receptor perceives _Ib_Pep1 with high sensitivity and specificity

Using the heterologous expression system as previously described, we conducted experiments to assess the sensitivity and specificity of the potential *Ib*Pep1-*Ib*LRR-RK1 interaction. The application of *Ib*Pep1 resulted in the dose-dependent production of reactive oxygen species (ROS), exhibiting a clear response in the sub-nanomolar concentration range. The estimated half-maximal activation (EC_{50}) was determined to be approximately 1 nM (Figure 16A). In a comparative analysis, it was observed that the tomato peptide (*Sl*Pep6) displayed approximately 10 times lower efficacy in activating *Ib*LRR-RK1 compared to *Ib*Pep1 in this bioassay (Figure 16A). To further investigate the specificity of the receptor-ligand interactions, the tomato peptide receptor (*Sl*PEPR1) was cloned and expressed in *N. benthamiana*. The efficiencies of the two peptides, *Ib*Pep1 and *Sl*Pep6, in inducing the production of ROS were compared. The *Ib*LRR-RK1/*Ib*Pep1 pair and the *Sl*PEPR1/*Sl*Pep6 pair demonstrated similar efficiencies, with both exhibiting an estimated EC_{50} value of 1 nM (Figure 16B). Interestingly, the sweet potato *Ib*Pep1 peptide was also recognized by the tomato *Sl*PEPR1 receptor, albeit with significantly lower sensitivity, as indicated by the estimated EC_{50} values above 100 nM (Figure 16B). These findings highlight the specificity of the *Ib*LRR-RK1 receptor for *Ib*Pep1 and the cross-

doi:10.6342/NTU202302113

recognition of *Ib*Pep1 by the tomato *Sl*PEPR1 receptor, albeit with reduced sensitivity.

*Sl*Pep6 and *Ib*Pep1 shared only 37% identity but both peptides were functional in activating *Ib*LRR-RK1 (Figure 8B, 13A, Table 5). By alignment of amino acids sequences of *Ib*Pep1 and *Sl*Pep6 revealed that both Peps share part of the similar amino acids residues such as RPP (*Ib*Pep1: $R^4P^5P^6$, *Sl*Pep6: $R^7P^8P^9$), RPXXG (*Ib*Pep1: $R^7P^8GLG^{11}$, *Sl*Pep6: $R^{11}P^{12}KVG^{15}$), and PQXN (*Ib*Pep1: $P^{16}Q^{17}TN^{19}$, *Sl*Pep6: $P^{20}Q^{21}NN^{23}$) (Figure 17). It suggests these amino acids residues might play critical functional role in activating corresponding receptor. To investigate the specificity of predicted sweet potato *Ib*Pep1 peptide ligand for its receptor *Ib*LRR-RK1, we synthesized N-terminal and C-terminal truncated versions of *Ib*Pep1 (Figure 18). Deleting the three N-terminal amino acids residues of *Ib*Pep1 (named *Ib*Pep1 (4-23)) did not significantly affect its perception by *Ib*LRR-RK1 receptor, but the loss of arginine at position 4 of *Ib*Pep1 resulted in a significant increase in the EC^{50} value when either deleted (*Ib*Pep1 (5-23)) or replaced with alanine (*Ib*Pep1 (A4)). On the other hand, the presence of the *Ib*Pep1 C-terminus was necessary for its sensitive perception by *Ib*LRR-RK1 receptor, although the last two serine residues substituted by alanine (*Ib*Pep1 (A22A23)) did not significantly affect its function (Figure 18, 19).

doi:10.6342/NTU202302113

_Ib_PROPEP1 localizes to the tonoplast and forms aggregates within the vacuole

We generated a fusion construct of *Ib*PROPEP1 (OP311829) with GFP at the C-terminus and transiently expressed it in *N. benthamiana* leaves and *A. thaliana* protoplasts to investigate its subcellular localization using confocal microscopy. *Ib*PROPEP1-GFP exhibited a localization pattern consistent with tonoplast localization (Figure 20), similar to the localization of *At*PROPEP1-YFP as previously reported (Hander et al., 2019). Interestingly, we observed that *Ib*PROPEP1-GFP also aggregated inside the vacuole of Arabidopsis mesophyll protoplasts. Aggregated *Ib*PROPEP1 formed the formation of bright, small globular structures, resembling bulbs (Saito et al., 2002) (Figure 20). Similarly, *Ib*PROPEP1-GFP also accumulated in the tonoplast and formed multiple bright small globular bulbs structures that exhibited movement within the vacuole in *N. benthamiana* (Figure 21, Video 1).

A specific _Ib_LRR-RK1-activating DAMP is present in sweet potato leaves

The previous results showed that the sweet potato extracts contained endogenous ligands which exhibited the function in activating *Ib*LRR-RK1 receptor (Figure 11). Previous researches have demonstrated that PROPEPs undergo cleavage by wounding-activated proteases, resulting in the release of immunomodulatory Peps (Bartels and Boller, 2015; Hander et al., 2019). To simulate a similar scenario, we performed

doi:10.6342/NTU202302113

additional experiments where sweet potato leaves were damaged by squeezing them with tweezers and allowing a 10-min interval before harvesting the tissue. Oxidative burst experiment showed that extracts from wounded leaves displayed higher elicitor activity compared to directly extracted leaves from non-wounded plants. Notably, the observed activity was dependent on the expression of *Ib*LRR-RK1 (Figure 22). These findings suggest that crude extracts of *I. batatas* leaves contain endogenous ligands for *Ib*LRR-RK1, and their accumulation may be induced by wounding stress.

Wounding triggers *Ib*PROPEP1 processing

Previous research showed that damage induces instant processing and generates the plant elicitor peptide 1 (*At*Pep1) from C-terminal of its precursor protein *At*PROPEP1 (Hander et al., 2019). To ascertain whether our candidate peptide ligand *Ib*Pep1 can be processed by wounding from C-terminal of its precursor protein *Ib*PROPEP1, *N. benthamiana* leaves transiently expressing with *Ib*PROPEP1-GFP were damaged with tweezers and collected quantitative samples at different time points. Then crushed tissue with liquid nitrogen immediately and extracted the proteins. The immunoblot result showed that *Ib*PROPEP1-GFP fusion protein can be cleaved into a smaller C-terminal of *Ib*PROPEP1-GFP which has the approximate molecular weight of an *Ib*Pep1-GFP fusion protein. The band estimated as *Ib*Pep1-GFP rose immediately after the damage, peaking

doi:10.6342/NTU202302113

at around 2 min, followed by gradually disappearing speculation fades with general protein degradation or *Ib*PepI-GFP binding to other proteins (Figure 23). Taken together, *Ib*Pep1 peptide ligand can be derived from *Ib*PROPEP1 due to tissue damage. This experiment supports that *Ib*Pep1 has a high probability of being an endogenous ligand of *Ib*LRR-RK1 receptor.

_Ib_HypSysIV and _Ib_Pep1 activate complementary signaling cascades to induce defense responses

To investigate the potential involvement of *Ib*Pep1 in herbivore resistance responses in sweet potato and other processes, we conducted experiments on whole sweet potato plants. Plants were subjected to foliar spraying with a concentration of 25 μM *Ib*Pep1, and the expression of *SPORAMIN* and other well-characterized defense-related genes, as reported in previous studies (Chen et al., 2016b), was analyzed. For comparative analysis, we also treated the plants with a synthetic hydroxyproline-rich glycopeptide, *Ib*HypSysIV, known to induce *SPORAMIN* expression (Chen et al., 2008), at the same concentration. Quantitative real-time PCR (qRT-PCR) analysis the sweet potato leaves at 30 min and 1 h after peptides treatment revealed transient increases in transcript levels of *IbWIPK1* (HQ434622) (68-fold), *IbNAC1* (GQ280387.1) (22-fold), and *SPORAMIN* (X60930.1) (16-fold) in response to *Ib*HypSysIV treatment (Figure 24A), confirming the activity of

doi:10.6342/NTU202302113

*Ib*HypSys peptides to rapidly initiate SPORAMIN-related signaling pathways. On the other hands, *Ib*Pep1 only induced a 3.5-fold increase in *SPORAMIN* expression after 30 min, while *IbWIPK1* and *IbNAC1* showed longer and stronger expression levels compared to *Ib*HypSysIV treatment (Figure 24B). Furthermore, analysis of other defense-related genes revealed that both treatments with *Ib*Pep1 and *Ib*HypSysIV led to an upregulation of *Ib*CML1 (calmodulin-like protein 1; OP311828) and *Ib*LRR-RK1 gene expression (Figure 24A, B). Additionally, compared to the control treatment with *Ib*Pep1 and water, the *Ib*HypSysIV treatment induced a significantly increased of the wound-inducible volatile DMNT ((E)-4,8-dimethyl-1,3,7-nonatriene) emmision (Meents et al., 2019) (Supplementary Figure S3). Leaves treated with an inactive scrambled peptide or the tomato *Sl*Pep6 peptide exhibited DMNT levels comparable to the control treatment, which validates the functionality of the peptide application technique and confirms the specific elicitation of DMNT by *Ib*HypSysIV in sweet potato.

To investigate the role of peptides in the defense mechanisms of Ipomoea, we analyzed the levels of phytohormones in both local and systemic leaves of *I. batatas* TN57 plants after peptide treatment. Comparative analysis with controls (water treatment) revealed no significant alterations in the levels of jasmonic acid (JA) following treatment with *Ib*HypSysIV in local and systemic leaves (Supplementary Figure S4A). Intriguingly, the locally treated leaves with *Ib*HypSysIV displayed a substantial increase in the

doi:10.6342/NTU202302113

concentration of bioactive JA-Ile, while the systemic leaves did not show a similar response (Supplementary Figure S4B). In the case of stress-related hormones, such as salicylic acid (SA) and abscisic acid (ABA), no significant differences were observed compared to control (water) treatments, except for a reduction in SA concentrations in the local *Ib*HypSysIV-treated leaves (Supplementary Figure S4C). Treatment with *Ib*Pep1 did not significantly alter JA, JA-Ile, and SA levels, although the effects might be masked by low concentrations. However, sweet potato leaves treated with *Ib*Pep1 led to a decrease amount in ABA levels, predominantly observed in the local leaves (Supplementary Figure S4D). Although there were no dramatic changes in overall phytohormone levels, a clear tendency was observed: for phytohormones regulated by *Ib*HypSysIV, no response was observed during treatment with *Ib*Pep1, and vice versa.

Differentially expressed genes (DEGs) between *Ib*Pep1 and *Ib*HypSysIV treatment in sweet potato leaves

To further gain a deeper understanding of the similarities and functional characteristics of *Ib*Pep1 and *Ib*HypSysIV, we performed RNA sequencing (RNA-seq) experiments on individual leaves treated with *Ib*Pep1, *Ib*HypSysIV, or water (control) for 1 h, respectively (Supplementary Figure S5). A total of 29385 expressed genes were identified by mapping them to the reference sweet potato genome database. Among them,

doi:10.6342/NTU202302113

27521 genes were shared across all samples, including *Ib*Pep1, *Ib*HypSysIV, and control (water) treatment. Specifically, 383 genes were exclusively detected after *Ib*Pep1 treatment, while 261 genes were exclusively detected after *Ib*HypSysIV treatment. Additionally, we identified 356 common transcripts that were present in both peptide treatments but not in the control (Supplementary Figure S5A). Interestingly, 253 expressed genes were mapped to the *I. trifida* genome but were only observed in control plants, indicating that the expression of these genes is suppressed upon peptide treatments.

Moreover, treatment with *Ib*HypSysIV resulted in the significant upregulation of 261 genes and downregulation of 294 genes compared to control (water) leaves. Conversely, incubation with *Ib*Pep1 elicited an even stronger response, leading to the upregulation of 769 genes and downregulation of 706 genes compared to control (water) leaves (data not shown). A comparative analysis of the two peptide treatments revealed that 1923 genes exhibited significant differential regulation between *Ib*HypSysIV and *Ib*Pep1 treatments. *Ib*HypSysIV treatment led to 889 genes being upregulated and 1,034 genes being downregulated compared to *Ib*Pep1 treatment (Supplementary Figure S5B). These findings support the notion that the two sweet potato peptides have distinct functions, potentially attributed to their ability to modulate different sets of genes. To further validate this hypothesis, additional confirmation through GO and KEGG pathway analyses, as well as qRT-PCR, is necessary and will be conducted. The complete original RNA-seq

doi:10.6342/NTU202302113

data can be accessed through NCBI with the accession number GSE227409.

Establishment of transgenic sweet potato lines

Based on the previous experiments, we have found that the *Ib*LRR-RK1 receptor and the *Ib*Pep1 peptide ligand derived from the precursor protein *Ib*PROPEP1 are both involved in the defense responses of sweet potato. We aim to further investigate the physiological functions of these proteins in sweet potato by establishing overexpress/silence transgenic plants. To establish transgenic sweet potato plants overexpressing *Ib*PROPEP1 and *Ib*LRR-RK1, we cloned the genes and used restriction enzyme digestion for inserting them into the pCAMBIA2300 vector containing the 35S promoter. The resulting constructs, pCAMBIA2300-35s-*Ib*LRR-RK1 and pCAMBIA2300-35s-*Ib*PROPEP1, were transformed into sweet potato *(Ipomoea batatas* cv. KS57) via Agrobacterium-mediated transformation to achieve gene overexpression. To establish transgenic sweet potato plants with gene silencing of *Ib*PROPEP1 and *Ib*LRR-RK1, we used the gateway system to clone gene fragments into the pK7GWIWG2(II) vector. The constructs, pK7GWIWG2(II)-*Ib*LRR-RK1 and pK7GWIWG2(II)-*Ib*PROPEP1, were also introduced into sweet potato *(Ipomoea batatas* cv. KS57) via *Agrobacterium*-mediated transformation to achieve gene silencing using RNAi.

doi:10.6342/NTU202302113

So far, we have successfully obtained transgenic sweet potato plants overexpressing *Ib*LRR-RK1, and the successful transformation was confirmed through genomic DNA extraction and PCR analysis (Supplementary Figure S6A). Initial physiological observations of the transgenic plants in culture media and soil revealed that the roots of the *Ib*LRR-RK1 overexpressing sweet potato plants were more abundant compared to the control group, exhibiting unusual anti-gravitropism patterns (Supplementary Figure S6B). Additionally, the size of the *Ib*LRR-RK1 overexpressing plants was significantly smaller, with fewer leaves, compared to the wild-type plants after the same duration of cultivation (Supplementary Figure S6C). Further quantification of these physiological phenomena and assessment of stress tolerance characteristics have not yet been examined, and is required to fully understand the impact of *Ib*LRR-RK1 overexpression on sweet potato.

doi:10.6342/NTU202302113

Discussion

Activation of *Ib*LRR-RK1 receptor starts up plant immune responses

By exploring the genomic databases of sweet potato, we successfully identified a gene which can be induced upon herbivore attack and wounding, encoding a typical leucine-rich repeat receptor kinase called *Ib*LRR-RK1 (Figures 2, 3, 4). We employed a chimeric receptor strategy to generate a functional receptor by combining the extracellular recognition domain of *Sl*SYR1 with the cytosolic kinase domain of *Ib*LRR-RK1 (Supplementary Figure S1). Heterologous expression of this chimeric receptor in both *A. thaliana* and *N. benthamiana* confirmed its functionality in initiating the defense responses, including oxidative burst, induction of defense-related genes, and ethylene biosynthesis (Figure 7, 8, 9, 10). Phylogenetic analysis indicated that *Ib*LRR-RK1 belongs to the PEPR (plant elicitor peptide receptor) family (Figure 6). The sweet potato *Ib*LRR-RK1 receptor recognized and responded to *Sl*Pep6 peptide ligand from tomato, but not to *At*Pep1 from Arabidopsis. Remarkably, the sweet potato endogenous peptide ligand *Ib*HypSysIV, known for its involvement in wound responses (Chen et al., 2008), was found to be non-recognizable by *Ib*LRR-RK1 (Figure 8, 9, 10).

*Ib*Pep1 is a functional peptide ligand for *Ib*LRR-RK1 receptor

Based on the known results, we conducted a search for cognate peptides of *Ib*LRR-

doi:10.6342/NTU202302113

RK1 in the sweet potato genome utilizing sequences of *Sl*Pep6, Peps from other Solanaceae plants, and their precursor proteins (PROPEPs). As a result, a novel peptide ligand called *Ib*Pep1 consisting of 23 amino acids was discovered, originating from the C-terminus of its precursor protein *Ib*PROPEP1 (Figure 12, 13, 14). *Ib*Pep1 displayed a significantly higher sensitivity, approximately 10 times greater, in triggering the oxidative burst in *N. benthamiana* leaves expressing *Ib*LRR-RK1 compared to *Sl*Pep6 (Figure 16A). Interestingly, the cross-recognition between the tomato peptide and sweet potato receptors prompted us to explore the reverse situation. Specifically, we examined the interaction between the tomato receptor *Sl*PEPR1, known as the endogenous receptor for the *Sl*Pep6 ligand (Lori et al., 2015), and sweet potato peptide ligand *Ib*Pep1. *Sl*PEPR1 is indeed capable to recognize and response to *Ib*Pep1, although its sensitivity is relatively lower compared to *Sl*Pep6. These results providing novel evidence for the compatibility of Peps and PEPRs across different families, specifically between Solanaceae and Convolvulaceae.

The activity of *Ib*Pep1 requires specific amino acid residues and structure

The structure-activity relationship of peptide ligand *Ib*Pep1 and its receptor *Ib*LRR-RK1 was investigated by analyzing different synthetic derivatives of *Ib*Pep1. This investigation unveiled specific structural features necessary for the interaction between

doi:10.6342/NTU202302113

the *Ib*Pep1 peptide and the *Ib*LRR-RK1 receptor, as depicted in Figure 19. Consistent with the findings regarding other Peps, the C-terminus of *Ib*Pep1 was determined to be crucial for its activity. Specifically, the C-terminally truncated form of *Ib*Pep1 (*Ib*Pep1(1-20)) showed a significant reduction in activity, with at least a 100-fold decrease compared to the full-length 23-mer *Ib*Pep1 (Figure 19, 20). Interestingly, unlike Peps from other plant families (Tang et al., 2015), the specific amino acid composition at the C-terminus of *Ib*Pep1 seemed to have less significance. Substitution of the last two residues with alanine (*Ib*Pep1(A22A23)) only resulted in a marginal decrease in affinity. In the conserved region spanning the overlapping 20 amino acids, sweet potato Peps shared five out of the twelve highly conserved amino acid residues observed in the Pep-motif specific to the Solanaceae family (Lori et al., 2015) (Figure 18, 25A). The significance of one of these highly conserved residues (Arginine^4) was confirmed, as the substitution of arginine with alanine (*Ib*Pep1(A4)) significantly decreased the activity of *Ib*Pep1, highlighting the crucial of the arginine residue at the position. A composite consensus sequence of Peps in Solanaceae and Convolvulaceae families revealed conserved clusters of proline and arginine residues at the N-terminus, while asparagine and proline residues were conserved at the C-terminus (Figure 25B).

doi:10.6342/NTU202302113

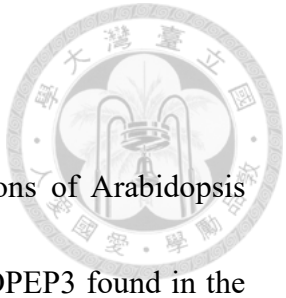

Is *Ib*PROPEP1 stored in the bulb, in addition to the tonoplast?

Previous studies have indicated distinct subcellular localizations of Arabidopsis PROPEPs, with *At*PROPEP1/6 localized at the tonoplast and *At*PROPEP3 found in the cytosol (Bartels et al., 2013). Our investigation revealed that *Ib*PROPEP1-GFP also localizes at the tonoplast (Figure 20, 21). Interestingly, *Ib*PROPEP1-GFP was additionally observed in bright vesicle-like structures attached to the tonoplast, which exhibited dynamic fusion with the vacuole (Vedio 1). Whether these structures, characterized as cytoplasmic projections enclosed by a double membrane derived from the tonoplast and extending into the vacuole, remains uncertain as to whether they represent bulbs (Madina et al., 2018; Saito et al., 2002), or artifacts resulting from the tagging of overexpressed PROPEP with dimerizing GFP (Segami et al., 2014), warrants further investigation. Notably, this specific localization has not been previously reported for other PROPEPs. Our hypothesis is that the enrichment of *Ib*PROPEP1 in bulbs serves to store sufficient amounts of the precursor, enabling rapid release upon cellular and vacuolar injury for efficient cleavage into active *Ib*Pep1. The release of a specific agonist of *Ib*LRR-RK1 receptor were found in sweet potato leaves (Figure 11). Incubation of wounded sweet potato leaves for only 10 min resulted in increased levels of the elicitor in a partially purified fraction compared to non-wounded leaves material (Figure 22). Immunoblotting experiments also demonstrated that *Ib*PROPEP1 can be rapidly cleaved

doi:10.6342/NTU202302113

into *Ib*Pep1 upon injury (Figure 23), providing further evidence for our hypothesis that the endogenous peptide *Ib*Pep1 can be released by sweet potato leaves upon injury to initiate defense responses.

_Ib_Pep1 might work in a complementary and/or parallel pathway with _Ib_HypSys to regulate defense responses

SPORAMIN, known for its trypsin inhibitory activity, plays a crucial role in providing robust herbivory protection in sweet potato and other plants species engineered to express *SPORAMIN* (Chen et al., 2006; Meents et al., 2019; Yeh et al., 1997a). The expression of *SPORAMIN* is prominently induced in sweet potato leaves in response to pest attack and injury stress (Yeh et al., 1997b). In a previous study, it was demonstrated that the 18-amino acid hydroxyproline-rich peptide *Ib*HypSysIV possesses the ability to activate *SPORAMIN* expression and enhance the wound signaling cascade. *Ib*HypSysIV as an endogenous peptide ligand can also be extracted from sweet potato leaves (Chen et al., 2008). In our present investigation, we observed that the treatments of either *Ib*Pep1 or *Ib*HypSysIV peptides rapidly initiated the induction of several wound-induced defense-related genes in sweet potato leaves, such as *SPORAMIN*, *IbNAC1*, *IbWIPK1*, and even *IbLRR-RK1* (Figure 24A, B). However, the expression of *SPORAMIN* was significantly more strongly induced by *Ib*HypSysIV treatment compared to *Ib*Pep1

doi:10.6342/NTU202302113

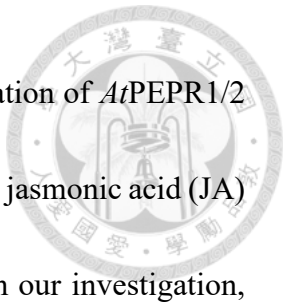

treatment. Previous studies in Arabidopsis have shown that the activation of *At*PEPR1/2 receptors and the application of *At*Peps peptides lead to an elevation in jasmonic acid (JA) levels and the induction of JA-responsive genes (Huffaker, 2015). In our investigation, we observed that the application of *Ib*Pep1 peptide did not result in an increase in JA levels in sweet potato leaves. In the contrast, the application of *Ib*HypSysIV peptide induced a slight accumulation of JA-Ile in sweet potato leaves (Supplementary Figure S4A, B). This finding suggests that *Ib*HypSysIV may activate the jasmonate pathway and its associated responses, while *Ib*Pep1 may not have a direct impact on jasmonate signaling. There is a noticeable contrast between the effects of the two peptides on the regulation of the homoterpene DMNT synthesis and release. DMNT functions as a volatile signal that is triggered in sweet potato upon herbivory attack and wounding (Meents et al., 2019). Only the treatment with *Ib*HypSysIV peptide, and not *Sl*Pep6, *Ib*Pep1, or control scrambled peptide, was able to induce DMNT emission (Supplementary Figure S3). In summary, these results demonstrate that although *Ib*Pep1 and *Ib*HypSysIV can collectively regulate the expression of some wound-related defense genes, each of them independently regulates additional defense mechanisms through distinct pathways. Our results also suggest that in addition to our newly identified *Ib*Pep1/*Ib*LRR-RK1 peptide/receptor pair, there might be another unidentified receptor involved in DAMP recognition in sweet potato, specifically interacting with the

doi:10.6342/NTU202302113

*Ib*HypSysIV ligand. This *Ib*HypSysIV/unknown receptor pair appears to exert a more prominent role than the *Ib*Pep1/*Ib*LRR-RK1 pair in regulating the JA pathway and controlling the expression of *SPORAMIN*. Figure 26 presents a summarized model of both peptide-induced pathways. Although we have demonstrated the ability of both *Ib*Pep1 and *Ib*HypSysIV to regulate defense responses against herbivory and wounding, with varying efficiencies, further research is needed to elucidate the key signaling pathway(s) governed by *Ib*Pep1. Preliminary analyses of RNAseq data revealed that *Ib*Pep1 and *Ib*HypSysIV control partially distinct signaling pathways and responses (Supplementary Figure S5), which should be further explored in combination with actual infestation and infection assays in future studies.

doi:10.6342/NTU202302113

Conclusions and future perspectives

Recent studies have highlighted the involvement of damage-associated molecular pattern (DAMP)-mediated defense activation in sweet potato. Notably, it has been demonstrated that the homoterpene volatile compound, DMNT, possesses the ability to provide defense against insect feeding by eliciting defense mechanisms in sweet potato leaves (Meents et al., 2019; Meents and Mithofer, 2020). Furthermore, previous studies have reported the activation of defense responses in sweet potato through peptide-based mechanisms (Chen et al., 2008). However, the biological significance of these processes and their connection to induced resistance against insects have remained unknown. This investigation aims to establish the presence of a novel Pep/PEPR-like ligand/receptor system in sweet potato and explore its functionality to regulate the defense responses. In summary, our findings demonstrate that *Ib*LRR-RK1 can be activated by an endogenous elicitor, which undergoes amplification in response to damage. We provide indirect evidence suggesting that this elicitor may be *Ib*Pep1, a peptide ligand generated through the cleavage of its precursor protein *Ib*PROPEP1. We also demonstrated that this *Ib*Pep1/*Ib*LRR-RK1 system operates in synergy and in parallel with a *Ib*HypSysIV-dependent signaling pathway.

In previous studies, the widespread presence of Peps/PEPR ligand/receptor systems in plants have been established. In our research, we have identified a novel peptide ligand

doi:10.6342/NTU202302113

*Ib*Pep1 and its corresponding receptor *Ib*LRR-RK1 in sweet potato. Contributing to the expanding ligand/receptor pair to the list of DAMP perception systems. Future investigations should focus on understanding the coordination of downstream signaling pathways or genes, such as MAPK cascades, responses to different ligands within the genetic network. Although the treatment of *Ib*Pep1 did not induce the emission of DMNT in sweet potato, it upregulates the *SPORAMIN* gene and its activator gene *IbNAC1.* And it simultaneously induced other defense responses, suggesting a modular mechanism for enhancing insect resistance. However, further evidence is required to validate the hypothesis of potential enhancement in insect resistance. While Peps exhibit substantial variation among different species, the presence of conserved family-specific residues in Peps are necessary for Pep recognition by PEPRs within the same plant family (Lori et al., 2015). In our experimental observations, we found that the sweet potato receptor kinase *Ib*LRR-RK1, belonging to the Convolvulaceae family, interacted with the tomato peptide ligand *Sl*Pep6, belonging to the Solanaceae family, and initiated downstream defense responses. Remarkably, the reverse combination also showed functionality. To our knowledge, this is the first instance where a peptide ligand deviates from the general rule of family-specific incompatibility among Peps/PEPRs, suggesting the existence of an order-specific incompatibility conserved among Peps/PEPRs in the Solanales plant families Solanaceae and Convolvulaceae.

doi:10.6342/NTU202302113

For future prospects, we can expand our research by exploring the Peps/PEPRs systems in different plants. The compatibility of various plant Peps/PEPRs systems can be verified using the oxidative burst assay system. By analyzing the amino acid sequences of peptide ligands and receptor proteins, we can investigate the crucial amino acid regions involved in the recognition and activation of PEPRs receptors by Peps ligands. This will allow for a deeper understanding of the mechanisms underlying receptor-ligand interactions. By elucidating these mechanisms, we can gain insights into the molecular basis of receptor-ligand recognition and activation in the Peps/PEPRs signaling pathway. On the other hand, although this study has discovered that the *Ib*Pep1 peptide ligand activates *Ib*LRR-RK1, initiating DTI responses in sweet potato and inducing the expression of defense genes related to injury and insect resistance, such as *IbWIPK1*, *IbbHLH3*, *IbNAC1*, and *SPORAMIN*, the mechanism by which *Ib*LRR-RK1 activation leads to the induction of these defense genes remains unknown. In the future, further investigations can be conducted to explore the interactions of *Ib*LRR-RK1 with other proteins and the mechanisms involving phosphorylation cascades to elucidate whether these mechanisms can connect to previously reported pathways such as CDPKs and MAPK cascades, thus linking to downstream PTI responses.

We have initiated the establishment of transgenic plants overexpressing or silencing *Ib*LRR-RK1 and *Ib*PROPEP1, including both Arabidopsis and sweet potato. Through

doi:10.6342/NTU202302113

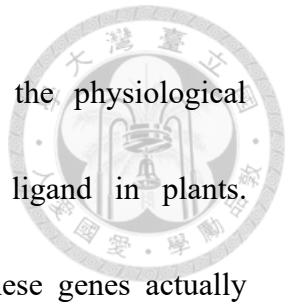

these transgenic plants, we will be able to further investigate the physiological significance of the *Ib*LRR-RK1 receptor and *Ib*Pep1 peptide ligand in plants. Physiological experiments will be conducted to verify whether these genes actually impact plant growth, development, stress tolerance, and insect resistance, providing direct evidence for their involvement in these responses and valuable insights into the functional role of these proteins in sweet potato. Furthermore, we will explore the practical application value of the Pep/PEPR system such as the potential of plant peptide ligands as new biological fertilizers or pesticides.

One limitation of this experiment is the lack of direct analysis of the endogenous *Ib*Pep1 peptide sequence from the extracted solution of sweet potato leaves. In future studies, we will refer methods used in other research to extensively extract sweet potato leaf samples, purify their proteins and peptides, fractionate them using FPLC, and test the ability of different fractions to activate IbLRR-RK1 through oxidative burst assays. Subsequently, LC-MS/MS sequencing will be performed to analyze the peptide ligands present in the extracted solution (Chen et al., 2015). We hope to identify the endogenous *Ib*Pep1 peptide ligands and even discover novel endogenous peptide ligands that can activate IbLRR-RK1 or other receptors. This approach will provide valuable insights into the molecular interactions and signaling pathways involved in the defense response of sweet potato. Another limitation of this experiment is that the identified *Ib*LRR-RK1

doi:10.6342/NTU202302113

receptors cannot recognize *Ib*HypSysIV, indicating that the receptors capable of sensing *Ib*HypSysIV are still remain unknown. Through the RNA-seq database, we have further screened numerous receptors, which contain LRR extracellular domains, and showed significant induction upon injury and treatment with the *Ib*HypSysIV peptide ligand (Data not shown). By cloning and transiently expressing these receptors, we can verify their ability to recognize *Ib*HypSysIV and induce defense responses through experiments such as oxidative burst, ethylene biosynthesis, and defense-related gene expression. Moreover, the RNA-seq database constructed in this experiment has the potential for further exploration. Through in-depth analysis of the database, we can better determine the specific growth, development, stress tolerance, and insect resistance capabilities and pathway regulated by *Ib*Pep1 and *Ib*HypSysIV in sweet potato.

doi:10.6342/NTU202302113

References

Albert, M., Jehle, A.K., Mueller, K., Eisele, C., Lipschis, M., and Felix, G. (2010). *Arabidopsis thaliana* pattern recognition receptors for bacterial elongation factor Tu and flagellin can be combined to form functional chimeric receptors. *Journal of Biological Chemistry,* **285**, 19035-19042.

Asai, T., Tena, G., Plotnikova, J., Willmann, M.R., Chiu, W.L., Gomez-Gomez, L., Boller, T., Ausubel, F.M., and Sheen, J. (2002). MAP kinase signalling cascade in Arabidopsis innate immunity. *Nature,* **415**, 977-983.

Bartels, S., and Boller, T. (2015). Quo vadis, Pep? Plant elicitor peptides at the crossroads of immunity, stress, and development. *Journal of Experimental Botany,* **66**, 5183-5193.

Bartels, S., Lori, M., Mbengue, M., van Verk, M., Klauser, D., Hander, T., Boni, R., Robatzek, S., and Boller, T. (2013). The family of Peps and their precursors in Arabidopsis: differential expression and localization but similar induction of pattern-triggered immune responses. *Journal of Experimental Botany,* **64**, 5309-5321.

Beloshistov, R.E., Dreizler, K., Galiullina, R.A., Tuzhikov, A.I., Serebryakova, M.V., Reichardt, S., Shaw, J., Taliansky, M.E., Pfannstiel, J., Chichkova, N.V., Stintzi, A., Schaller, A., and Vartapetian, A.B. (2018). Phytaspase-mediated precursor processing and maturation of the wound hormone systemin. *New Phytologist,* **218**, 1167-1178.

Binder, A., Lambert, J., Morbitzer, R., Popp, C., Ott, T., Lahaye, T., and Parniske, M. (2014). A modular plasmid assembly kit for multigene expression, gene silencing and silencing rescue in plants. *Plos One,* **9**, e88218.

Boehm, H., Albert, I., Fan, L., Reinhard, A., and Nuernberger, T. (2014). Immune receptor complexes at the plant cell surface. *Current Opinion in Plant Biology,* **20**,

doi:10.6342/NTU202302113

47-54.

Boller, T., and Felix, G. (2009). A renaissance of elicitors: perception of microbe-associated molecular patterns and danger signals by pattern-recognition receptors. *Annual Review of Plant Biology,* **60**, 379-406.

Brutus, A., Sicilia, F., Macone, A., Cervone, F., and De Lorenzo, G. (2010). A domain swap approach reveals a role of the plant wall-associated kinase 1 (WAK1) as a receptor of oligogalacturonides. *Proceedings of the National Academy of Sciences of the United States of America,* **107,** 9452-9457.

Butenko, M.A., Wildhagen, M., Albert, M., Jehle, A., Kalbacher, H., Aalen, R.B., and Felix, G. (2014). Tools and strategies to match peptide-ligand receptor pairs. *Plant Cell,* **26**, 1838-1847.

Cederholm, H.M., and Benfey, P.N. (2015). Distinct sensitivities to phosphate deprivation suggest that RGF peptides play disparate roles in *Arabidopsis thaliana* root development. *New Phytologist,* **207,** 683-691.

Chen, H.J., Wang, S.J., Chen, C.C., and Yeh, K.W. (2006). New gene construction strategy in T-DNA vector to enhance expression level of sweet potato *sporamin* and insect resistance in transgenic *Brassica oleracea*. *Plant Science,* **171**, 367-374.

Chen, S.P., Kuo, C.H., Lu, H.H., Lo, H.S., and Yeh, K.W. (2016a). The sweet potato NAC-Domain transcription factor *Ib*NAC1 is dynamically coordinated by the activator *Ib*bHLH3 and the repressor *Ib*bHLH4 to reprogram the defense mechanism against wounding. *Plos Genetics,* **12**, e1006397.

Chen, S.P., Lin, I.W., Chen, X.Y., Huang, Y.H., Chang, S.C., Lo, H.S., Lu, H.H., and Yeh, K.W. (2016b). Sweet potato NAC transcription factor, *Ib*NAC1, upregulates sporamin gene expression by binding the SWRE motif against mechanical wounding and herbivore attack. *Plant Journal,* **86**, 234-248.

doi:10.6342/NTU202302113

Chen, Y.C., Siems, W.F., Pearce, G., and Ryan, C.A. (2008). Six peptide wound signals derived from a single precursor protein in *Ipomoea batatas* leaves activate the expression of the defense gene sporamin. *Journal of Biological Chemistry,* **283**, 11469-11476.

Chen, Y.L., Lee, C.Y., Cheng, K.T., Chang, W.H., Huang, R.N., Nam, H.G., and Chen, Y. R. (2014). Quantitative peptidomics study reveals that a wound-induced peptide from PR-1 regulates immune signaling in tomato. *Plant Cell,* **26,** 4135-4148.

Chen, Y.L., Fan, K.T., Hung, S.C., and Chen, Y.R. (2020). The role of peptides cleaved from protein precursors in eliciting plant stress reactions. *New Phytologist,* **225**, 2267-2282.

Chien, P.S., Nam, H.G., and Chen, Y.R. (2015). A salt-regulated peptide derived from the CAP superfamily protein negatively regulates salt-stress tolerance in Arabidopsis. *Journal of Experimental Botany,* **66**, 5301-5313.

Chinchilla, D., Bauer, Z., Regenass, M., Boller, T., and Felix, G. (2006). The Arabidopsis receptor kinase FLS2 binds flg22 and determines the specificity of flagellin perception. *Plant Cell,* **18**, 465-476.

Choi, J., Tanaka, K., Cao, Y., Qi, Y., Qiu, J., Liang, Y., Lee, S.Y., and Stacey, G. (2014). Identification of a plant receptor for extracellular ATP. *Science*, **343,** 290-294.

Costa, L.M., Marshall, E., Tesfaye, M., Silverstein, K.A.T., Mori, M., Umetsu, Y., Otterbach, S.L., Papareddy, R., Dickinson, H.G., Boutiller, K., VandenBosch, K.A., Ohki, S., and Gutierrez-Marcos, J.F. (2014). Central cell-derived peptides regulate early embryo patterning in flowering plants. *Science*, **344,** 168-172.

Curtis, M.D., and Grossniklaus, U. (2003). A gateway cloning vector set for high-throughput functional analysis of genes in planta. *Plant Physiology,* **133**, 462-469.

doi:10.6342/NTU202302113

Grienenberger, E., and Fletcher, J.C. (2015). Polypeptide signaling molecules in plant development. *Current Opinion in Plant Biology,* **23,** 8-14.

Hander, T., Fernandez-Fernandez, A.D., Kumpf, R.P., Willems, P., Schatowitz, H., Rombaut, D., Staes, A., Nolf, J., Pottie, R., Yao, P.F., Goncalves, A., Pavie, B., Boller, T., Gevaert, K., Van Breusegem, F., Bartels, S., and Stael, S. (2019). Damage on plants activates Ca^{2+}-dependent metacaspases for release of immunomodulatory peptides. *Science,* **363**, eaar7486.

Huffaker, A. (2015). Plant elicitor peptides in induced defense against insects. *Current Research in Insect Science,* **9**, 44-50.

Huffaker, A., Pearce, G., and Ryan, C.A. (2006). An endogenous peptide signal in Arabidopsis activates components of the innate immune response. *Proceedings of the National Academy of Sciences of the United States of America,* **103**, 10098-10103.

Huffaker, A., Pearce, G., Veyrat, N., Erb, M., Turlings, T.C., Sartor, R., Shen, Z., Briggs, S.P., Vaughan, M.M., Alborn, H.T., Teal, P.E., and Schmelz, E.A. (2013). Plant elicitor peptides are conserved signals regulating direct and indirect antiherbivore defense. *Proceedings of the National Academy of Sciences of the United States of America,* **110**, 5707-5712.

Iizasa, E., Mitsutomi, M., and Nagano, Y. (2010). Direct binding of a plant LysM receptor-like kinase, LysM RLK1/CERK1, to chitin in vitro. *Journal of Biological Chemistry,* **285,** 2996-3004.

Imanishi, S., KitoNakamura, K., Matsuoka, K., Morikami, A., and Nakamura, K. (1997). A major jasmonate-inducible protein of sweet potato, ipomoelin, is an ABA-independent wound-inducible protein. *Plant and Cell Physiology,* **38**, 643-652.

Kim, J.S., Jeon, B.W., and Kim, J. (2021). Signaling Peptides Regulating Abiotic Stress

doi:10.6342/NTU202302113

Responses in Plants. *Frontiers in Plant Science*, **12**.

Klauser, D., Desurmont, G.A., Glauser, G., Vallat, A., Flury, P., Boller, T., Turlings, T.C.J., and Bartels, S. (2015). The Arabidopsis Pep-PEPR system is induced by herbivore feeding and contributes to JA-mediated plant defence against herbivory. *Journal of Experimental Botany,* **66**, 5327-5336.

Krol, E., Mentzel, T., Chinchilla, D., Boller, T., Felix, G., Kemmerling, B., Postel, S., Arents, M., Jeworutzki, E., Al-Rasheid, K.A.S., Becker, D., and Hedrich, R. (2010). Perception of the Arabidopsis danger signal peptide 1 involves the pattern recognition receptor *At*PEPR1 and its close homologue *At*PEPR2. *Journal of Biological Chemistry,* **285**, 13471-13479.

Kunert, M., David, A., Becher, J., and Boland, W. (2009). Volatile sampling from biological sources by the closed-loop-stripping technique. *Cold Spring Harbor Protocols,* **2009**, pdb.prot5233.

Li, Y.C., Wan, W.L., Lin, J.S., Kuo, Y.W., King, Y.C., Chen, Y.C., and Jeng, S.T. (2016). Signal transduction and regulation of *Ib*preproHypSys in sweet potato. *Plant Cell and Environment,* **39**, 1576-1587.

Liu, P. L., Du, L., Huang, Y., Gao, S. M., and Yu, M. (2017). Origin and diversification of leucine-rich repeat receptor-like protein kinase (LRR-RLK) genes in plants. *BMC Evolutionary Biology*, **17**, 47.

Lori, M., van Verk, M.C., Hander, T., Schatowitz, H., Klauser, D., Flury, P., Gehring, C.A., Boller, T., and Bartels, S. (2015). Evolutionary divergence of the plant elicitor peptides (Peps) and their receptors: interfamily incompatibility of perception but compatibility of downstream signalling. *Journal of Experimental Botany,* **66**, 5315-5325.

Ma, D., Endo, S., Betsuyaku, S., Shimotohno, A., and Fukuda, H. (2020). CLE2 regulates light-dependent carbohydrate metabolism in Arabidopsis shoots. *Plant*

doi:10.6342/NTU202302113

Molecular Biology, **104,** 561-574.

Madina, M.H., Zheng, H.Q., and Germain, H. (2018). New insight into bulb dynamics in the vacuolar lumen of Arabidopsis cells. *Botany,* **96**, 511-520.

Meents, A.K., and Mithofer, A. (2020). Plant-plant communication: is there a role for volatile damage-associated molecular patterns? *Frontiers in Plant Science,* **11**, 583275.

Meents, A.K., Chen, S.P., Reichelt, M., Lu, H.H., Bartram, S., Yeh, K.W., and Mithofer, A. (2019). Volatile DMNT systemically induces jasmonate-independent direct anti-herbivore defense in leaves of sweet potato (*Ipomoea batatas*) plants. *Scientific Reports,* **9**, 17431.

Murphy, E., and De Smet, I. (2014). Understanding the RALF family: a tale of many species. *Trends in Plant Science*, **19**, 664-671.

Narvaez-Vasquez, J., Pearce, G., and Ryan, C.A. (2005). The plant cell wall matrix harbors a precursor of defense signaling peptides. *Proceedings of the National Academy of Sciences of the United States of America,* **102**, 12974-12977.

Nelson, B.K., Cai, X., and Nebenfuhr, A. (2007). A multicolored set of in *vivo* organelle markers for co-localization studies in Arabidopsis and other plants. *Plant Journal,* **51**, 1126-1136.

Orozcocardenas, M., Mcgurl, B., and Ryan, C.A. (1993). Expression of an antisense prosystemin gene in tomato plants reduces resistance toward *Manduca Sexta* larvae. *Proceedings of the National Academy of Sciences of the United States of America,* **90**, 8273-8276.

Patharkar, O.R., and Walker, J.C. (2016). Core Mechanisms Regulating Developmentally Timed and Environmentally Triggered Abscission. *Plant Physiology,* **172,** 510-520.

Pearce, G. (2011). Systemin, hydroxyproline-rich systemin and the induction of protease

doi:10.6342/NTU202302113

Inhibitors. *Current Protein and Peptide Science,* **12**, 399-408.

Pearce, G., Strydom, D., Johnson, S., and Ryan, C.A. (1991). A polypeptide from tomato leaves induces wound-inducible proteinase-inhibitor proteins. *Science,* **253**, 895-898.

Pearce, G., Siems, W.F., Bhattacharya, R., Chen, Y.C., and Ryan, C.A. (2007). Three hydroxyproline-rich glycopeptides derived from a single petunia polyprotein precursor activate defensin I, a pathogen defense response gene. *Journal of Biological Chemistry,* **282**, 17777-17784.

Rajendran, S., Lin, I.W., Chen, M.J., Chen, C.Y., and Yeh, K.W. (2014). Differential activation of sporamin expression in response to abiotic mechanical wounding and biotic herbivore attack in the sweet potato. *BMC Plant Biology,* **14**, 112.

Ron, M., and Avni, A. (2004). The receptor for the fungal elicitor ethylene-inducing xylanase is a member of a resistance-like gene family in tomato. *Plant Cell,* **16**, 1604-1615.

Ross, A., Yamada, K., Hiruma, K., Yamashita-Yamada, M., Lu, X.L., Takano, Y., Tsuda, K., and Saijo, Y. (2014). The Arabidopsis PEPR pathway couples local and systemic plant immunity. *Embo Journal,* **33**, 62-75.

Saito, C., Ueda, T., Abe, H., Wada, Y., Kuroiwa, T., Hisada, A., Furuya, M., and Nakano, A. (2002). A complex and mobile structure forms a distinct subregion within the continuous vacuolar membrane in young cotyledons of Arabidopsis. *Plant Journal,* **29**, 245-255.

Schmelz, E.A., Carroll, M.J., LeClere, S., Phipps, S.M., Meredith, J., Chourey, P.S., Alborn, H.T., and Teal, P.E.A. (2006). Fragments of ATP synthase mediate plant perception of insect attack. *Proceedings of the National Academy of Sciences of the United States of America,* **103,** 8894-8899.

Segami, S., Makino, S., Miyake, A., Asaoka, M., and Maeshima, M. (2014). Dynamics

doi:10.6342/NTU202302113

of vacuoles and H^+-Pyrophosphatase visualized by monomeric green fluorescent protein in Arabidopsis: artifactual bulbs and native intravacuolar spherical structures. *Plant Cell ,* **26**, 3416-3434.

Sher Khan, R., Iqbal, A., Malak, R., Shehryar, K., Attia, S., Ahmed, T., Ali Khan, M., Arif, M., and Mii, M. (2019). Plant defensins: types, mechanism of action and prospects of genetic engineering for enhanced disease resistance in plants. *3 Biotech*, **9,** 192.

Shimizu, T., Nakano, T., Takamizawa, D., Desaki, Y., Ishii-Minami, N., Nishizawa, Y., Minami, E., Okada, K., Yamane, H., Kaku, H., and Shibuya, N. (2010). Two LysM receptor molecules, CEBiP and *Os*CERK1, cooperatively regulate chitin elicitor signaling in rice. *Plant Journal,* **64,** 204-214.

Tabata, R., Sumida, K., Yoshii, T., Ohyama, K., Shinohara, H., and Matsubayashi, Y. (2014). Perception of root-derived peptides by shoot LRR-RKs mediates systemic N-demand signaling. *Science*, **346,** 343-346.

Takahashi, F., Suzuki, T., Osakabe, Y., Betsuyaku, S., Kondo, Y., Dohmae, N., Fukuda, H., Yamaguchi-Shinozaki, K., and Shinozaki, K. (2018). A small peptide modulates stomatal control via abscisic acid in long-distance signalling. *Nature*, **556,** 235-238.

Tang, J., Han, Z., Sun, Y., Zhang, H., Gong, X., and Chai, J. (2015). Structural basis for recognition of an endogenous peptide by the plant receptor kinase PEPR1. *Cell Research*, **25,** 110-120.

Tavormina, P., De Coninck, B., Nikonorova, N., De Smet, I., and Cammue, B.P.A. (2015). The Plant Peptidome: An Expanding Repertoire of Structural Features and Biological Functions. *Plant Cell*, **27,** 2095-2118.

Thuerig, B., Felix, G., Binder, A., Boller, T., and Tamm, L. (2005). An extract of *Penicillium chrysogenum* elicits early defense-related responses and induces

doi:10.6342/NTU202302113

resistance in *Arabidopsis thaliana* independently of known signalling pathways. *Physiological and Molecular Plant Pathology,* **67**, 180-193.

Wang, L., Albert, M., Einig, E., Furst, U., Krust, D., and Felix, G. (2016). The pattern-recognition receptor CORE of Solanaceae detects bacterial cold-shock protein. *Nature Plants,* **2**, 16185.

Wang, L., Einig, E., Almeida-Trapp, M., Albert, M., Fliegmann, J., Mithofer, A., Kalbacher, H., and Felix, G. (2018). The systemin receptor SYR1 enhances resistance of tomato against herbivorous insects. *Nature Plants,* **4**, 152-156.

Xie, H., Zhao, W., Li, W., Zhang, Y., Hajný, J., and Han, H. (2022). Small signaling peptides mediate plant adaptions to abiotic environmental stress. *Planta,* **255,** 72.

Yamaguchi, Y., Huffaker, A., Bryan, A.C., Tax, F.E., and Ryan, C.A. (2010). PEPR2 is a second receptor for the Pep1 and Pep2 peptides and contributes to defense responses in Arabidopsis. *Plant Cell,* **22**, 508-522.

Yamaguchi, Y.L., Ishida, T., and Sawa, S. (2016). CLE peptides and their signaling pathways in plant development. *Journal of Experimental Botany,* **67,** 4813-4826.

Yeh, K.W., Chen, J.C., Lin, M.I., Chen, Y.M., and Lin, C.Y. (1997a). Functional activity of sporamin from sweet potato (*Ipomoea batatas* Lam): A tuber storage protein with trypsin inhibitory activity. *Plant Molecular Biology,* **33**, 565-570.

Yeh, K.W., Lin, M.I., Tuan, S.J., Chen, Y.M., Lin, C.Y., and Kao, S.S. (1997b). Sweet potato (*Ipomoea batatas*) trypsin inhibitors expressed in transgenic tobacco plants confer resistance against *Spodoptera litura*. *Plant Cell Reports,* **16**, 696-699.

Yoo, S.D., Cho, Y.H., and Sheen, J. (2007). Arabidopsis mesophyll protoplasts: a versatile cell system for transient gene expression analysis. *Nature Protocols,* **2**, 1565-1572.

Zhao, C., Zayed, O., Yu, Z., Jiang, W., Zhu, P., Hsu, C.-C., Zhang, L., Tao, W.A., Lozano-Durán, R., and Zhu, J.-K. (2018). Leucine-rich repeat extensin proteins

doi:10.6342/NTU202302113

regulate plant salt tolerance in Arabidopsis. *Proceedings of the National Academy of Sciences of the United States of America,* **115,** 13123-13128.

Zipfel, C., Kunze, G., Chinchilla, D., Caniard, A., Jones, J.D.G., Boller, T., and Felix, G. (2006). Perception of the bacterial PAMP EF-Tu by the receptor EFR restricts Agrobacterium-mediated transformation. *Cell,* **125**, 749-760.

doi:10.6342/NTU202302113

Tables

Table 1. List of peptides used for signaling activity experiments.

Name	Sequence
elf18	ac-SKEKFERTKPHVNVGTIG
systemin	AVQSKPPSKRDPPKMQTD
IbHypSysIV	REEKPOOOAOETDDPNRP
C-IbHypSysIV	CREEKPOOOAOETDDPNRP
IbPepI	LSSRPPRPGLGNSGDPQTNDTSS
SlPep6	ATDRRGRPPSRPKVGSGPPPQNN
SlHypSysIII	GRHDSVLPPPSPKTD
AtPep1	ATKVKAKQRGKEKVSSGRPGQHN
Scramble peptide	PEROEDDNEOPKORPC

O: hydroxyproline

doi:10.6342/NTU202302113

Table 2. List of oligonucleotides used for this study.

Primer Name	Sequence (5' to 3')	Amplification of
*Ib*LRR-RK1_RT_F	TGGCCCATTTCCTGAGTCTTTAC	real-time PCR
*Ib*LRR-RK1_RT_R	GACAGGCAAGGTTCCAACAAGATT	
*Ib*LRR-RK2_RT_F	GATATGGTTTACAAGGTACGCTCG	
*Ib*LRR-RK2_RT_R	CTGTGGCGAAGATACAACCCTTT	
*Ib*LRR-RK3_RT_F	ACTTTCAGGCCACATCCCTC	
*Ib*LRR-RK3_RT_R	GTGGCCTGAAAGTTGGTTATTGAG	
*Ib*LRR-RK4_RT_F	ACAGCCTTAATGGGTCAATTCC	
*Ib*LRR-RK4_RT_R	CCAGACAAGTCTAAGCTCTGAAGA	
*Ib*LRR-RK5_RT_F	GCATTGTGGGTAGTGTTCCATCC	
*Ib*LRR-RK5_RT_R	CACCTGCCCTGAGAACCTCAA	
*Ib*Actin_RT_F	GACTACCATGTTCCCCGGTA	
*Ib*Actin_RT_R	TTGTATGCCACGAGCATCTT	
SPORAMIN _RT_F	ATGTCCAAATGCGCCAGCG	
SPORAMIN _RT_R	TTTCAGGAAATACTGCCCGGA	
*Ib*WIPK_RT_F	ACATCACCATGGTGGGCG	
*Ib*WIPK_RT_R	CGTTCAAAGCCGAACAGACGATT	
*Ib*NAC1_RT_F	CGGCCGGGGATACAAATTTGTAAGCTT	
*Ib*NAC1_RT_R	GAATCGGAATCCCGGCGGCATCTC	
*Ib*CML_RT_F	AAGTGGAGAAGGTGTTCAGGAAG	
*Ib*CML_RT_R	CCTTGTCCTCAGAGTCGGATC	
*Ib*PROPEP1_FL_F	ATGGAGAAGGGTGGAGAGGA	*Ib*PROPEP1 CDS
*Ib*PROPEP1_FL_R	TTAAGAAGAGGTGTCGTTAGTCTGA	
*Ib*LRR-RK1_FL_F	ATGAAGGTTGCTGTGATCACATTCT	*Ib*LRR-RK CDS
*Ib*LRR-RK1_FL_R	CTACTTAGACTTGTTTCTAACACTCGA	

doi:10.6342/NTU202302113

*Sl*PEPR_FL_F	ATGAAGATAGCTGTTCATAATTTGATCT	*Sl*PEPR CDS
*Sl*PEPR_FL_R	CTAGTACTTGCTTCGTATACTCGAA	
B-5*_*Ib*RK1_fw	tatggtctcaTCTGaacaATGAAGCTTGCTGTGAACATATTC	*Ib*LRR-RK ectodomain (for GoldenGate)
B-5*_*Ib*RK1_rev	ttaggtctcCCgATAACATACTTATCATTTAGGTTC	
5*-D_*Ib*RK1_fw	ataggtctcTATcGGGAAGGGAGCACATG	*Ib*LRR-RK kinase (for GoldenGate)
5*-D_*Ib*RK1_rev	attggtctcTcCTTAGATTTGTTTCTAACACTCGAG	
B-5*_SYR1_fw	atggtctcATctgaacaATGTTCTTGTTTGATGTTGTTCAT	SYR1 ectodomain (for GoldenGate)
B-5*_SYR1_rev	tatggTCTcCCgATAACATAGTTTTCACTCCAGC	
NptII_F	GAGAAAGTATCCATCATGGCTGATG	Transgenic plants
NptII-R	GTAGCCAACGCTATGTCCTGATAG	

doi:10.6342/NTU202302113

Table 3. Comparison of the full-length amino acid sequence of *Ib*LRR-RK1 with related sequences, calculation of % identity by Vector NTI.

	*It*LRR-RLK1	*Sl*PEPR1	*At*PEPR1	*At*PEPR2	*Sl*SYR1	*Sl*SYR2
*Ib*LRR-RK1	97	65	50	49	36	35
*It*LRR-RK1		64	50	49	36	35
*Sl*PEPR1			51	48	35	35
*At*PEPR1				66	36	34
*At*PEPR2					36	35
*Sl*SYR1						79

At, Arabidopsis thaliana; Ib, Ipomoea batatas; It, Ipomoea trifida; Sl, Solanum lycopersicum.

doi:10.6342/NTU202302113

Table 4. Comparison of the amino acid sequence of the extracellular domain of *Ib*LRR-RK1 with *At*PEPR1, *Sl*PEPR1, and *Sl*SYR1, calculation of % identity by Vector NTI.

	*Sl*PEPR1	*At*PEPR1	*Sl*SYR1
*Ib*LRR-RK1	60	48	36
*Sl*PEPR1		49	36
*At*PEPR1			36

At, Arabidopsis thaliana; Ib, Ipomoea batatas; Sl, Solanum lycopersicum.

doi:10.6342/NTU202302113

Table 5. Identity table of *Ib*Pep1 and other Peps by Vector NTI.

	*At*Pep1	*At*Pep2	*At*Pep8	*At*Pep6	***Ib*Pep1**	*Nb*Pep6	*Ns*Pep6	*Nt*Pep6	*Sl*Pep6	*St*Pep1	*Sm*Pep1	*At*Pep3	*At*Pep5	*At*Pep4	*At*Pep7
*At*Pep1		65	43	43	**10**	30	30	30	39	39	35	39	39	35	35
*At*Pep2			52	35	**21**	22	22	22	26	26	26	43	30	39	30
*At*Pep8				30	**16**	22	22	22	22	22	17	35	35	39	26
*At*Pep6					**32**	39	39	39	43	43	48	26	39	26	26
***Ib*Pep1**						**42**	**42**	**42**	**37**	**37**	**37**	**10**	**5**	**10**	**16**
*Nb*Pep6							100	100	65	65	65	26	17	17	13
*Ns*Pep6								100	65	65	65	26	17	17	13
*Nt*Pep6									65	65	65	26	17	17	13
*Sl*Pep6										96	74	26	17	17	13
*St*Pep1											74	26	17	17	13
*Sm*Pep1												30	22	22	17
*At*Pep3													35	30	39
*At*Pep5														39	39
*At*Pep4															39
*At*Pep7															

At, Arabidopsis thaliana; Ib, Ipomoea batatas; Nb, Nicotiana benthamiana; Ns, Nicotiana sylvestris; Nt, Nicotiana tomentosiformis; Sl, Solanum lycopersicum; Sm; Solanum melongena; St, Solanum tuberosum.

doi:10.6342/NTU202302113

Figures

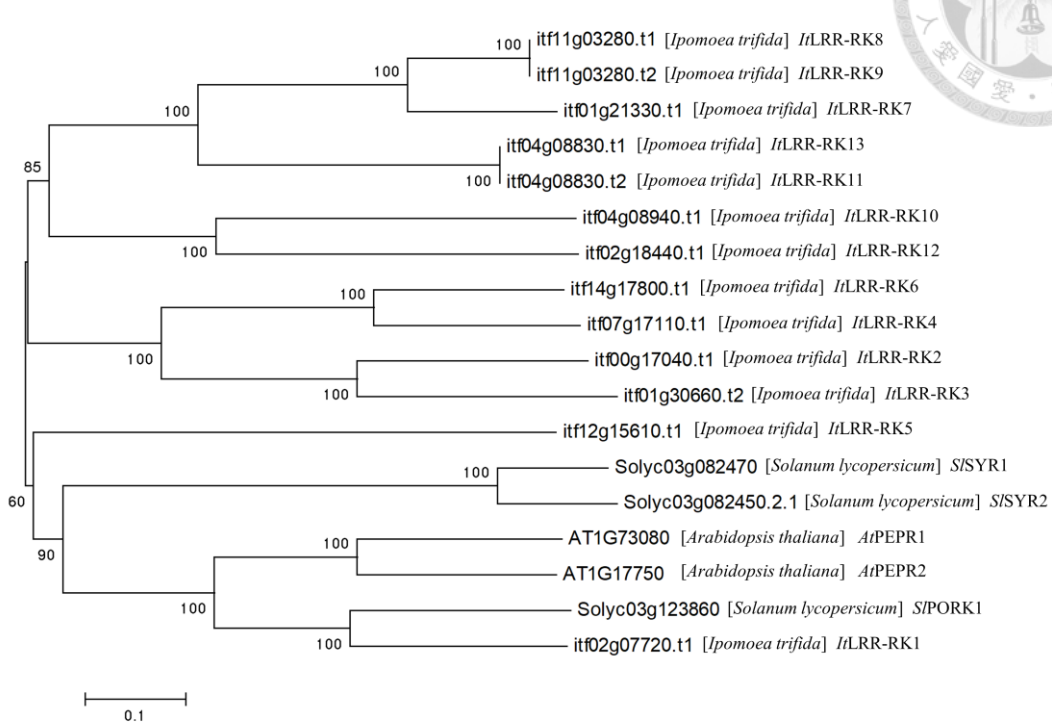

Figure 1. Phylogenetic tree of *Ipomoea trifida* receptor-like kinases. A phylogenetic tree was constructed using a Neighbor-Joining method (1000 bootstrap replicates), depicting the evolutionary relationships among receptor-like genes from *Ipomoea trifida*. The gene sequences used for this analysis were obtained through BLASTx searches, employing *At*PEPR1/2 and *Sl*SYR1/2 sequences as queries against the *Ipomoea trifida* database (http://sweetpotato.plantbiology.msu.edu/index.shtml). The tree provides insights into the genetic homologies and potential functional similarities of these receptor-like genes in *Ipomoea trifida*.

doi:10.6342/NTU202302113

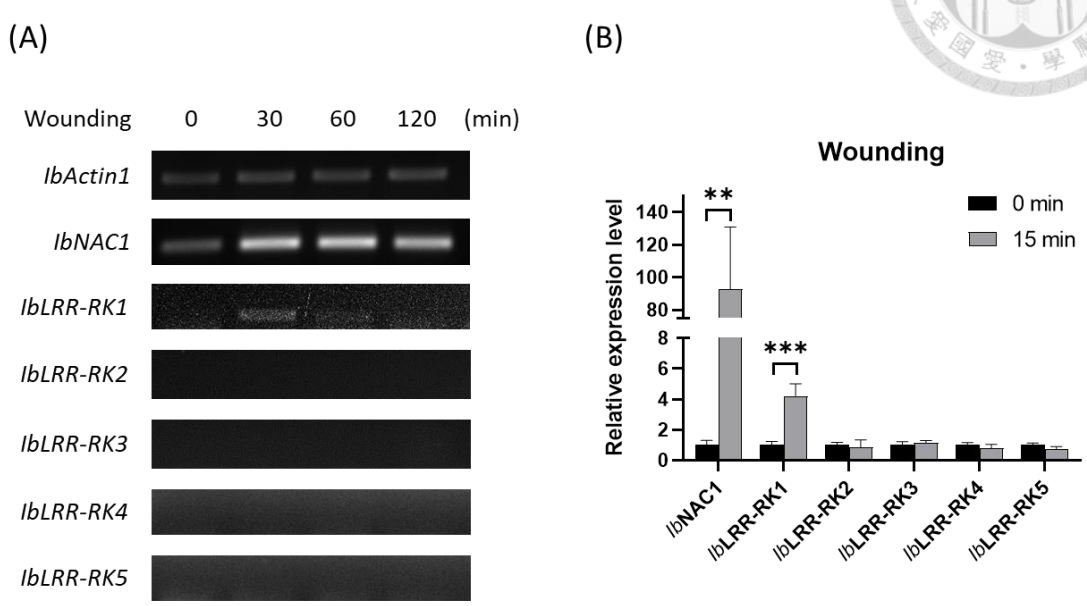

Figure 2. Expression levels of *IbLRR-RKs* in response to wound treatments. The expression level of *IbLRR-RK1* to *IbLRR-RK5* receptor-like genes in sweet potato leaves upon wounding stress. The mRNA levels of these genes were quantified using **(A)** RT-PCR and **(B)** quantitative RT-PCR, with *Ib*Actin1 serving as the internal control for normalization. The expression of *Ib*NAC1, a known marker of wounding response in sweet potato leaves, was used as a positive control. The bar graph represents the mean expression level, and the error bars indicate the standard deviation (n = 4), indicating the reproducibility of the results in Figure 2B.

doi:10.6342/NTU202302113

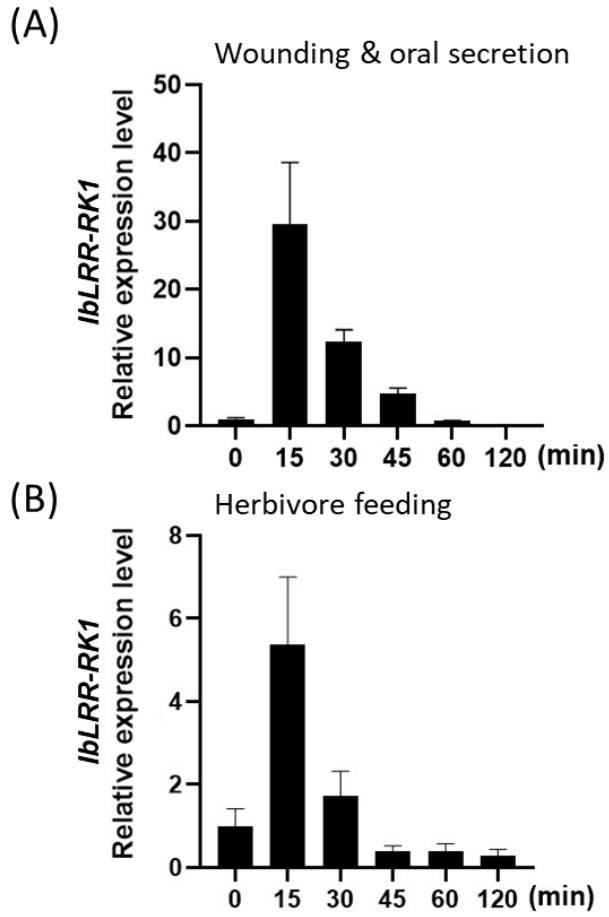

Figure 3. Expression levels of *IbLRR-RK1* in response to herbivory attack. Sweet potato leaves were **(A)** subjected to mechanical injury by wounding and treated with oral secretions of *Spodoptera litura* larvae, or **(B)** directly exposed to feeding *S. litura* larvae. The expression of *IbLRR-RK1* was analyzed using quantitative RT-PCR. The bar graph displays the mean expression level of IbLRR-RK1, and the error bars indicate the standard deviation (n = 4), reflecting the variability in the results.

doi:10.6342/NTU202302113

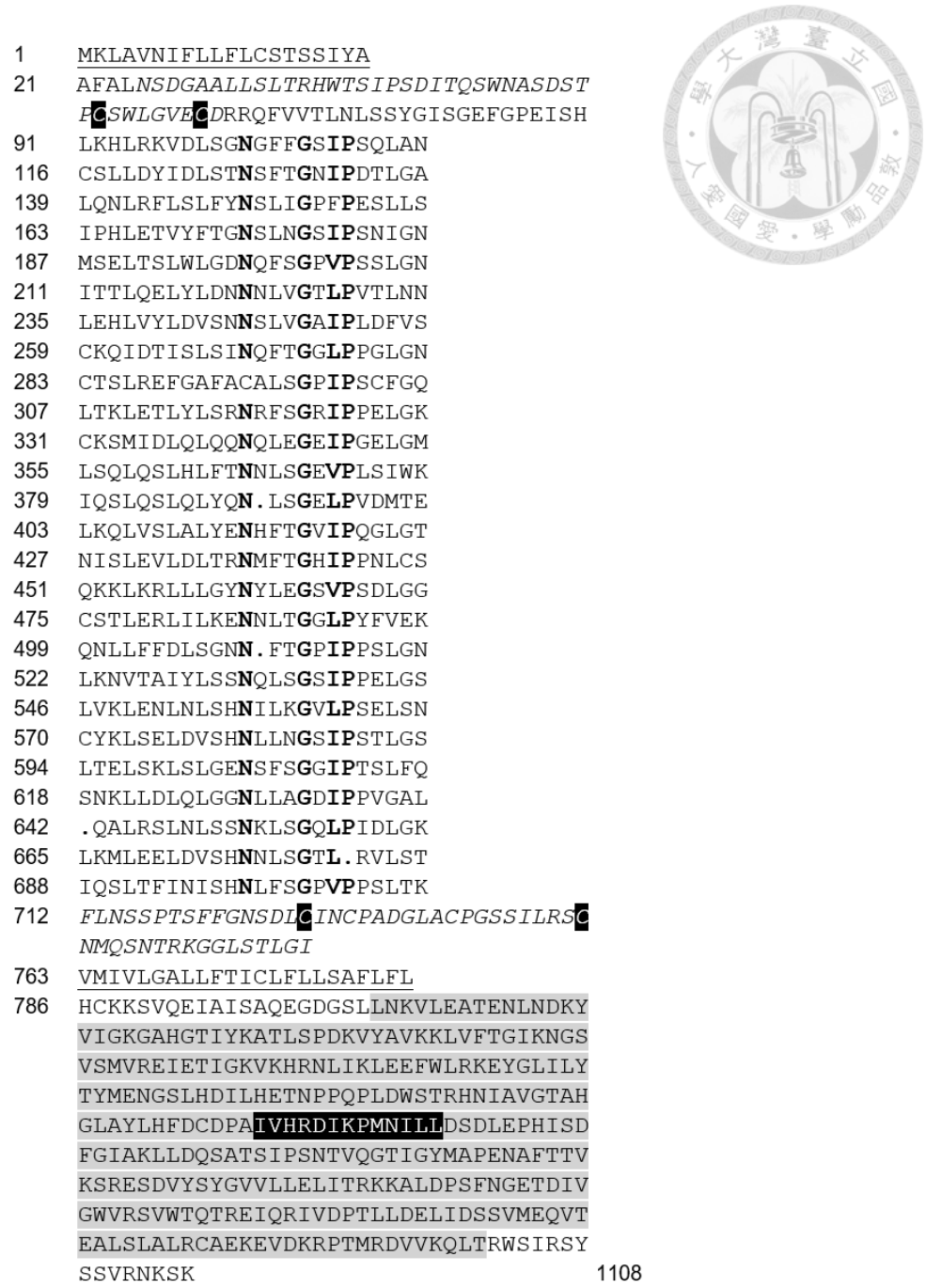

Figure 4. Primary structure of the *Ib*LRR-RK1 receptor kinase from sweet potato. The primary structure of IbLRR-RK1, a leucine-rich repeat receptor kinase from sweet potato, is depicted in the figure. The coding sequence of IbLRR-RK1 consists of various functional domains and regions. It begins with a signal peptide (amino acids 1-20, underlined). The N-terminal cap region (italic) encompasses two conserved cysteine residues (white on black) embedded within the N-terminus (amino acids 21-90).

doi:10.6342/NTU202302113

Following this, there are 26 repetitions of the leucine-rich repeat (LRR) motif (amino acids 91-711). The LRR motif contains highly conserved residues indicated in bold, according to the consensus sequence of plant LRRs (Liu et al., 2017). Gaps (dots) are introduced to optimize alignment during sequence comparison. The outer juxtamembrane region (amino acids 712-762) also harbors two conserved cysteine residues (white on black). This is followed by a transmembrane domain (amino acids 763-785, underlined), which anchors the protein to the cell membrane. Finally, the cytoplasmic domain (amino acids 786-1108) contains a serine/threonine kinase domain (shaded light gray) with a conserved active site (shaded in black), indicating its potential role in kinase activity and downstream signaling.

doi:10.6342/NTU202302113

(A)

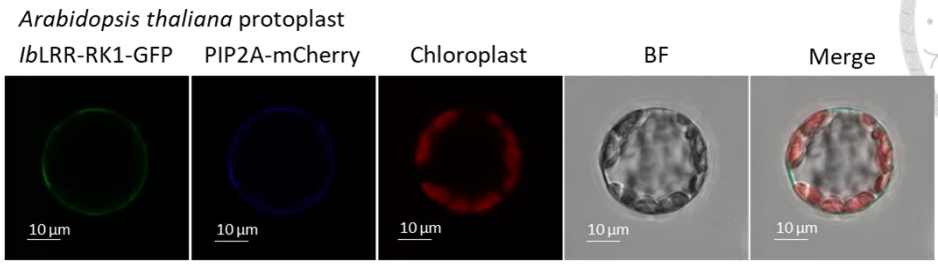

(B)

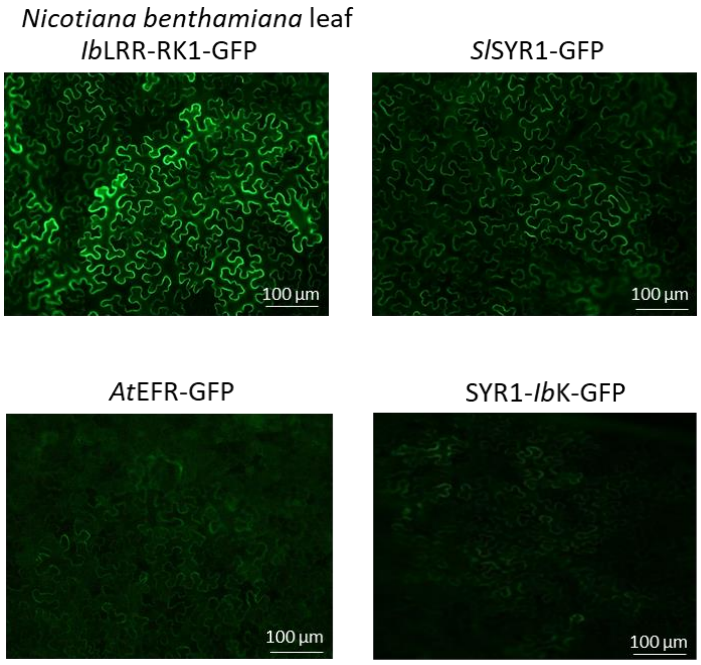

Figure 5. Chimeric receptors localized on the cell membrane. Cell membrane localization of GFP-tagged *Ib*LRR-RK1 and SYR1-*Ib*K was examined by confocal microscope (TCS SP5 Confocal, Leica) in transiently transformed **(A)** protoplasts of *A. thaliana* or **(B)** leaf samples of *N. benthamiana* (Collaborated with Prof. Georg Felix 's lab). To confirm the plasma membrane localization, PIP2A (plasma membrane-intrinsic protein 2A) and well-characterized plasma membrane-localized receptor proteins, such as SYR1 from tomato and EFR from *A. thaliana* (Wang et al., 2018; Zipfel et al., 2006), were used as positive controls in *Arabidopsis thaliana* and *Nicotiana benthamiana*, respectively.

doi:10.6342/NTU202302113

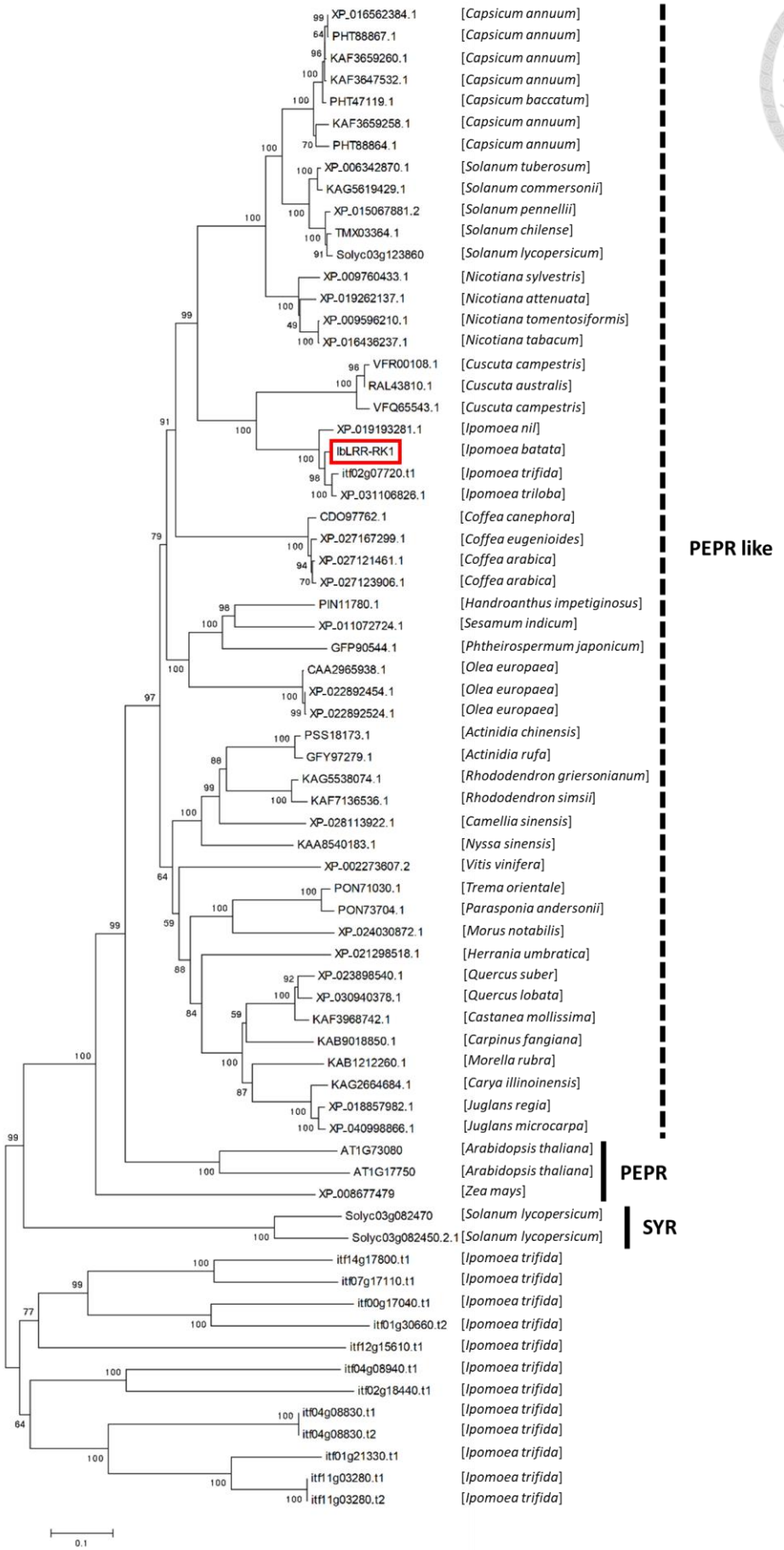

doi:10.6342/NTU202302113

Figure 6. Phylogenetic tree established with *Ib*LRR-RK1-related receptors in different plant species. A phylogenetic tree was constructed using the Neighbor-joining method (1000 bootstrap replicates), based on sequences homologous to *Ib*LRR-RK1 from various plant species. These sequences were obtained through BLASTx searches using IbLRR-RK1 as a query against public databases such as PubMed, NCBI, and the Sweet Potato Genomics Resource database.

doi:10.6342/NTU202302113

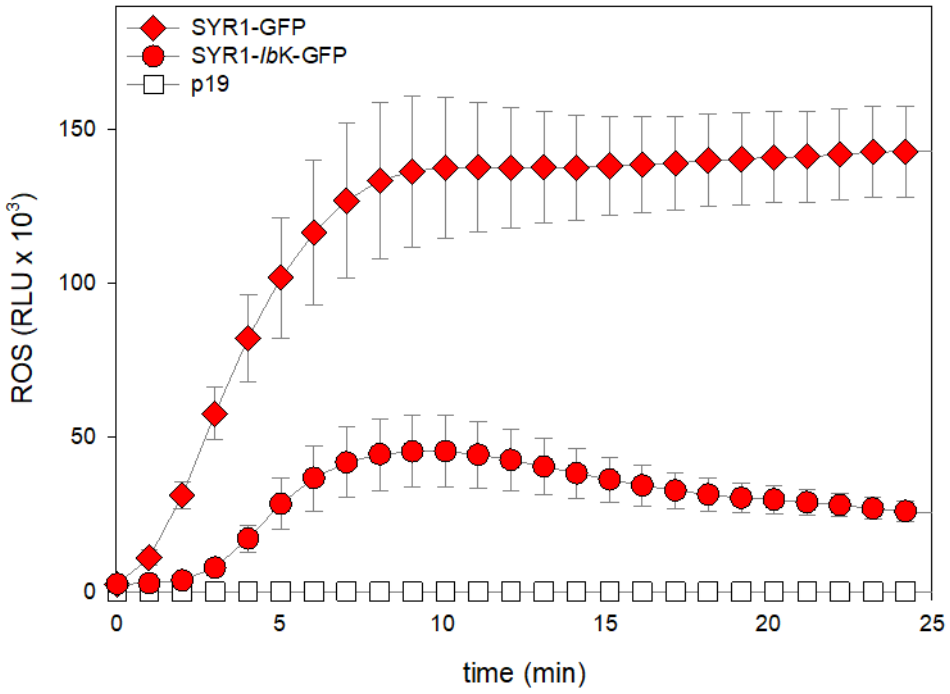

Figure 7. The oxidative burst assays demonstrated the kinase activity of *Ib*LRR-RK1. Transiently expressing the chimeric receptors (SYR1-*Ib*K) in combination of kinase domain of *Ib*LRR-RK1 with the ectodomain of SYR1. Reactive oxygen species (ROS) were induced in the leaf discs when treated with 10 nM systemin (represented by red circles), similar to the response observed with SYR1 (represented by red diamonds). In contrast, control leaf samples expressing only p19 did not exhibit a ROS burst upon systemin treatment (represented by open squares). The data presented here represent the mean values ± standard error (s.e.) of four replicates.

doi:10.6342/NTU202302113

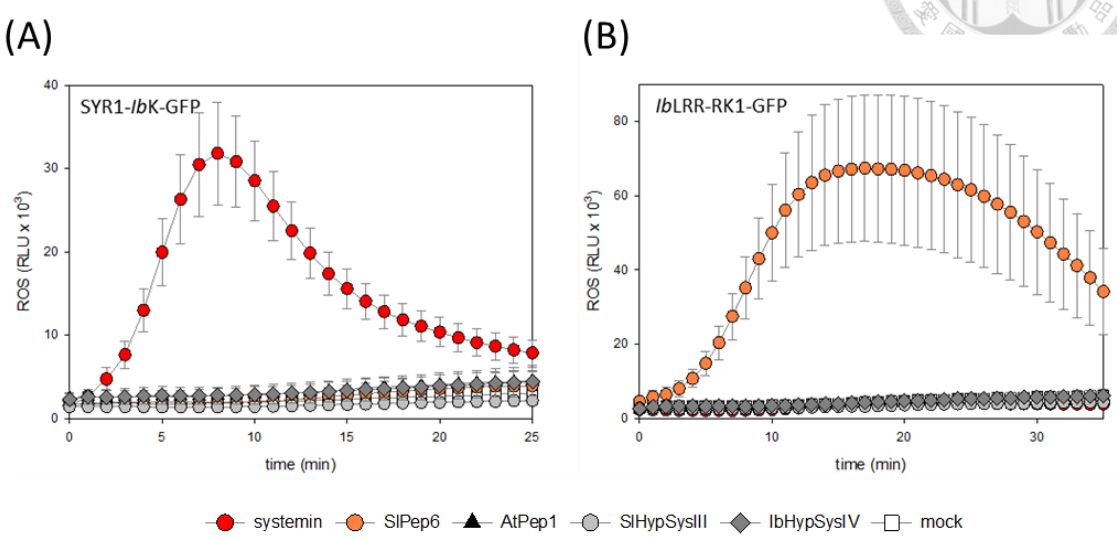

Figure 8. Activation of *Ib*LRR-RK1 by *Sl*Pep6 from tomato induced ROS burst. The generation of ROS burst was examined in *N. benthamiana* leaves transiently expressing **(A)** SYR1-*Ib*K or **(B)** *Ib*LRR-RK1 upon treatment with various stimuli. The stimuli included 1 μM *At*Pep1 (black triangles), *Sl*Pep6 (orange circles), systemin (red circles), *Ib*HypSysIV (dark gray diamonds), *Sl*HypSysIII (gray circles), or the control (BSA/NaCl, open squares). The values and error bars represent the mean ± standard error (s.e.) of four independent replicates.

doi:10.6342/NTU202302113

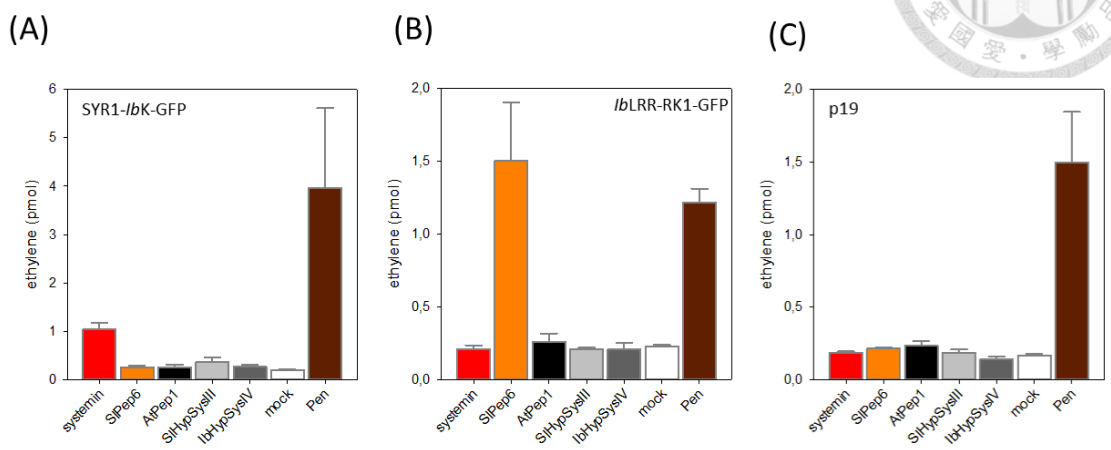

Figure 9. Activation of *Ib*LRR-RK1 by *Sl*Pep6 from tomato induced ethylene production. Ethylene production was measured in leaf discs of *N. benthamiana* expressing **(A)** SYR1-*Ib*K, **(B)** *Ib*LRR-RK1, or **(C)** only p19 upon treatment with a panel of peptides at a concentration of 1 µM including systemin, *Sl*Pep6, *At*Pep1, *Sl*HypSysIII, *Ib*HypSysIV. Additionally, plants treated with water were included as mock control and 90 ng/µl Pen extract (Thuerig et al., 2005) was included as a positive control. The values and error bars represent the mean ± standard deviation (s.d.) of three independent replicates.

doi:10.6342/NTU202302113

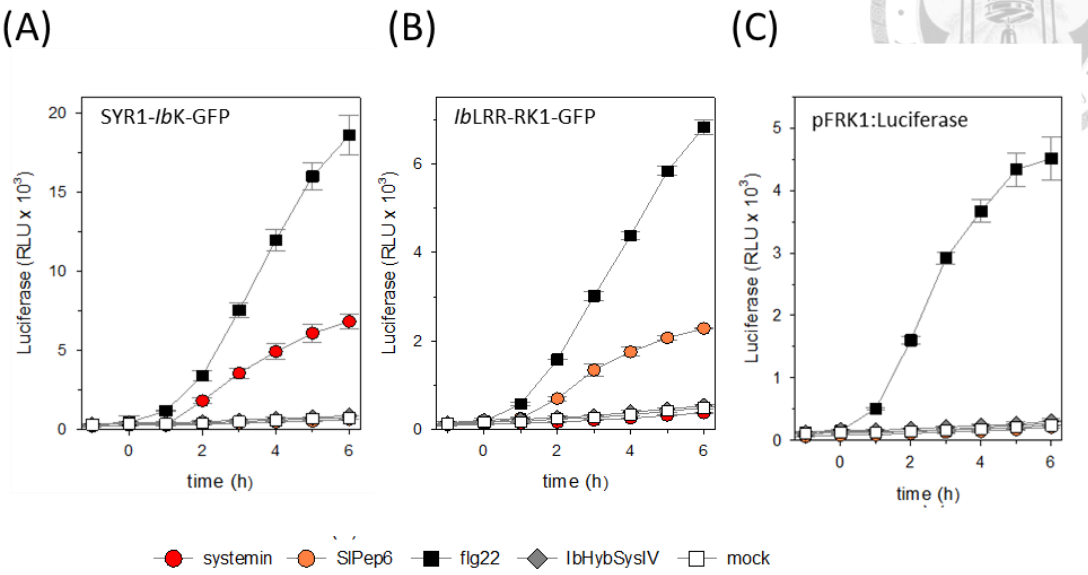

Figure 10. Activation of *Ib*LRR-RK1 by *Sl*Pep6 from tomato induced the expression of defense genes. Mesophyll protoplasts isolated from *Arabidopsis thaliana* Col-0 were co-transformed with **(A)** SYR1-*Ib*K or **(B)** *Ib*LRR-RK1, along with the reporter construct *pFRK1:luciferase*. Protoplasts were transformed with **(C)** *pFRK1:luciferase* alone were used as a control. Luminescence induction was monitored following treatment with various peptides: 10 nM *Sl*Pep6 (orange circles), systemin (red circles), *Ib*HypSysIV (dark gray diamonds), or flg22 (black squares, positive control) at time point 0. A mock control was included, represented by white squares. The values and error bars represent the mean ± standard deviation (s.d.) of two independent experiments.

doi:10.6342/NTU202302113

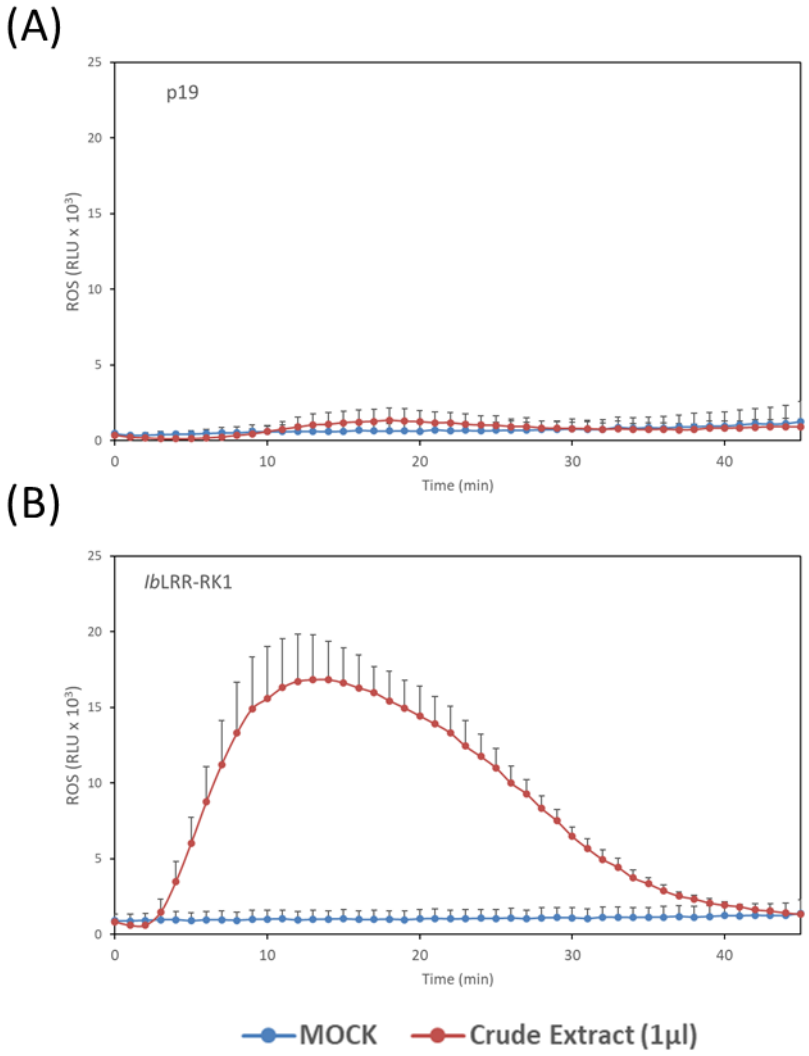

Figure 11. Activation of *Ib*LRR-RK1 by crude extracts from sweet potato induced ROS burst. The generation of ROS burst was examined in *N. benthamiana* leaves transiently expressing **(A)** p19 along or **(B)** *Ib*LRR-RK1 with p19 upon treatment with crude extracts from sweet potato leaves (red circle and red line) or the mock control. (BSA/NaCl, blue circle and blue line). The values and error bars represent the mean ± standard error (s.e.) of four independent replicates.

doi:10.6342/NTU202302113

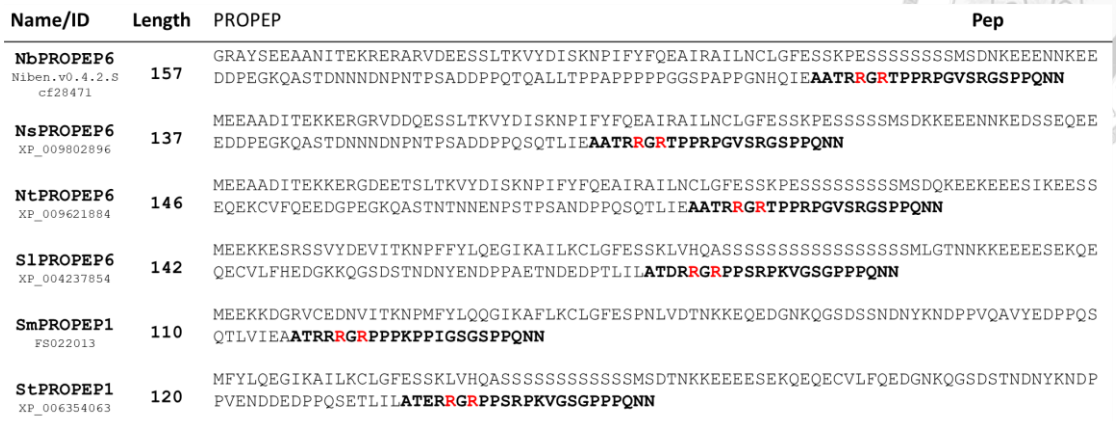

Name/ID	Length	PROPEP	Pep
NbPROPEP6 Niben.v0.4.2.Scf28471	157	GRAYSEEAANITEKRERARVDEESSLTKVYDISKNPIFYFQEAIRAILNCLGFESSKPESSSSSSSSMSDNKEEENNKEE DDPEGKQASTDNNNDNPNTPSADDPPQTQALLTPPAPPPPPGGSPAPPGNHQIE	**AATRRGRTPPRPGVSRGSPPQNN**
NsPROPEP6 XP_009802896	137	MEEAADITEKKERGRVDDQESSLTKVYDISKNPIFYFQEAIRAILNCLGFESSKPESSSSSMSDKKEEENNKEDSSEQEE EDDPEGKQASTDNNNDNPNTPSADDPPQSQTLIE	**AATRRGRTPPRPGVSRGSPPQNN**
NtPROPEP6 XP_009621884	146	MEEAADITEKKERGDEETSLTKVYDISKNPIFYFQEAIRAILNCLGFESSKPESSSSSSSSSMSDQKEEKEEESIKEESS EQEKCVFQEEDGPEGKQASTNTNNENPSTPSANDPPQSQTLIE	**AATRRGRTPPRPGVSRGSPPQNN**
SlPROPEP6 XP_004237854	142	MEEKKESRSSVYDEVITKNPFFYLQEGIKAILKCLGFESSKLVHQASSSSSSSSSSSSSSSSSSMLGTNNKKEEEESEKQE QECVLFHEDGKKQGSDSTNDNYENDPPAETNDEDPTLIL	**ATDRRGRPPSRPKVGSGPPPQNN**
SmPROPEP1 FS022013	110	MEEKKDGRVCEDNVITKNPMFYLQQGIKAFLKCLGFESPNLVDTNKKEQEDGNKQGSDSSNDNYKNDPPVQAVYEDPPQS QTLVIEA	**ATRRRGRPPPKPPIGSGSPPQNN**
StPROPEP1 XP_006354063	120	MFYLQEGIKAILKCLGFESSKLVHQASSSSSSSSSSSSMSDTNKKEEEESEKQEQECVLFQEDGNKQGSDSTNDNYKNDP PVENDDEDPPQSETLIL	**ATERRGRPPSRPKVGSGPPPQNN**

Figure 12. PROPEPs and Peps in Solanaceae family plants. Sweet potato, a member of the Convolvulaceae family, is closely related to the Solanaceae family. In previous studies, genes encoding PROPEPs have been reported in the Solanaceae family, including *Sl*PROPEP6 (Lori et al., 2015). In this study, we retrieved the sequences of six PROPEPs from different species (*Ns, Nicotiana sylvestris; Nb, Nicotiana benthamiana; Nt, Nicotiana tomentosiformis; Sl, Solanum lycopersicum; St, Solanum tuberosum; Sm, Solanum melongena*). The last 23 amino acid residues of the precursor protein (putative mature Peps) are highlighted in bold. These sequences were then used for tBlastn searches of the sweet potato databases available at http://sweetpotato.plantbiology.msu.edu/index.shtml.

doi:10.6342/NTU202302113

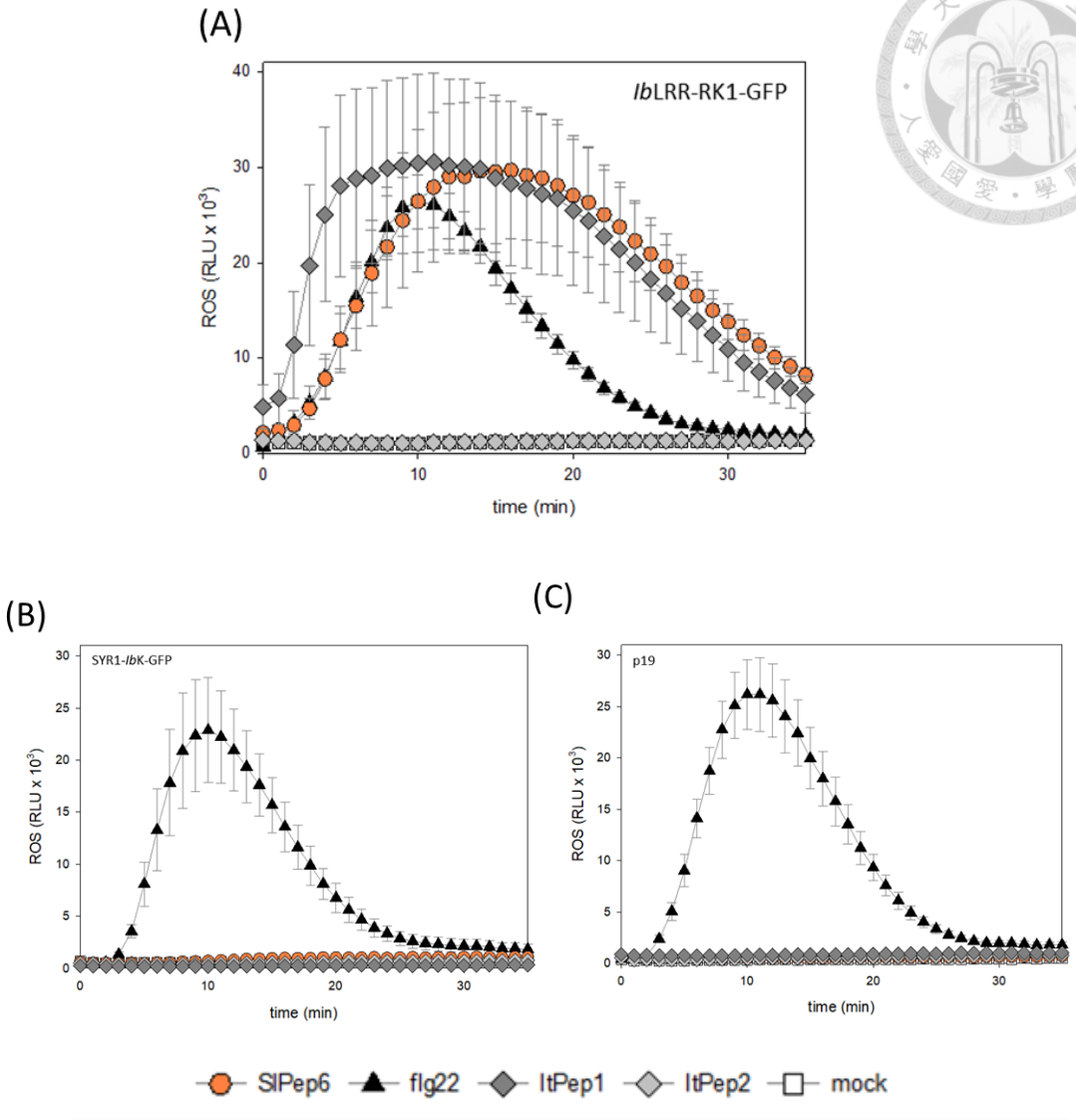

Figure 13. Identification of putative *Ib*Peps ligands for *Ib*LRR-RK. ROS burst was measured in *Nicotiana benthamiana* leaves expressing **(A)** p19 and *Ib*LRR-RK1-GFP, **(B)** p19 and SYR1-*Ib*K-GFP, or **(C)** p19 only (negative control) upon treatment with various peptides, including 1 μM *It*Pep1 (dark grey diamonds), *It*Pep2 (grey diamonds), and *Sl*Pep6 (orange circles), as well as 10 nM flg22 (black triangles), or a control treatment with BSA/NaCl (mock, white squares).

doi:10.6342/NTU202302113

>*Ib*PROPEP1 - 125aa
MEKGGEEGERVRIISSINDPCKWLQELSRAMLKCLGFEICSDQPSPLAAAAASSSSPSSYSDEN
GEDHQKCCFQQLPIAADNKDPDPPPPSTTDPPQLIVSLSSRPPRPGLGNSGDPQTNDTSS*

Comparison of *I. batata* and *I. trifida* PROPEPs; Identity: 86.4%

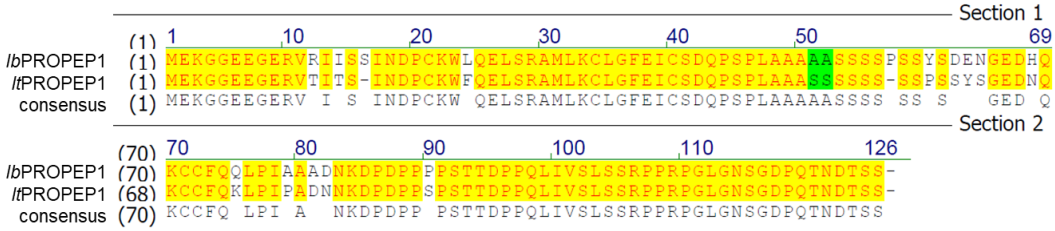

Figure 14. The amino acid sequence of *Ib*Pep1 and its precursor protein *Ib*PROPEP1.

The amino acid sequence of *Ib*PROPEP1 and its corresponding peptide, *Ib*Pep1 (highlighted in red), were deduced. A comparison of PROPEP amino acid sequences between *Ipomoea trifida* and *Ipomoea batata* showed an identity of 86.4%. The putative mature 23-mer peptides located at the C-terminus were found to be 100% identical.

doi:10.6342/NTU202302113

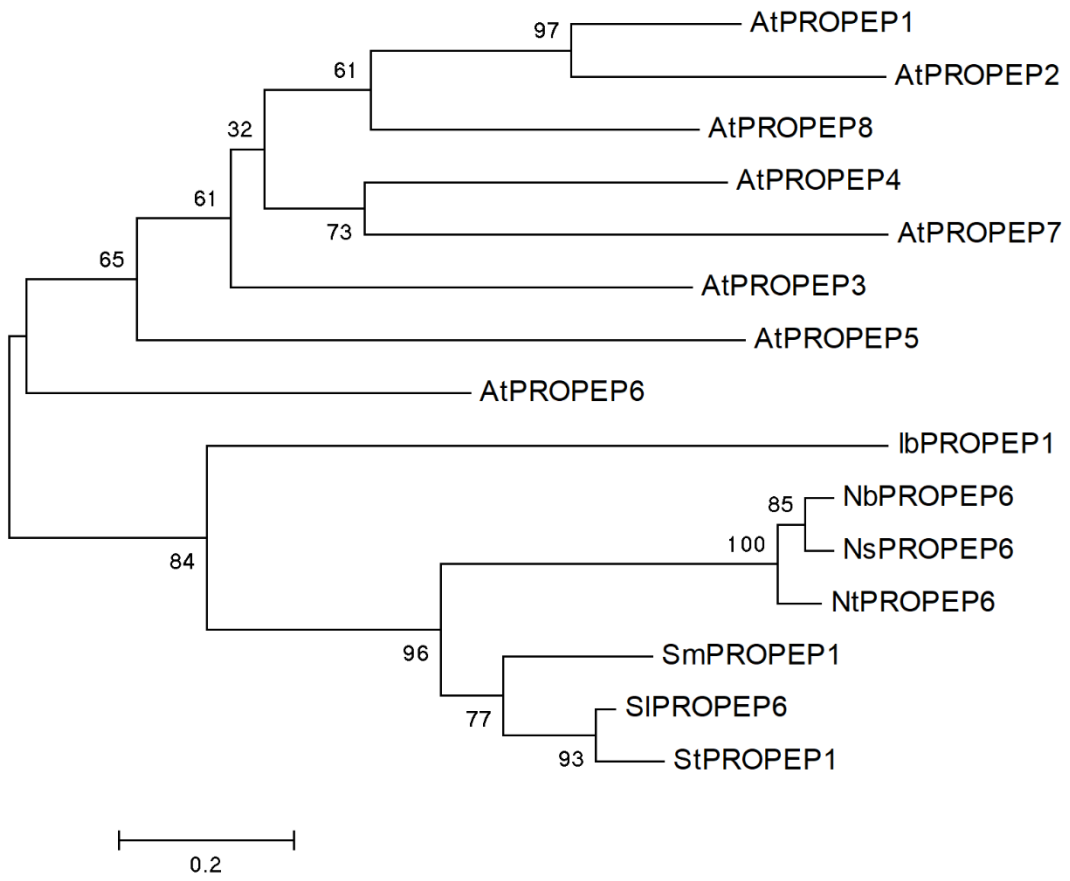

Figure 15. Phylogenetic tree established with *Ib*PROPEP1-related PROPEPs in different plant species. A phylogenetic tree was constructed using a Neighbor-Joining method, depicting the evolutionary relationships among *Ib*PROPEP1 and PROPEPs from various plant species. The tree illustrates the evolutionary relationships among the sequences. *At, Arabidopsis thaliana; Ib, Ipomoea batatas; Nt, Nicotiana tomentosiformis; Nb, Nicotiana benthamiana; Ns, Nicotiana sylvestris; Sm; Solanum melongena; Sl, Solanum lycopersicum; St, Solanum tuberosum.*

doi:10.6342/NTU202302113

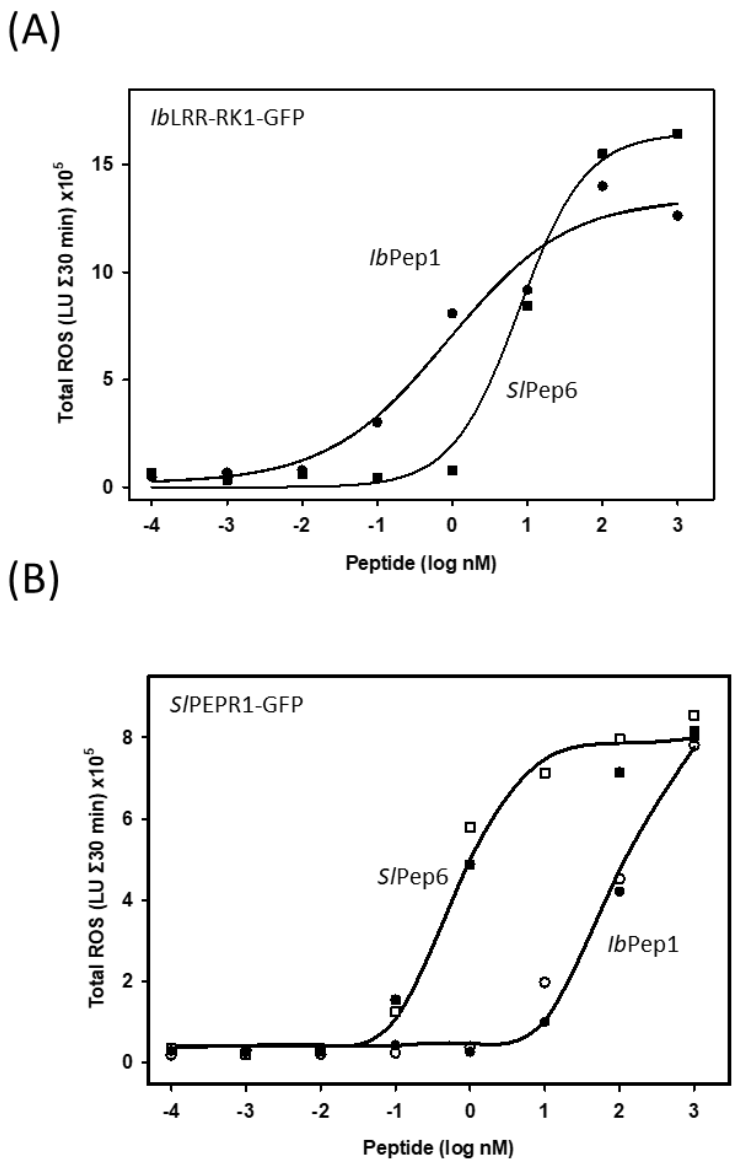

Figure 16. *Ib*LRR-RK1 and *Sl*PEPR1 exhibit cross-recognition of each other's ligands. ROS burst and dose-response curves were analyzed in *N. benthamiana* leaves that were transformed with p19 plus **(A)** *Ib*LRR-RK1-GFP or **(B)** *Sl*PEPR1-GFP. The response of these transformed leaves to different concentrations of *Ib*Pep1 (indicated by circles) and *Sl*Pep6 (indicated by squares) was measured. Filled and open symbols represent data from independent experiments. The integrated ROS response over a 30-min period was recorded for each concentration. Nonlinear regression was performed to fit the curves.

doi:10.6342/NTU202302113

>*Ib*PROPEP1 - 125aa
MEKGGEEGERVRIISSINDPCKWLQELSRAMLKCLGFEICSDQPSPLAAAAASSSSPSSYSDEN
GEDHQKCCFQQLPIAAADNKDPDPPPPSTTDPPQLIVSLSS**RPPRP**GL**G**NSGD**PQ**T**N**DTSS*
>*Sl*PROPEP6 -143aa
MEEKKESRSSVYDEVITKNPFFYLQEGIKAILKCLGFESSKLVHQASSSSSSSSSSSSSSSSSML
GTNNKKEEEESEKQEQECVLFHEDGKKQGSDSTNDNYENDPPAETNDEDPTLILATDRRG**RP**
PSRPKV**G**SGPP**PQ**NN*

Comparison of *Ib*Pep1 and *Sl*Pep6; Identity: 37%

```
            1         10                  27
IbPep1      ---LSSRPP-RPGLGNSGDPQTNDTSS
SlPep6      ATDRRGRPPSRPKVGSGPPPQNN----
consensus          RPP RP LG     PQ N
```

Figure 17. The amino acid sequence of *Ib*PROPEP1, *Sl*PROPEP6 and their derived Peps. The amino acid sequence of *Ib*PROPEP1, *Sl*PROPEP6 and their corresponding peptide *Ib*Pep1, *Sl*Pep6 (highlighted in red) were deduced. A comparison of Peps amino acid sequences between *Ipomoea batatas* and *Solanum lycopersicum* showed an identity of 37%.

doi:10.6342/NTU202302113

	*Ib*LRR-RK1	
Peptide	**Sequence**	**EC_{50} (nM)**
***Sl*Pep6**	ATDRRGRPPSRPKVGSGPPPQNN	**9,8**
***Ib*Pep1**	LSSRPPRPGLGNSGDPQTNDTSS	**0,9**
***Ib*Pep1 (4-23)**	RPPRPGLGNSGDPQTNDTSS	**3,1**
***Ib*Pep1 (5-23)**	PPRPGLGNSGDPQTNDTSS	**> 100**
***Ib*Pep1 (A4)**	LSSAPPRPGLGNSGDPQTNDTSS	**> 100**
***Ib*Pep1 (7-23)**	RPGLGNSGDPQTNDTSS	**n.d.**
***Ib*Pep1 (1-20)**	LSSRPPRPGLGNSGDPQTND	**> 100**
***Ib*Pep1 (1-17)**	LSSRPPRPGLGNSGDPQ	**n.d.**
***Ib*Pep1 (A22A23)**	LSSRPPRPGLGNSGDPQTNDTAA	**2,3**
***Ib*Pep1 (4-22)**	RPPRPGLGNSGDPQTNDTS	**> 100**

Figure 18. Sequences and ROS-inducing activities of different peptide derivatives derived from *Ib*Pep1. Amino acids sequences and specific ROS-inducing activities of various peptide derivatives of *Ib*Pep1. EC_{50} values represent the concentrations needed to elicit half-maximal ROS production in *N. benthamiana* leaves expressing *Ib*LRR-RK1-GFP. Nonlinear regression was performed to calculate the EC_{50} values.

doi:10.6342/NTU202302113

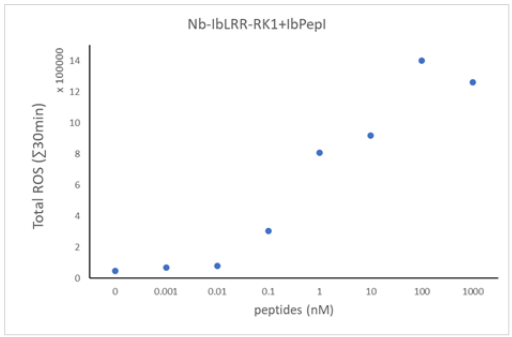

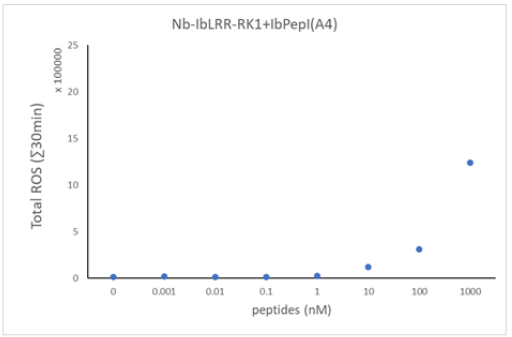

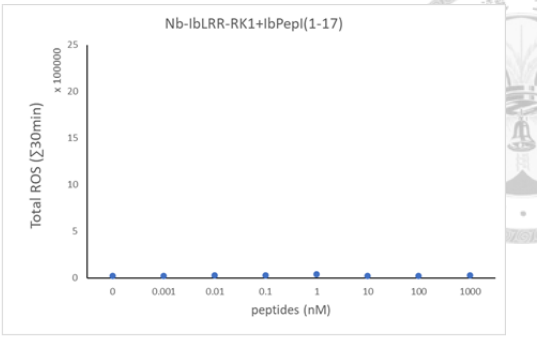

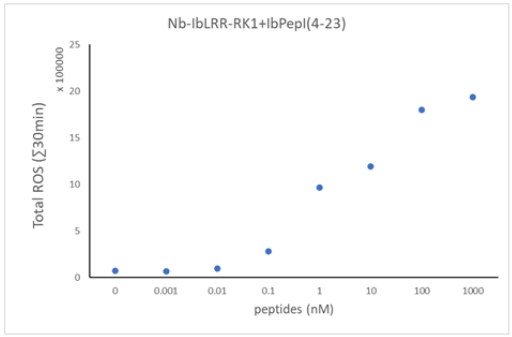

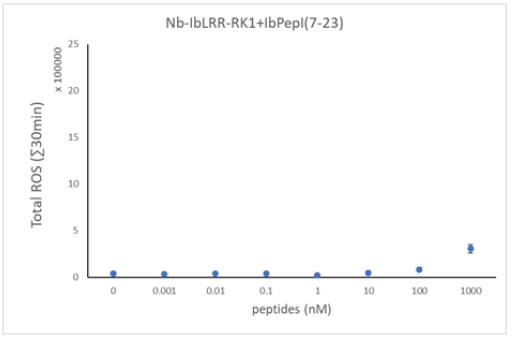

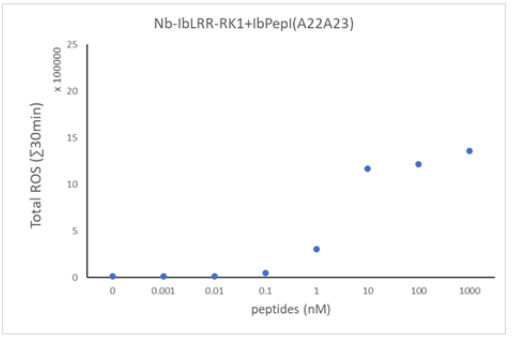

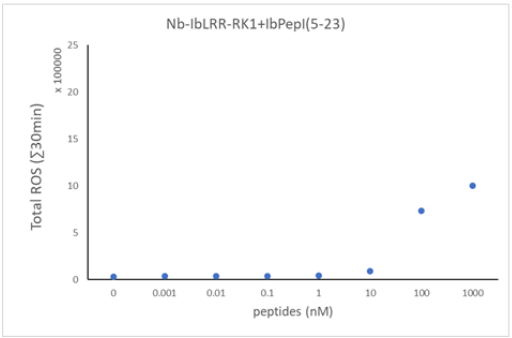

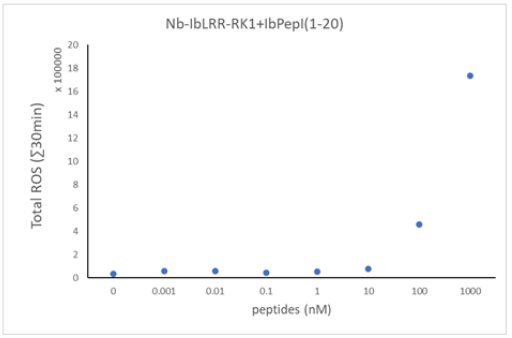

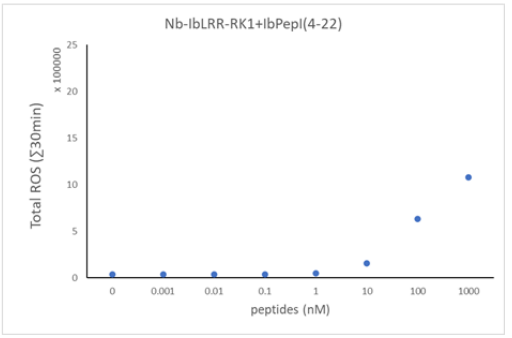

doi:10.6342/NTU202302113

Figure 19. Activity of peptide derivatives derived from *Ib*Pep1. ROS burst and dose-response curves were analyzed in *N. benthamiana* leaves that were transformed with p19 plus *Ib*LRR-RK1-GFP. The response of these transformed leaves to various peptide derivatives of *Ib*Pep1 (see Figure 18) was measured. The integrated ROS response over a 30-min period was recorded for each concentration.

doi:10.6342/NTU202302113

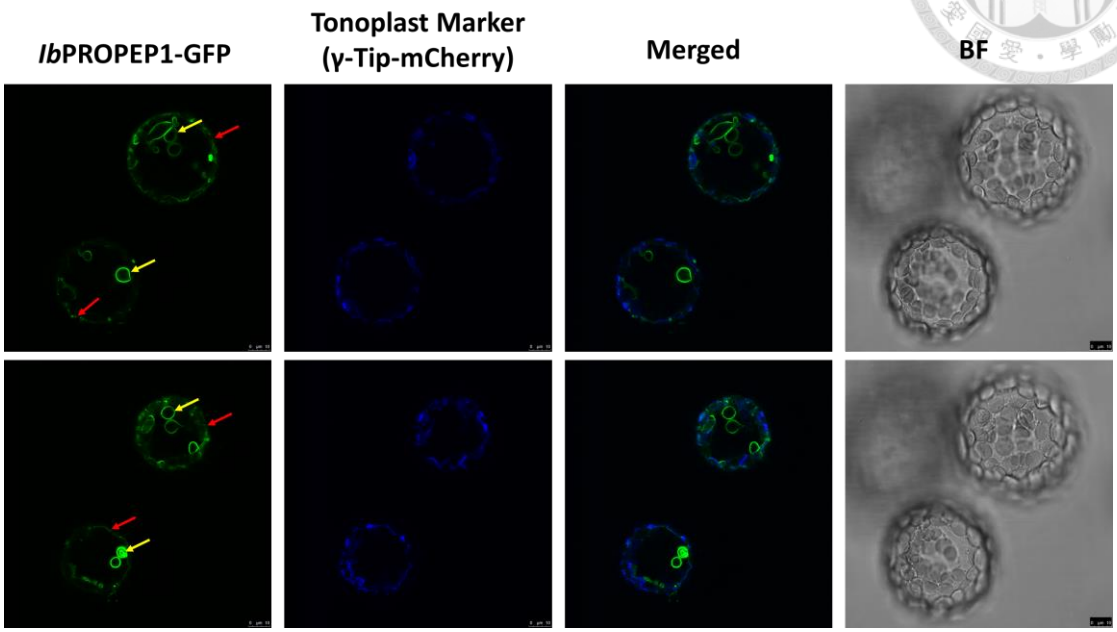

Figure 20. *Ib*PROPEP1 predominantly localizes to the tonoplast membrane. To investigate the subcellular localization, *Ib*PROPEP1-GFP was transiently expressing in mesophyll protoplasts of *Arabidopsis thaliana*. Confocal microscopy was used to observe the subcellular distribution of *Ib*PROPEP1. Partial colocalization was observed between *Ib*PROPEP1-GFP and the tonoplast marker γ-Tip-mCherry. The tonoplast is indicated by red arrows, and bulb structures are indicated by yellow arrows.

doi:10.6342/NTU202302113

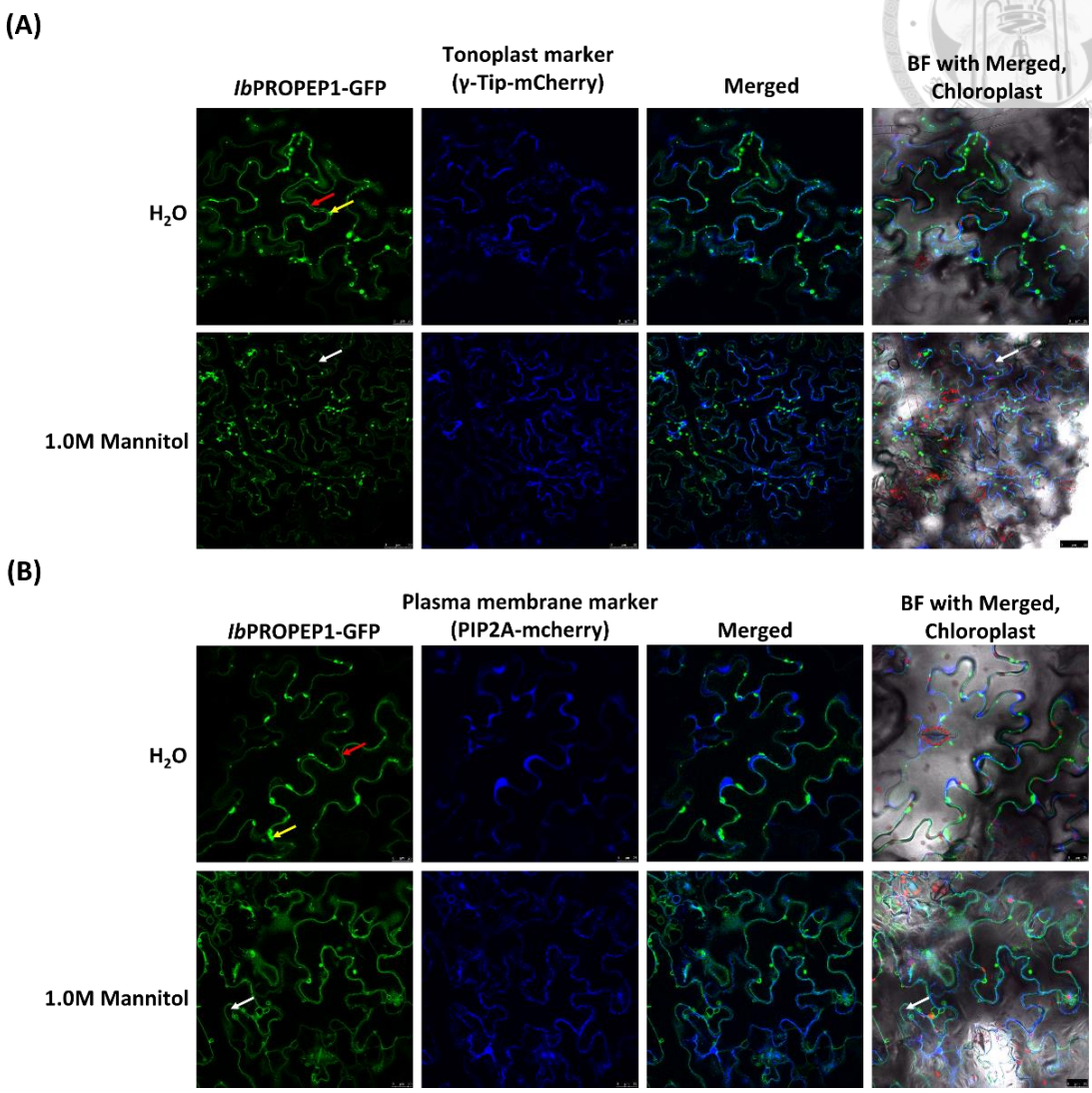

Figure 21. Subcellular localization of *Ib*PROPEP1 in *N. benthamiana* leaves. *N. benthamiana* leaves were transiently transformed with *Ib*PROPEP1-GFP and observed at 3 dpi using confocal microscopy (TCS SP5 Confocal; Leica). The subcellular distribution of *Ib*PROPEP1-GFP was assessed in conjunction with either **(A)** the tonoplast marker γ-Tip-mCherry (Nelson, Cai, & Nebenfuhr, 2007) or **(B)** the plasma membrane marker PIP2A-mCherry (plasma membrane intrinsic protein 2A). Fluorescence signals were also observed after inducing plasmolysis through infiltration with 1.0 M mannitol. The position of the tonoplast is indicated by red arrows, bulb structures within vacuoles are

doi:10.6342/NTU202302113

indicated by yellow arrows, and areas where plasmolysis occurred are indicated by white arrows. The final panels show bright field (BF) images overlaid with merged fluorescence signals, including the red autofluorescence emitted by chloroplasts.

doi:10.6342/NTU202302113

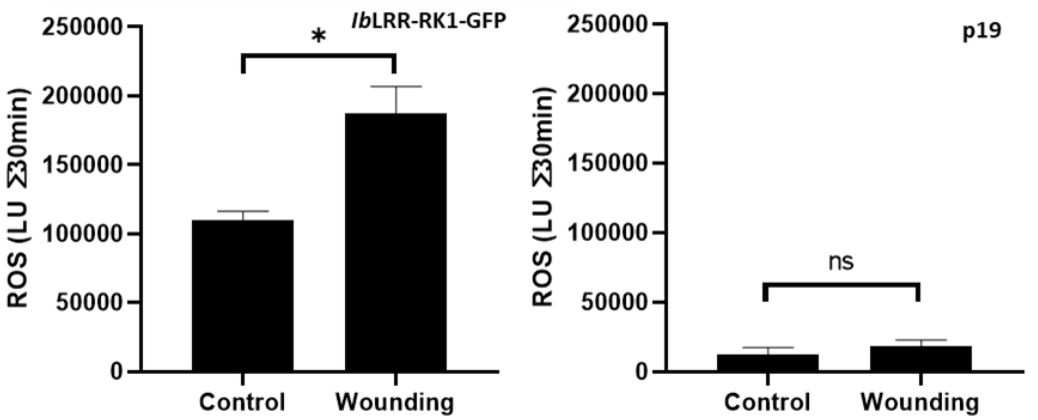

Figure 22. *Ib*LRR-RK1 recognized wound-induced endogenous compounds extracted from sweet potato leaves. ROS burst, integrated over a period of 30 min, was measured in *N. benthamiana* leaves. Control leaves expressing p19 alone and leaves expressing *Ib*LRR-RK1 were treated with either 1 μl of partially purified extract from unwounded sweet potato leaves (control) or 10 min wounded sweet potato leaves. The bars and error bars represent the mean ± standard error (s.e.) of n = 4 replicates.

doi:10.6342/NTU202302113

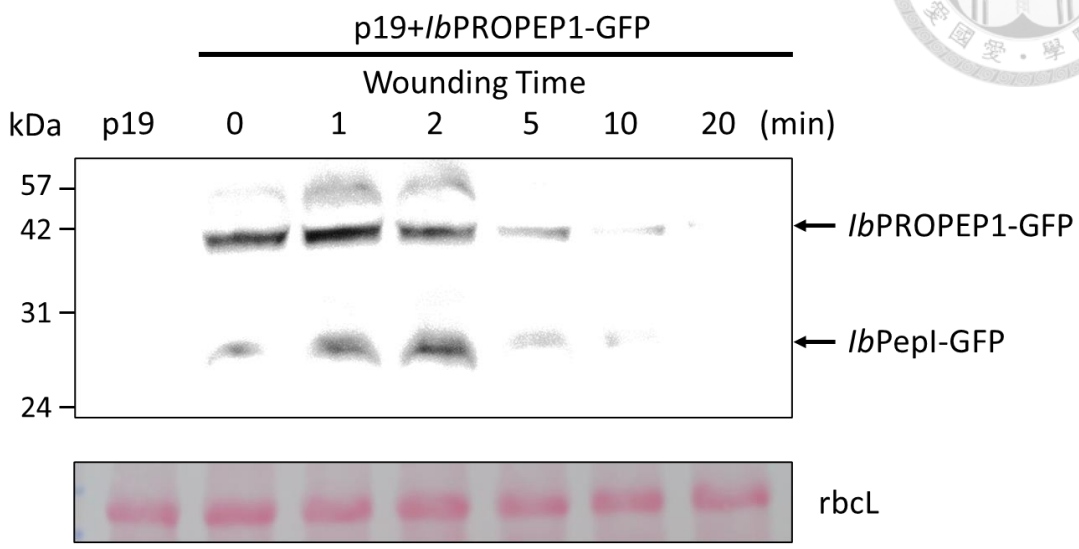

Figure 23. Wounding induced the processing of *Ib*PROPEP1. Total crude proteins were extracted from *N. benthamiana* leaves transiently transformed with p19 or p19 plus *Ib*PROPEP1-GFP at the indicated time after wounding. Western blots were developed with antibodies against the GFP-tag present on the *Ib*PROPEP1-GFP (~40kDa) and *Ib*PepI-GFP (~28kDa). Ponceau-S staining of rbcL shows equal loading of proteins on blots with crude extracts. Data are representative of at least three independent experiments.

doi:10.6342/NTU202302113

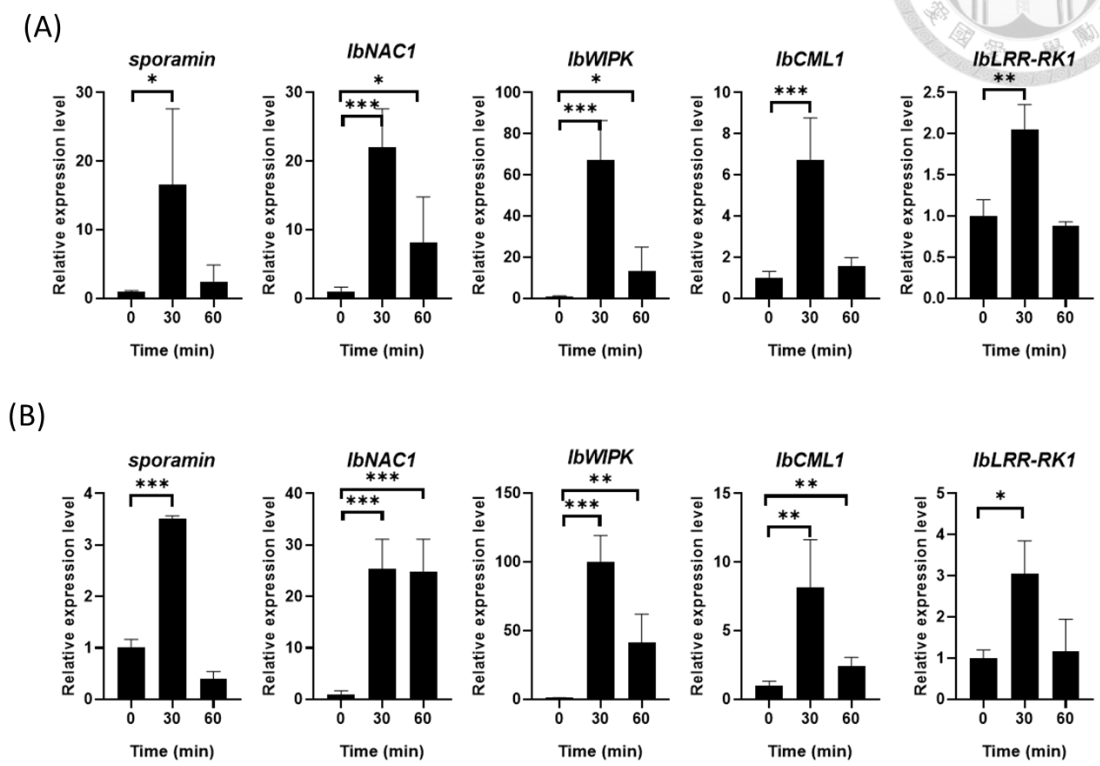

Figure 24. Induction of defense-related genes in response to *Ib*Pep1 and *Ib*HypSysIV in sweet potato. Sweet potato leaves were subjected to treatment with 25 μM of **(A)** *Ib*HypSysIV or **(B)** *Ib*Pep1, and the expression levels of herbivore defense-related genes were examined. The expression level of *SPORAMIN, IbNAC1, IbWIPK1, IbCML1,* and *IbLRR-RK1* was analyzed using quantitative RT-PCR. The bars and error bars in the graph represent the mean ± s.e. of n = 4 replicates. Significance levels are indicated as * = $p<0.05$, ** = $p<0.01$, *** = $p<0.001$, based on a one-tailed t-test.

doi:10.6342/NTU202302113

(A)

		Solanales aligned sequence 1 20 23
Ipomoea batatas	*Ib*PepI	LSS**R**P**P**RPGLGNS**G**D**P**QT**N**DTSS
Ipomoea triloba	*Itl*PepI	LSS**R**PLRPGLGNS**G**D**P**QT**N**DTSS
Ipomoea trifida	*Itf*PepI	LSS**R**P**P**RPGLGNS**G**D**P**QT**N**DTSS
Ipomoea nil	*In*PepI	QSS**R**P**P**RPGLGNS**G**D**P**QT**N**DTSS
Nicotiana benthamiana	*Nb*Pep6	**A**AT**RRGR**T**P**PR**P**GVSR**G**S**PPQNN**
Nicotiana sylvestris	*Ns*Pep6	**A**AT**RRGR**T**P**PR**P**GVSR**G**S**PPQNN**
Nicotiana tomentosiformis	*Nt*Pep6	**A**AT**RRGR**T**P**PR**P**GVSR**G**S**PPQNN**
Solanum lycopersicum	*Sl*Pep6	**A**TD**RRGR**P**P**SR**P**KVGS**G**P**PPQNN**
Solanum melongena	*Sm*Pep1	**A**TR**RRGR**P**P**PK**P**PIGS**G**S**PPQNN**
Solanum tuberosum	*St*Pep1	**A**TE**RRGR**P**P**SR**P**KVGS**G**P**PPQNN**
		1 4 23

(B)

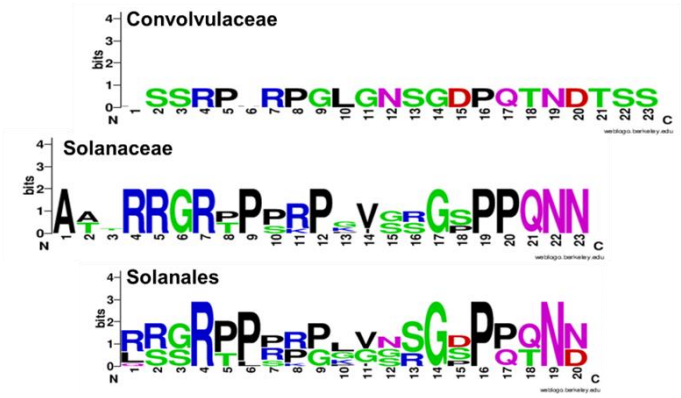

Figure 25. Comparison of Peps from Convolvulaceae and Solanaceae. (A) Pep sequences from the genera *Ipomoea* (Convolvulaceae) and Solanum and *Nicotiana* (Solanaceae) . Both Convolvulaceae and Solanaceae families utilized for the analysis of consensus sequences belonging to order Solanales. (B) WebLogos were generated to compare the consensus sequences of Convolvulaceae (*Ib*Pep1, *Itl*Pep1, *Itf*Pep1, *In*Pep1) and Solanaceae (*Nb*Pep6, *Ns*Pep6, *Nt*Pep6, *Sl*Pep6, *Sm*Pep6, *St*Pep6) Peps with the combined consensus (based on overlapping 20 residues). The WebLogos provide a visual representation of the amino acid sequence conservation in the Peps.

doi:10.6342/NTU202302113

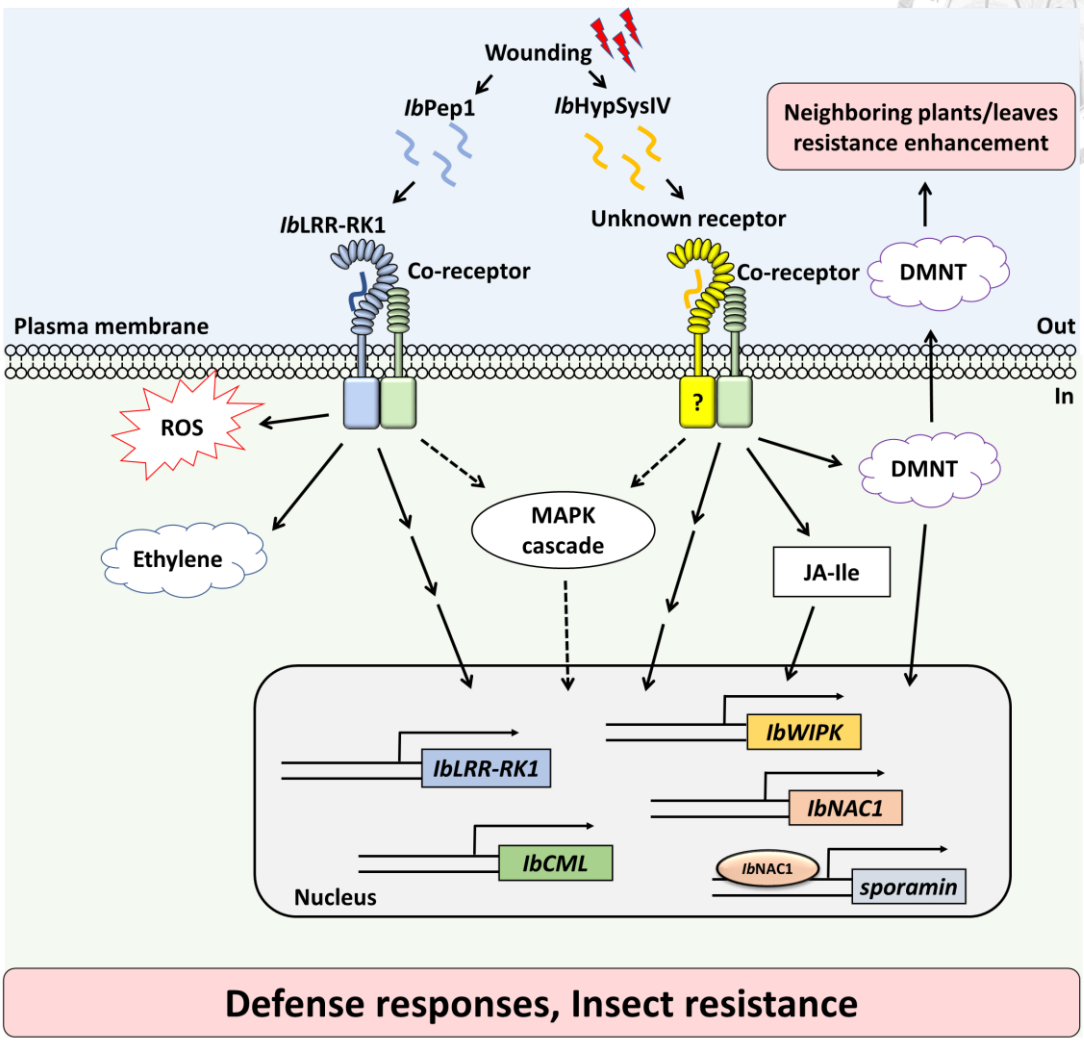

Figure 26. Proposed model of *Ib*Pep1 and *Ib*HypSysIV triggered defense responses in sweet potato leaves. Peptide ligands *Ib*Pep1 and *Ib*HypSysIV are activated/induced in the wounded leaf (Chen et al., 2008; Li et al., 2016). *Ib*Pep1 activates the *Ib*LRR-RK1 receptor, leading to the initiation of defense responses such as the production of reactive oxygen species (ROS) and ethylene. In contrast, *Ib*HypSysIV induces the emission of the volatile compound DMNT as an anti-herbivore defense signal (Meents et al., 2019) and the accumulation of jasmonate derivative JA-Ile.. Both *Ib*Pep1 and *Ib*HypSysIV contribute to the upregulation of various genes associated with wound and defense responses, including *IbLRR-RK1, IbWIPK, IbNAC1, IbCML,* and the trypsin inhibitor

doi:10.6342/NTU202302113

gene *SPORAMIN* (Chen et al., 2016a; Chen et al., 2016b; Yeh et al., 1997a; Yeh et al., 1997b). Collectively, *Ib*Pep1 and *Ib*HypSysIV may function through complementary and/or parallel pathways to enhance plant resistance against biotic threats. Dashed arrows indicate pathways that are yet to be fully elucidated, such as the MAPK cascade.

doi:10.6342/NTU202302113

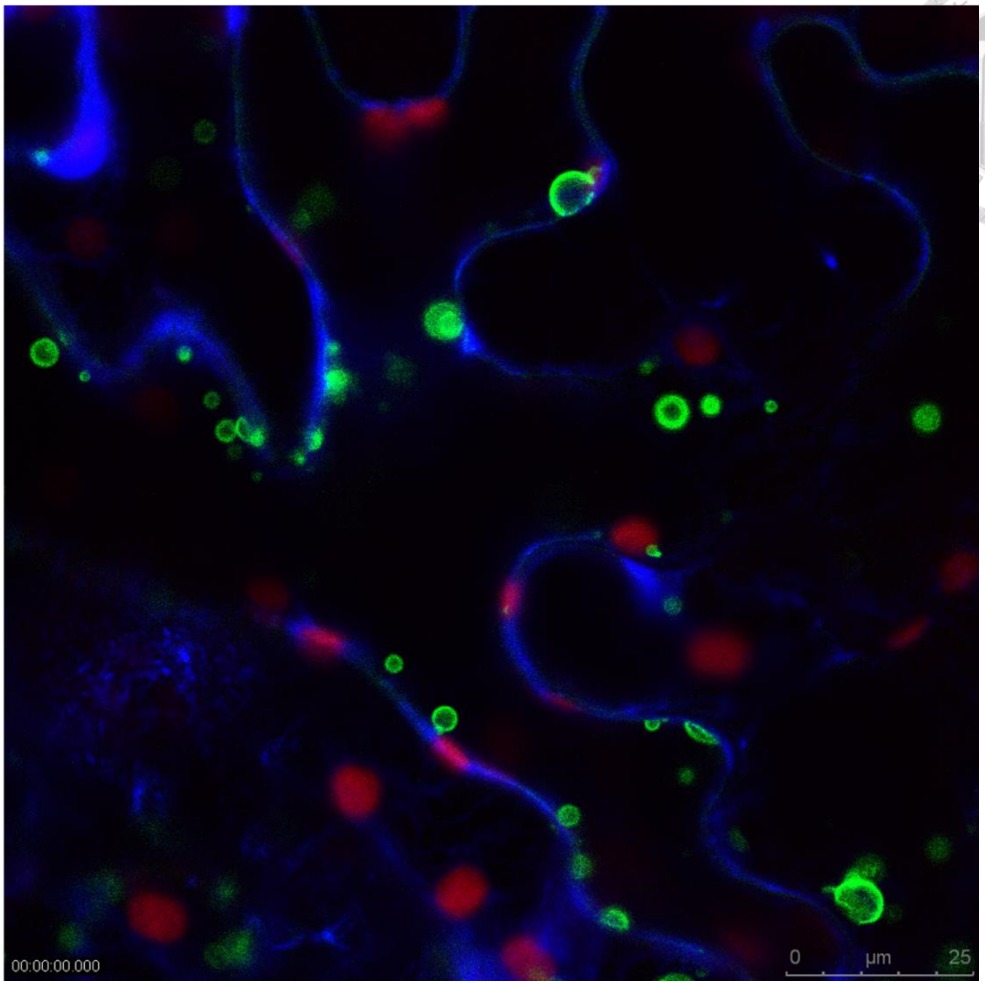

Video 1. Subcellular localization and movement of GFP-tagged *Ib*PROPEP1. To investigate the subcellular localization and movement of *Ib*PROPEP1, *N. benthamiana* leaves were transiently transformed with *Ib*PROPEP1-GFP fusion construct (*Ib*PROPEP1-pMDC83). Confocal microscopy (TCS SP5 Confocal; Leica) was used to visualize and track the movement of *Ib*PROPEP1-GFP within the cells. The tonoplast, marked by γ-Tip-mCherry co-transformation (Nelson, Cai, & Nebenfuhr, 2007), was labeled in blue for reference. The observed movement of *Ib*PROPEP1-GFP was captured in Vedio 1 (https://reurl.cc/qLk6eN), demonstrating its localization in vesicles.

doi:10.6342/NTU202302113

Supplementary Figures

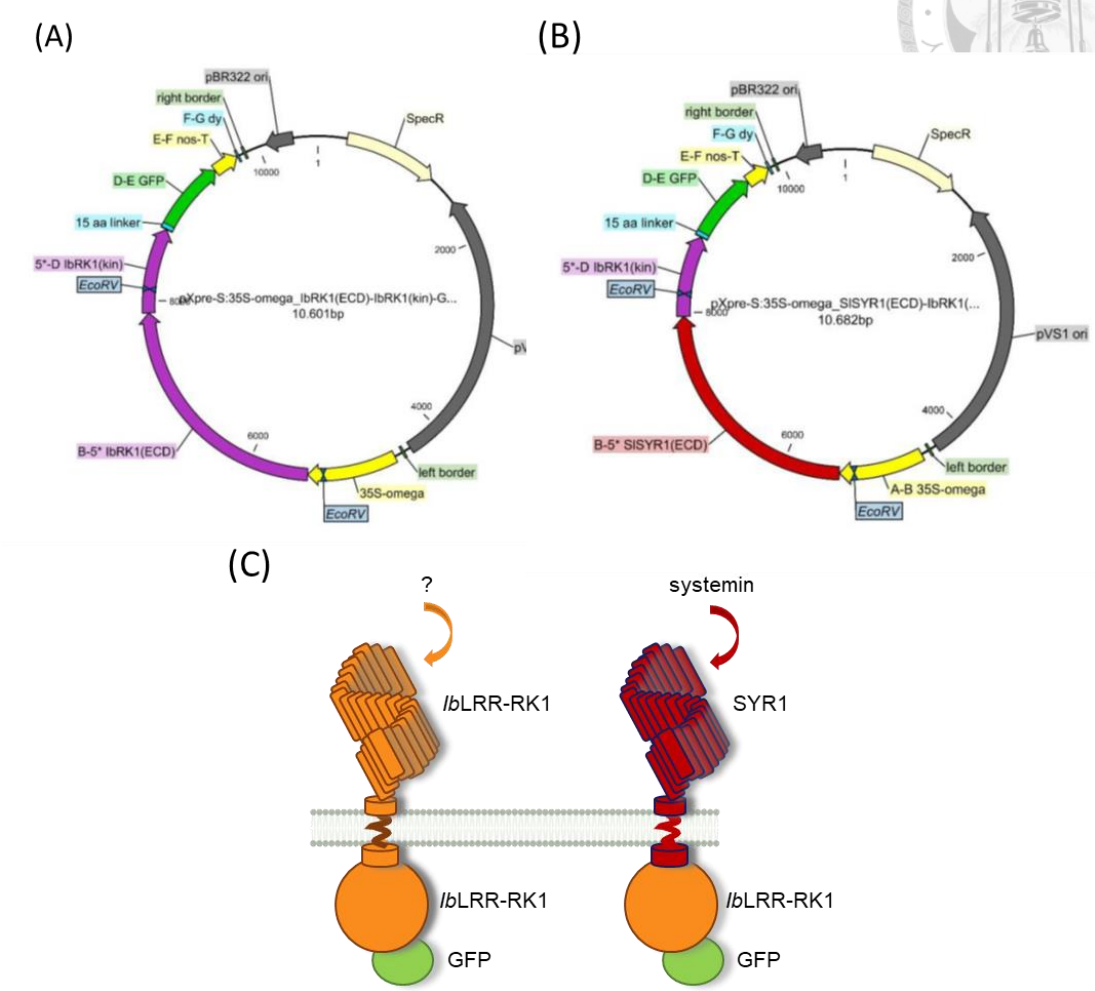

Supplementary Figure S1. Generation of chimeric receptors IbLRR-RK1-GFP and SYR1-*Ib*K-GFP. (Collaborated with Prof. Georg Felix's lab) Golden Gate system was utilized to generate the chimeric receptors **(A)** *Ib*LRR-RK1-GFP and **(B)** SYR1-*Ib*K-GFP. To create SYR1-*Ib*K-GFP chimeric receptor, the core kinase domain of SYR1 was replaced with the corresponding domain from *Ib*LRR-RK1. (C) The resulting chimeric proteins was transiently expressed in *Nicotiana benthamiana*, allowing for functional analysis and characterization of their signaling properties in the plant system.

doi:10.6342/NTU202302113

(A)

PROPEP	*Ipomoea nil*	*Ipomoea trifida*	*Ipomoea Batatas*
NbPROPEP6	No hit	(2) itf01g30920.t1	No hit
NsPROPEP6	No hit	itf01g30920.t1	(4) G19268|TU31487
NtPROPEP6	(1) XM_019318849 XP_019174394	itf01g30920.t1	(5) G34072|TU55871
SlPROPEP6	No hit	itf07g19300.t1	G34395|TU56413
SmPROPEP1	No hit	(3) itf03g29180.t1	G6779|TU11193
StPROPEP1	No hit	No hit	(6) G21027|TU34394

putative *It*PROPEP1 (itf01g30920.t1)

>itf01g30920.t1|Protein - 123aa
MEKGGEEGERVTITSINDPCKWFQELSRAMLKCLGFEICSDQPSPLAAASSSSSSSS
PSSYSGEDNQKCCFQKLPIPADNNKDPDPPSPSTTDPPQLIVSLSSRPPRPGLGNSG
DPQTNDTSS*

*It*Pep1: LSS**R**PP**R**PGLGNSGDPQTNDTSS

(B)

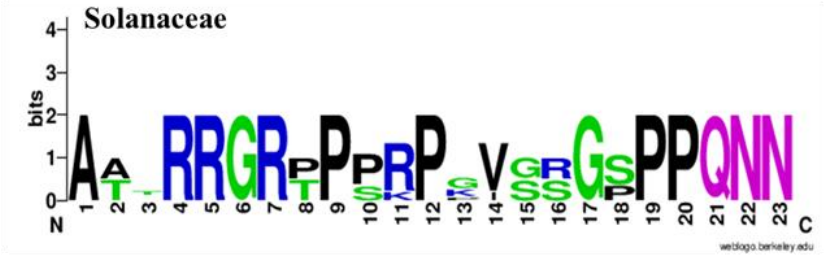

putative *It*PROPEP2 (itf07g21780.t1)

>itf07g21780.t1|Protein - 289aa
MDSLSSVSPSFVLPPGKLLRHHHHRRRISVSSKVKLARQLRLSF
SSGIPRSSFGRTSDNLDRRRTPEAYCKLGGGGGGGGGGGEGGD
HDEEGRRRDEEVESALRMDGTIPGTPNEFVKQVSSRAYDMRRH
LQQSFDSSSYDVLEANPWRETSKPVYVLTHRENQLCTMKTRRN
QSEVERELGLLFSKGGKWRNQAKQTGTGTKFQMVVEDVREG
VLVFEDGDEAVKYCDLLQGGGQDCEGVAEIEASSVFDLCRKMR
ALAVLFRRGRTPPRPENLKLNLRARKHSLEDQ*

*It*Pep2: **RRGR**T**P**PRPENLKLNLRARKHSLEDQ

doi:10.6342/NTU202302113

Supplementary Figure S2. Identification of putative Peps and PROPEPs in sweet potato. (Collaborated with Prof. Ming-Jing Hwang's lab) (A) Through our analysis, we found that a specific gene, itf01g30920.t1, which is a putative *It*PROPEP1, was retrieved multiple times from the *I. trifida* dataset. **(B)** To further identify potential PROPEP genes in *I. trifida*, we employed a scanning sequence patterns strategy based on the consensus sequences derived from the Pep sequences of the Solanaceae family. This strategy, visualized using the WebLogo tool (Crooks, Hon, Chandonia, & Brenner, 2004), led us to discover another gene in *I. trifida*, itf07g21780.t1, which is a putative *It*PROPEP2.

doi:10.6342/NTU202302113

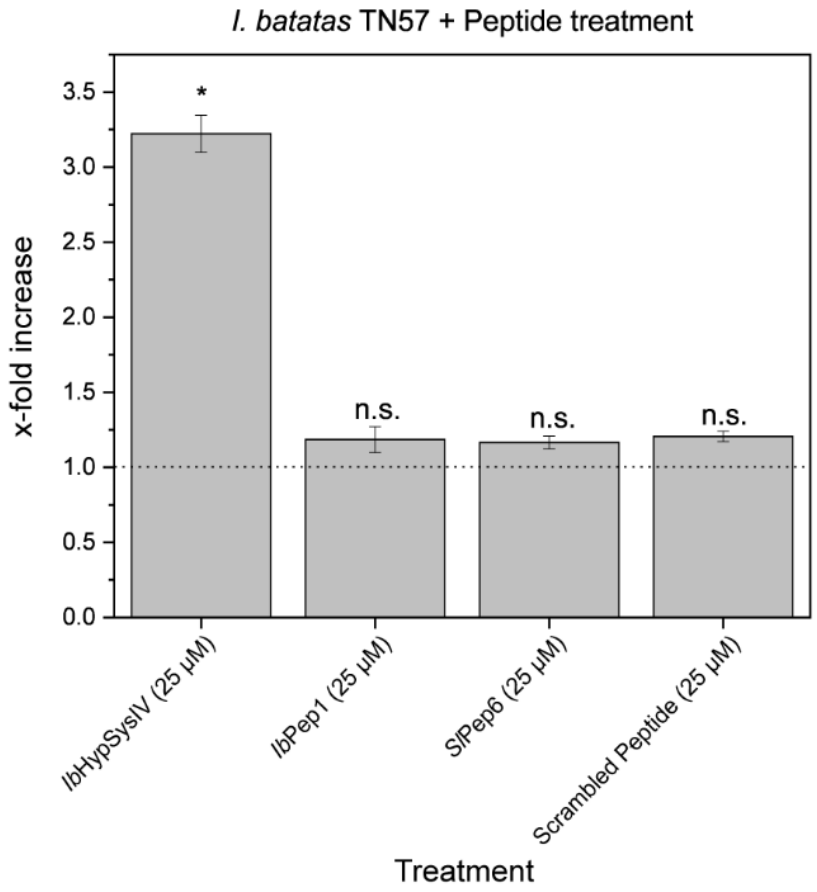

Supplementary Figure S3. Induction of defense-related DMNT volatiles in response to *Ib*Pep1 and *Ib*HypSysIV in sweet potato. (Collaborated with Prof. Axel Mithöfer's lab) The emission of (E)-4,8-dimethyl-nonatriene (DMNT) in sweet potato leaves was assessed by treating whole plants with 25 µM *Ib*HypSysIV (n = 10), *Ib*Pep1 (n = 10), *Sl*Pep6 (n = 11), or a scrambled peptide (n = 7). The fold-induction of DMNT emission was calculated relative to the respective water controls. The bars represent the mean ± s.e. of DMNT emission. Significance levels are denoted by asterisks (* = $p<0.05$) and were determined using a Shapiro-Wilk normality test followed by a Mann-Whitney rank sum test. Non-significant differences are indicated as n.s. (not significant).

doi:10.6342/NTU202302113

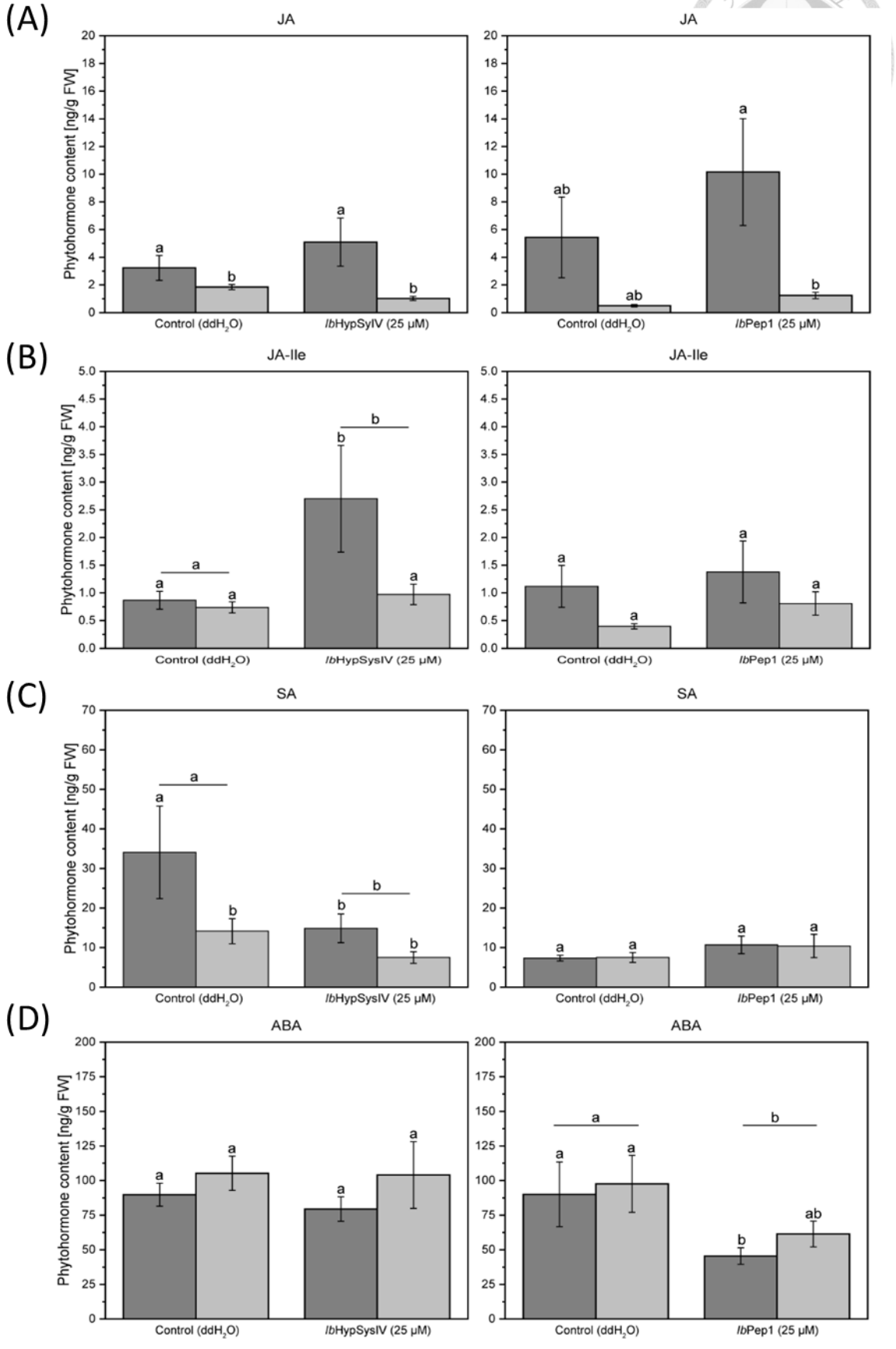

doi:10.6342/NTU202302113

Supplementary Figure S4. Phytohormone accumulation patterns in *I. batatas* leaves after treatment with *Ib*Pep1 or *Ib*HypSysIV. (Collaborated with Prof. Axel Mithöfer's lab) The levels of **(A, B)** jasmonates (JA, JA-Ile), **(C)** salicylic acid (SA), and **(D)** abscisic acid (ABA) were measured in *I. batatas* TN57 leaves after 1 h of treatment with 25 μM *Ib*HypSysIV (left) and *Ib*Pep1 (right). Phytohormone contents were analyzed in the locally treated 3rd leaf (dark gray bars) and the adjacent untreated 4th systemic leaf (light gray bars). Leaves from plants sprayed with ddH_2O served as controls. Statistical analysis was performed using a two-way ANOVA with initial tests for normality and equal variance. Different letters indicate significant differences among groups at $p<0.05$, determined using the Holm-Sidak method. Phytohormone content was set as the dependent variable, and treatment and leaf type were considered independent variables. Data are presented as mean ± s.e. of n = 8.

doi:10.6342/NTU202302113

(A)

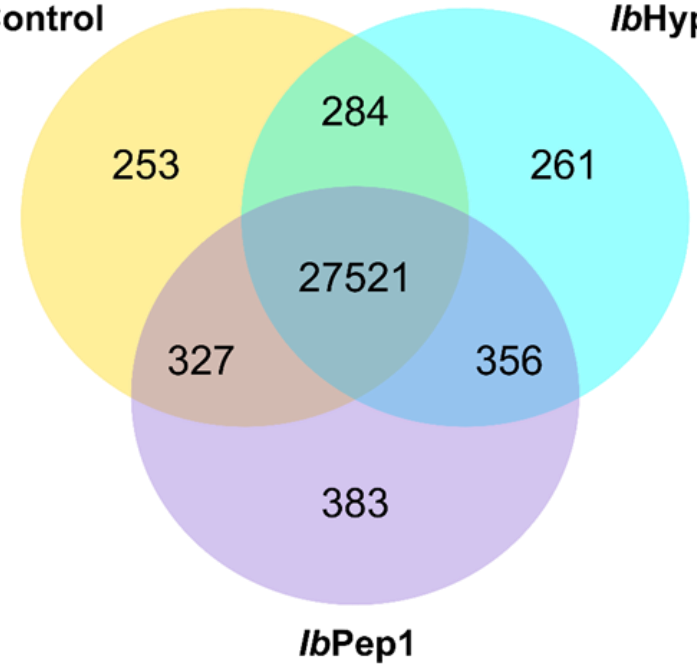

(B)

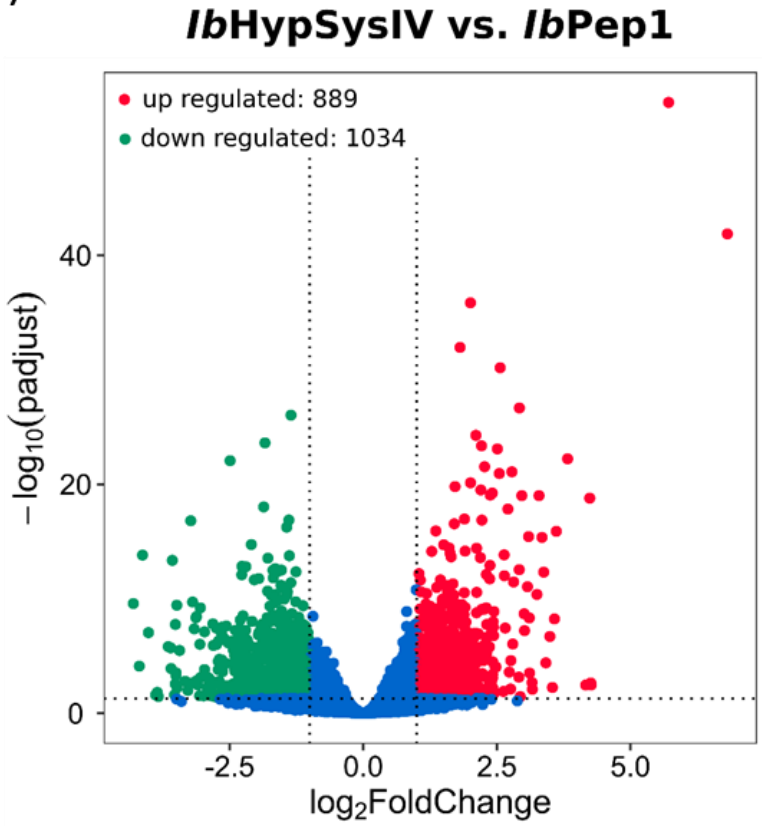

doi:10.6342/NTU202302113

Supplementary Figure S5. *Ib*Pep1 and *Ib*HypSysIV peptides exhibit differential effects on gene expression patterns in sweet potato leaves. (Collaborated with Prof. Axel Mithöfer's lab) (A) RNAseq data from *I. batatas* leaves treated with 25 μM *Ib*HypSysIV, *Ib*Pep1, or ddH2O (control) for 1 h were mapped to the sweet potato genome database. The Venn diagram illustrates the number of identified and expressed genes in each treatment (total of 29,385 genes). The overlapping regions represent the shared expressed genes among the treatments. **(B)** Volcano plot displaying statistical significance (-log10 adj. p-value >1.3, corresponding to adj. p-value <0.05) against differentially expressed genes (DEGs, log2-fold change >=1 and padj <0.05) obtained from a comparison of both peptide treatments (25 μM each peptide, 1 h). Upregulated genes (*Ib*HypSys vs. *Ib*Pep1) are depicted in red, while downregulated genes are highlighted in green. DEGs that do not meet the significance thresholds are represented in blue.

doi:10.6342/NTU202302113

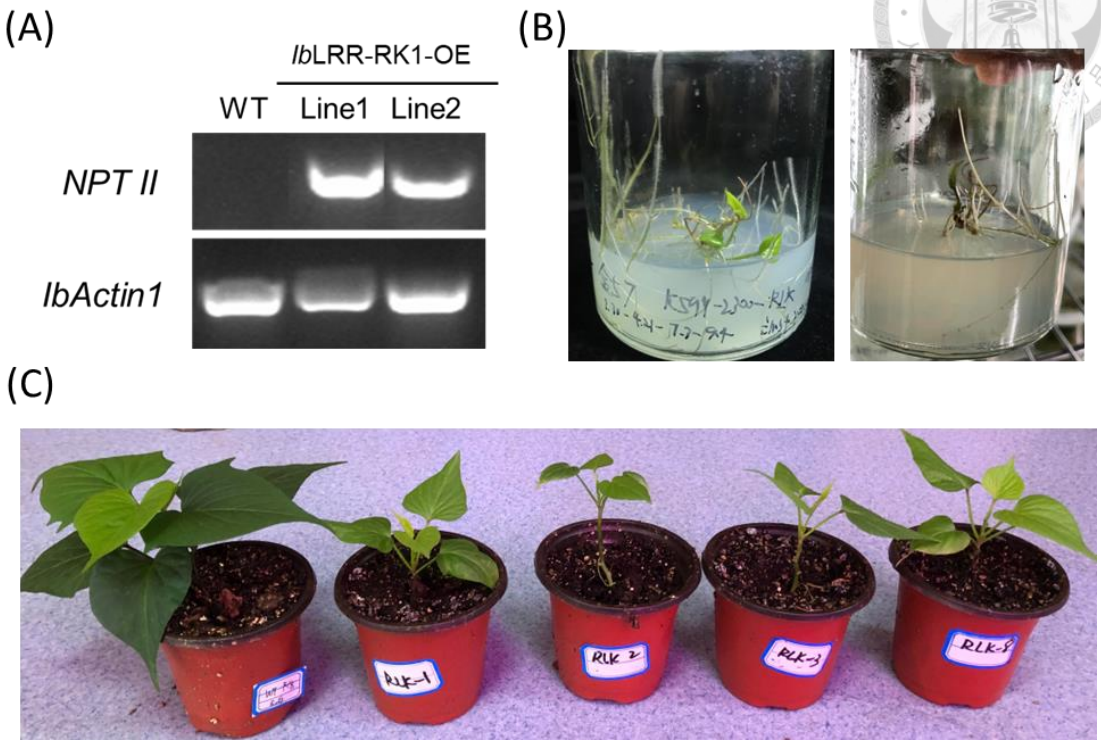

Supplementary Figure S6. Generation of transgenic sweet potato plants overexpressing *Ib*LRR-RK1. (Collaborated with Prof. Shi-Peng Chen's lab) In this study, transgenic sweet potato plants overexpressing IbLRR-RK1 were generated using an *Agrobacterium*-mediated transformation system. The pCAMBIA2300-35s-*Ib*LRR-RK1 vector was introduced into sweet potato (*Ipomoea batatas* cv. KS57) to obtain transgenic plants with overexpressed *Ib*LRR-RK1. **(A)** Genomic DNA was extracted from the transgenic sweet potato plants, and the successful integration of the transgene was confirmed by PCR amplification of the NPT II gene (Table 5). **(B)** Tissue culture-grown transgenic sweet potato plantlets overexpressing *Ib*LRR-RK1. **(C)** Transgenic sweet potato plants overexpressing *Ib*LRR-RK1 (Line 1, 2, 3, 8) compared with wild type sweet potato (WT, left).

doi:10.6342/NTU202302113

Appendix

Published article: Identification of a damage-associated molecular pattern (DAMP) receptor and its cognate peptide ligand in sweet potato (*Ipomoea batatas*)

doi:10.6342/NTU202302113

Received: 13 January 2023 | Revised: 25 April 2023 | Accepted: 19 May 2023

DOI: 10.1111/pce.14633

ORIGINAL ARTICLE

Plant, Cell & Environment | WILEY

Identification of a damage-associated molecular pattern (DAMP) receptor and its cognate peptide ligand in sweet potato (*Ipomoea batatas*)

Hsueh-Han Lu[1] | Anja K. Meents[2] | Judith Fliegmann[3] | Ming-Jing Hwang[4] | Ching-Shu Suen[4] | Diana Masch[2] | Georg Felix[3] | Axel Mithöfer[2] | Kai-Wun Yeh[1,5]

[1]Institute of Plant Biology, National Taiwan University, Taipei, Taiwan

[2]Research Group Plant Defense Physiology, Max Planck Institute for Chemical Ecology, Jena, Germany

[3]Center for Plant Molecular Biology (ZMBP), University of Tübingen, Tübingen, Germany

[4]Institute of Biomedical Sciences, Academia Sinica, Taipei, Taiwan

[5]The Weather Climate and Disaster Research Center, National Taiwan University, Taipei, Taiwan

Correspondence
Axel Mithöfer, Research Group Plant Defense Physiology, Max Planck Institute for Chemical Ecology, Hans-Knöll-Str. 8, 07745 Jena, Germany.
Email: amithoefer@ice.mpg.de

Funding information
Deutsche Forschungsgemeinschaft; Deutscher Akademischer Austauschdienst; National Science and Technology Council

Abstract

Sweet potato (*Ipomoea batatas*) is an important tuber crop, but also target of numerous insect pests. Intriguingly, the abundant storage protein in tubers, sporamin, has intrinsic trypsin protease inhibitory activity. In leaves, sporamin is induced by wounding or a volatile homoterpene and enhances insect resistance. While the signalling pathway leading to sporamin synthesis is partially established, the initial event, perception of a stress-related signal is still unknown. Here, we identified an *Ib*LRR-RK1 that is induced upon wounding and herbivory, and related to peptide-elicitor receptors (PEPRs) from tomato and Arabidopsis. We also identified a gene encoding a precursor protein comprising a peptide ligand (*Ib*Pep1) for *Ib*LRR-RK1. *Ib*Pep1 represents a distinct signal in sweet potato, which might work in a complementary and/or parallel pathway to the previously described hydroxyproline-rich systemin (HypSys) peptides to strengthen insect resistance. Notably, an interfamily compatibility in the Pep/PEPR system from Convolvulaceae and Solanaceae was identified.

KEYWORDS
DMNT, herbivory, LRR-RLK, plant defense, plant elicitor peptide receptor

1 | INTRODUCTION

Plants have evolved several mechanisms to cope with biotic and abiotic stresses. When encountering stresses, such as pathogen infection, insect feeding, and wounding, receptor kinases (RKs) or receptor-like proteins (RLPs) properly identify specific patterns derived either from the aggressors (microbe-associated molecular patterns, MAMPs; and herbivore-associated molecular patterns, HAMPs) or from the perturbation of cellular integrity (danger- or damage-associated molecular patterns, DAMPs). Subsequently, these pattern recognition receptors (PRRs) trigger signal transduction pathways to activate appropriate plant immune responses, leading

This article is dedicated to Prof. Dr. Kai-Wun Yeh, who is no longer with us. He passed away during the preparation of the final stages of this article. He will always be remembered as a passionate scientist and an excellent mentor.

[†]Died March 20, 2023.

doi:10.6342/NTU202302113

to pattern-triggered immunity (PTI) (Boller & Felix, 2009). PTI can reduce the damages caused by the invasion of many pathogens and insects (Böhm et al., 2014).

PRRs are usually composed of extracellular, transmembrane and intracellular domains. They are classified by their extracellular domains. The extracellular leucine-rich repeat domain, a single-pass transmembrane domain, and a cytoplasmic protein kinase domain characterize leucine-rich repeat receptor kinases (LRR-RKs). LRR-RKs and LRR-RLPs are sensors for proteinaceous immunogenic ligands, such as peptides and small proteins (Böhm et al., 2014). For example, the FLS2 receptor binds a 22-amino acid epitope (flg22) conserved in bacterial flagellins (Chinchilla et al., 2006), EFR recognizes a conserved N-terminal fragment of bacterial elongation factor Tu (Zipfel et al., 2006), and *Sl*Eix1 and *Sl*Eix2 bind *Trichoderma* cell wall-derived xylanase (Ron & Avni, 2004).

Peptide ligands play an important role in regulating the signal transduction of insect resistance and wound defense responses (Bartels & Boller, 2015; Huffaker, 2015). In *Arabidopsis thaliana*, eight plant elicitor peptides (*At*Pep1-*At*Pep8) are found to participate in damage-related defense responses after recognition by a pair of LRR-RKs, the PEP receptors 1 and 2 (*At*PEPR1 and 2) (Krol et al., 2010; Yamaguchi et al., 2010). Each of the *At*Peps is derived from the carboxy terminus of their precursor protein *At*PROPEP1-8 (Bartels et al., 2013; Huffaker et al., 2006), how and if the peptides are cleaved off is, however, mostly not known. However, a METACASPASE4 (MC4)-dependent maturation of *At*Pep1 was recently described. High levels of $[Ca^{2+}]_{cyt}$ that occur only in directly damaged cells bind to MC4, which in this activated form cleaves PROPEP1 and releases *At*Pep1 (Chen et al., 2020; Hander et al., 2019). *AtPROPEP2*, *AtPROPEP3* and the receptor genes *AtPEPR1/2* are strongly induced upon herbivore attack. Moreover, *pepr1 pepr2* double mutant plants display a reduced resistance to *Spodoptera littoralis* larvae (Huffaker, 2015; Klauser et al., 2015; Ross et al., 2014). In *Zea mays*, the precursor of *Zm*Pep3, an *At*Pep-ortholog, can be induced by insect oral secretion and insect HAMP. The application of *Zm*Pep3 can induce emission of some insect herbivory-related volatile organic compounds (VOCs), biosynthesis and accumulation of phytohormones and transcripts that are indirectly involved in defense against herbivores. *Zm*Pep3 also causes accumulation of proteinase inhibitor and contributes to the resistance to lepidopteran insects (Huffaker et al., 2013).

Systemin was the first peptide discovered in plants with signalling capacities. In *Solanum lycopersicum*, the injury-induced systemin can cause defense responses against insects (Orozcocardenas et al., 1993; Pearce et al., 1991). Tomato systemin is an endogenous peptide ligand composed of 18 amino acids, which is derived from a precursor protein by phytaspase-dependent cleavage at two aspartate residues (Beloshistov et al., 2018). Systemin induces proteinase inhibitors and activates phospholipase A2, thereby promoting the release of jasmonic acid precursors from the cell membrane. Induction of insect-resistance defense genes by jasmonic acid signalling pathways further contributes to the resistance of herbivore attack (Pearce et al., 1991), mediated by the LRR-RK receptor *Sl*SYR1, which, however, is not necessary for wound responses (Wang et al., 2018).

Hydroxyproline-rich systemins (HypSys) are systemin-like endogenous peptide ligands in *Solanaceae* plants. In addition to the hydroxyproline-rich conserved sequence, the HypSys precursor protein preproHypSys has a secretion sequence at the N-terminus, which is absent from Peps and systemin precursor proteins. Similar to systemin, HypSys induces the production of jasmonates and the expression of defense genes (Pearce, 2011). In petunia, HypSys is described to induce the expression of the immune gene *defensin1* (Pearce et al., 2007). The precursors of *Sl*HypSys I, II and III in tomato are synthesized and sequestered in the cell wall matrix of phloem parenchyma cells in response to systemin, wounding, and methyl jasmonate (Narváez-Vásquez et al., 2005). Moreover, the HypSys precursor gene *IbpreproHypSys* in sweet potato (*Ipomoea batatas*) can be induced by injury. The application of *Ib*HypSys in sweet potato induces downstream insect-resistance genes such as *sporamin* and *ipomoelin*, and improves the biosynthesis of lignin, to increase the ability to repel insects (Chen et al., 2008; Li et al., 2016). However, it is still unclear how HypSys binds to receptors and participates in defense responses.

Sweet potato is the fifth largest food crop in the world and has high nutritional and economic value. Several cultivars of sweet potato have higher insect resistance than others. For example, *I. batatas* cv. Tainong 57, which is widely cultivated in Taiwan, has strong insect resistance and represents a suitable model crop for studying insect resistance mechanisms (Meents et al., 2019). Sporamin, which was previously thought to be a unique storage protein in sweet potato tuberous roots, was recently described to be regulated by herbivore attack, injuries, jasmonic acid, and the homoterpene (*E*)-4,8–dimethyl–1,3,7-nonatriene (DMNT) in sweet potato leaves (Meents et al., 2019; Rajendran et al., 2014). Functional studies revealed that sporamin is a serine-type trypsin inhibitor, which acts in the insect intestine and retards insect growth and development (Imanishi et al., 1997; Yeh, Chen, et al., 1997). Transgenic *Nicotiana benthamiana* and *Brassica rapa* subsp. *chinensis* plants overexpressing sporamin demonstrated a strong pest resistance capacity (Chen et al., 2006; Yeh, Lin, et al., 1997), as did transgenic sweet potato plants overexpressing *IbNAC1*, which is a transcription factor (TF) binding to the sporamin wounding response element region of the *sporamin* promoter (Chen, Lin, et al., 2016). *Ib*NAC1 also regulates the jasmonic acid response and ROS signalling (Chen, Kuo, et al., 2016) and is regulated by TFs *Ibb*HLH3 and 4 (basic helix–loop–helix TF; aka MYC2, acting downstream of jasmonates), and *Ib*EIL1(ethylene-insensitive-like TF) as well as by *Ib*WIPK1 (wound-induced protein kinase) and *Ib*JAZ2 (jasmonate-ZIM domain protein, repressing MYC2), upon injury (Chen, Lin, et al., 2016). The MAPK pathway is also part of the signal transduction from wounding stress to *sporamin* expression (Chen, Lin, et al., 2016). However, the molecular connection between danger perception (ligands, receptors) and downstream defense responses is still elusive.

To discover the key players upstream of the intracellular signalling cascade leading to induced resistance against herbivores,

doi:10.6342/NTU202302113

we isolated candidates for both, a cell surface receptor and endogenous peptide ligands from sweet potato. Among the wound- and herbivore-induced genes in *I. batatas*, we detected a gene encoding a leucine-rich receptor kinase related to the plant elicitor peptide (Pep) receptor (PEPR) family, *Ib*LRR-RK1. When heterologously expressed in *N. benthamiana*, this receptor candidate did not provide responsiveness to HypSys but to extracts of damaged sweet potato leaf tissue. Finally, we identified the cognate peptide ligand, *Ib*Pep1, characterized the specificity and sensitivity of the new receptor/ligand-pair and compared the signalling capacities of the newly identified peptide with the previously described HypSys peptides.

2 | MATERIALS AND METHODS

2.1 | Plant material and growth conditions

Sweet potato scions (*I. batatas* Lam.; cultivar Tainong 57) were grown in phytochambers under long-day conditions (16 h light: 8 h dark) at 28°C (day) and 25°C (night) in 70% relative humidity for 3 weeks as previously described (Meents et al., 2019). When growing for 4–5 weeks, sweet potato and *N. benthamiana* plants were maintained in a greenhouse with a 16 h photoperiod and a 25°C/20°C day/night programme. *A. thaliana* ecotype Columbia-0 (Col-0) was grown at 22°C with an 8 h photoperiod in growth chambers for 4–5 weeks.

2.2 | Peptides

Peptides were ordered from GenScript Biotech (Leiden, Netherlands). They were dissolved before each experiment in BSA/NaCl (10 mg/mL, 0.1 M) solution. The list of peptides and their sequences can be found in Supporting Information: Table 1.

2.3 | RNA extraction and quantitative real-time polymerase chain reaction (qRT-PCR) analyses

Harvested sweet potato leaves were processed and used for qRT-PCR as described in (Meents et al., 2019) with the additional primer pairs for *IbLRR-RK1-5*, *sporamin*, *IbWIPK1*, *IbNAC1*, *IbCML1* (Supporting Information: Table 3) on a Bio-Rad CFX96 RT-PCR Detection System (Bio-Rad Laboratories).

2.4 | RNA-Seq analysis and processing

RNA from single third leaves treated for 1 h with *Ib*HypSysIV, *Ib*Pep1 and water (control) was extracted according to (Meents et al., 2019) using TRIzol Reagent (Invitrogen). Four biological replicates per treatment were used for RNA-Seq experiments conducted by Novogene Europe. RNA quality was monitored using NanoPhotometer® spectrophotometer (IMPLEN) and RNA Nano 6000 Assay Kit of the Bioanalyzer 2100 system (Agilent Technologies). A total of 1 μg of RNA per sample was used as template material for further sample preparations. Sequencing libraries were generated via NEBNext® UltraTM RNA Library Prep Kit for Illumina® (NEB) following manufacturer's instructions. A total of 20 M paired end reads of 150 bp per sample were generated, sequenced on an Illumina NovaSeq. A total of 6000 instrument. Raw reads were trimmed by in-house scripts. The clean reads were mapped onto *Ipomoea trifida* reference genome (http://sweetpotato.uga.edu/), using HISAT2 V2.0.5 with default parameter. HTSeq V0.6.1 software was used with the union mode to count read numbers mapped of genes for each sample.

R package from Bioconductor, DESeq. 2 V1.22.2 was used to estimate gene abundance and detect differentially expressed genes (DEGs) among the sample groups. A model based on the negative binomial distribution was carried out to determinate DEGs with an adjusted *p* value cutoff of 0.05 using the Benjamini-Hochberg correction. Genes with a log2-fold change ≥1 and *p*adj < 0.05 were considered as significantly DEGs. Gene ontology (GO) and Kyoto Encyclopaedia of Genes and Genomes (KEGG) pathway enrichment analyses of DEGs were implemented by the GOseq V1.34.1 R package and KOBAS V3.0 software.

2.5 | Wounding, insect feeding and peptide spray treatments

I. batatas and *N. benthamiana* plants with six to eight fully developed leaves were used in the study. For wound treatment, the third or fourth fully expanded leaves were wounded using tweezers and the wounded leaves samples were collected at different time points. For insect feeding treatment, starved *Spodoptera litura* larvae (second instar) were placed on the third or fourth fully expanded leaves and the treated leaves samples were collected at intervals.

To study the local effects of peptide solutions on DMNT emission and gene expression, whole sweet potato plants with six to eight fully expanded leaves were evenly sprayed with peptide solution or double-distilled water (control) until all leaves were fully covered in liquid. After a 1 h incubation period, single plants were placed for 24 h in 2.4 L glass desiccators (VWR international) for headspace volatile collection. For RNA-Seq, qRT-PCR and phytohormone analyses each third fully expanded leaf was locally sprayed with peptide solution or ddH_2O (control) and harvested together with the adjacent fourth leaf (systemic) after the indicated time points.

2.6 | VOC collection and quantification

Volatiles were collected over 24 h from peptide- or water-treated sweet potato plants enclosed in 2.4 L desiccators using the closed-loop stripping technique (Kunert et al., 2009). Throughout the headspace collection, each desiccator was connected to an air circulation pump (Fürgut GmbH) containing a charcoal trap with

doi:10.6342/NTU202302113

1.5 mg absorption material (CLSA filter, 6 cm long, 0.5 cm diameter, Gränicher & Quartero). After collection, volatiles were eluted and measured as described (Meents et al., 2019) with minor modifications. In this study, samples were eluted with 2 × 20 µL of dichloromethane containing 10 µg mL^{-1} *n*-bromodecane as internal standard used for further relative quantification.

2.7 | Cloning of receptor and propeptide gene candidates

*Ib*LRR-RK1 and *Ib*PROPEP1 genes were identified using blastn as well as tblastn on various databases using the receptor and propeptide sequences for Solanaceae plants from (Lori et al., 2015). Used databases included Sweet Potato Genomic Resource database (http://sweetpotato.plantbiology.msu.edu/index.shtml), *I. batatas* cv. TN57 transcriptome database (Rajendran et al., 2014), *I. batatas* database: Ipomoea Genome Hub (https://ipomoea-genome.org/), and NCBI (https://www.ncbi.nlm.nih.gov/). The *Ib*LRR-RK1 and *Ib*PROPEP1 coding sequences were amplified from sweet potato leaf cDNA using gene-specific primers (*Ib*LRR-RLK1_FL_F, *Ib*LRR-RLK1_FL_R, *Ib*PROPEP1_FL_F, *Ib*PROPEP1_FL_R, as shown in Supporting Information: Table 3) in a PCR reaction with Q5 High-Fidelity DNA Polymerase (NEB), respectively. The coding sequence encoding the tomato *Sl*PEPR1 (XP_004235511) was amplified using the primers *Sl*PEPR1_FL_F and *Sl*PEPR1_FL_R (Supporting Information: Table 3). All full-length coding sequences were cloned into the pCR8/GW/TOPO vector (Invitrogen). LR clonase (Invitrogen) was used to transfer these coding sequences from PCR8 to pMDC83 vectors (Curtis & Grossniklaus, 2003), generating C-terminal fusions with green fluorescent protein (GFP).

2.8 | Generation of chimeric receptors

Gene-specific level I modules for SYR1 (Wang et al., 2018) and *Ib*LRR-RK1 (see above) were generated by proofreading PCR (Phusion High Fidelity DNA Polymerase, ThermoFisher Scientific) from existing templates using the oligonucleotide primers listed in Supporting Information: Table 3, subcloned, and verified by sequencing. GoldenGate cloning was used to assemble the receptor expression constructs with general level I modules (A-B p35S (G005), D-E GFP (G011), E-F nos-T (G006) and dy F-G (BB09)) into the vector backbone LIIα F 1-2 (BB10) as described (Binder et al., 2014).

2.9 | Transient expression of receptor constructs and bioassays

Transient expression in *N. benthamiana* was performed as described (Albert et al., 2010). The oxidative burst was measured with leaf pieces floating on 100 µL water containing 20 µM L-012 (Wako) and 2 µg/mL horseradish peroxidase (Applichem), after addition of peptides, with a luminescence plate reader (Mithras LB 940, Berthold, or Infinite M200 PRO plant reader, TECAN). The amount of ethylene was measured by GC in the headspace of four leaf pieces floating on 500 µL water, treated for 4 h with the peptides or controls. Transient co-expression of the pFRK1:Luciferase reporter (Yoo et al., 2007) with the receptor expression constructs in mesophyll protoplasts of *A. thaliana* Col-0 wild-type was performed as described (Wang et al., 2016). Luminescence was recorded for up to 6 h in W5-medium containing 200 µM firefly luciferin (Synchem UG) after overnight incubation for 14 h and subsequent treatment with peptides or control solution.

2.10 | Subcellular localization

The *Ib*LRR-RK1-GFP, *Ib*PROPEP1-GFP, the tonoplast localization marker protein fusion γ-Tip-mCherry (Nelson et al., 2007) were transiently expressed in *N. benthamiana* leaves and *A. thaliana* mesophyll protoplast as described above. The plasma membrane marker PIP2A-mCherry was expressed in *N. benthamiana* leaves. Plasmolysis was induced by infiltration of 1.0 M mannitol before fluorescence images were taken. Fluorescence images were taken using a TCS SP5 Confocal microscope (Leica) and analyzed by LAS AF Lite application software (Leica) or a Zeiss Axio Zoom.V16.

2.11 | Crude endogenous ligand extraction

According to (Chien et al., 2015), 10 g injured and noninjured sweet potato leaves were harvested, respectively. Samples were homogenized with 1% cold trifluoroacetic acid (TFA) in a blender for 2 min. After filtering the extracts through four layers of Miracloth to remove plant debris and centrifuging at 8500 rpm for 20 min at 4°C, the supernatant was slowly pressed through a customized Sep-Pak C18 solid phase extraction cartridge (Waters) and eluted with 60% (v/v) methanol/0.1% (v/v) TFA. The eluate-containing peptides were dried in a speed vac and resuspended in 200 µL double-distilled H_2O.

2.12 | Phytohormone extraction and quantification

Local and systemic leaves collected after 1 h peptide treatment were extracted and measured as described (Meents et al., 2019) using an Agilent 1200 HPLC system (Agilent) with subsequent API 5000 tandem mass spectrometer (Applied Biosystems) equipped with a Turbo spray ion source employed in negative ionization mode.

2.13 | Statistical analysis

Data generated using qRT-PCR was analyzed as described in (Meents et al., 2019) followed by a Shapiro–Wilk normality test with

doi:10.6342/NTU202302113

subsequent t-test or Mann–Whitney rank sum test based on the data distribution. Phytohormone levels were analyzed using a two-way analysis of variance with initial Shapiro–Wilk-normality and equal variance test. For all analyses, phytohormone content was set as the dependent variable with treatment and leaf type as independent variables. For identification of significant differences between groups, pairwise multiple comparison procedure via the Holm–Sidak method was implemented with a significance level of $p < 0.05$. All statistical analyses were conducted in SigmaPlot (V 11.0).

3 | RESULTS

3.1 | Sweet potato encodes putative DAMP receptors

We based our search for receptors of sweet potato which are involved in responses to wounding and herbivore attack on published sequences for DAMP-related receptors in Arabidopsis (*At*PEPR1/2: AT1G73080/AT1G17750) and tomato, *S. lycopersicum* (*Sl*SYR1/2: *Solyc*03g082470/Solyc03g082450.2.1; *Sl*PEPR1: XP_004235511). Several closely related receptor genes, designated *ItLRR-RK1–ItLRR-RK13*, were mined from the *I. trifida* 'Sweet potato Genomic Resource database' (http://sweetpotato.plantbiology.msu.edu/index.shtml) (Supporting Information: Figure 1). Next, two transcriptomic databases, that is, the *I. batatas* cv. Tainong 57 transcriptome database (Rajendran et al., 2014) and *I. batatas* database, *Ipomoea* Genome Hub (https://ipomoea-genome.org/) were accessed to explore putative *LRR-RK* genes with sequence homology to *ItLRR-RKs*. Five putative *I. batatas* RK genes (*IbLRR-RK1* to *IbLRR-RK5*) were identified. Analysis by qRT-PCR experiments revealed that wound treatment did not induce the upregulation of *IbLRR-RK2* - *IbLRR-RK5* while both wounding and insect herbivory rapidly induced *IbLRR-RK1* (MT210638) (Figure 1a,b). Upon wounding and treatment with *Spodoptera* larvae-derived oral secretion, the relative expression level of *IbLRR-RK1* increased nearly 30-fold at 15 min, 12-fold at 30 min, and returned to normal levels at 60 min. Herbivory feeding also increased *IbLRR-RK1* expression level 5.4-fold at 15 min and 1.7-fold at 30 min (Figure 1b). These data demonstrate that mechanical wounding and herbivory induce the receptor-like kinase *Ib*LRR-RK1, suggesting that this receptor might be involved in perception of a wound-related signal.

3.2 | The receptor candidate *Ib*LRR-RK1 is related to PEPRs

The gene *IbLRR-RK1* from *I. batatas* cv. Tainong 57 encodes a typical member of the PEPR family. It consists of an ectodomain composed of a signal peptide, an N-terminal cap region typically found in plant LRR-RKs, 26 repetitions of the plant-specific version of the LRR motif, and an outer juxtamembrane; this is followed by a transmembrane domain; the cytosolic part contains the inner juxtamembrane domain and a serine/threonine kinase domain (Supporting Information: Figure 2). As expected, the GFP-tagged *Ib*LRR-RK1 protein, transiently expressed in either *A. thaliana* protoplasts or *N. benthamiana* leaves, localized to the plasma membrane (Figure 1c), like other plant LRRs such as *Sl*SYR1-GFP or *At*EFR-GFP, which were used as positive controls. *Ib*LRR-RK1 is most likely related to PEPRs from tomato (XP_004235511, *Sl*PEPR1) and Arabidopsis (*At*1g73080, *At*1g17750; PEPR1 and PEPR2; Supporting Information: Figure 3). *Ib*LRR-RK1, which is 97% identical with *It*LRR-RK1, shared 65% or 50% identical amino acid residues to *Sl*PEPR1 or *At*PEPR1, respectively, and 35% identity to *Sl*SYR1, while other putative RLK members selected from the Sweet Potato Databases never shared more than 36% identity to either of the mentioned receptors (Table 1). In addition, comparing the extracellular domains of different receptors also showed that *Ib*LRR-RK1 has a highly similar ligand-binding surface when compared with *Sl*PEPR1 and *At*PEPR1 (60% and 48% identity, respectively), and shares only 36% identical residues with tomato *Sl*SYR1 (Table 2). Thus, *Ib*LRR-RK1 is part of the plant elicitor peptide receptor (PEPR) group.

3.3 | *Ib*LRR-RK1 is a functional receptor

Establishing the functionality of new receptor candidates for which the ligands are not known is challenging, and can be overcome by approaches in which chimeric versions are ectopically expressed in suitable plants (Albert et al., 2010; Butenko et al., 2014). To test if the kinase domain of the putative receptor from sweet potato is able to feed into the immune response pathway, we generated a chimeric version with the ectodomain of tomato SYR1 a receptor with known ligand (Supporting Information: Figure 4a). The chimeric receptor SYR1-*Ib*K as well as the original *Ib*LRR-RK1 and SYR1 were transiently expressed in leaves of *N. benthamiana*. The GFP-tagged recombinant proteins localized to the cell surface, as predicted (Figure 1c, Supporting Information: Figure 4b). Treatment with the ligand of SYR1 resulted in the induction of an oxidative burst for the SYR1-*Ib*K expressing leaf pieces (Figure 2a, Supporting Information: Figure 4c), proving the functionality of the kinase domain of *Ib*LRR-RK1. Several other defense-related peptides from various plants such as *Sl*Pep6, *Sl*HypSysIII, *Ib*HypSysIV or *At*Pep1 were applied in addition to systemin (Supporting Information: Table 1) in bioassays with leaves expressing either the original *Ib*LRR-RK1 or SYR1-*Ib*K. Interestingly, *Sl*Pep6 triggered the defense pathway in the presence of *Ib*LRR-RK1, leading to ROS production and ethylene accumulation (Figure 2b,c). We then verified the recognition of *Sl*Pep6 by *Ib*LRR-RK1 in protoplasts, generated from *A. thaliana* Col-0 mesophyll cells. *FRK1* (flg22-induced receptor-like kinase 1) is a PTI marker gene of early defense responses in Arabidopsis (Asai et al., 2002) and its promoter is widely used in combination with a luciferase reporter gene to monitor PAMP activity (Yoo et al., 2007). The co-expression of *Ib*LRR-RK1 with p*FRK1:LUC* resulted in *Sl*Pep6-dependent induction of the reporter (Figure 2d), confirming the previous experiments

doi:10.6342/NTU202302113

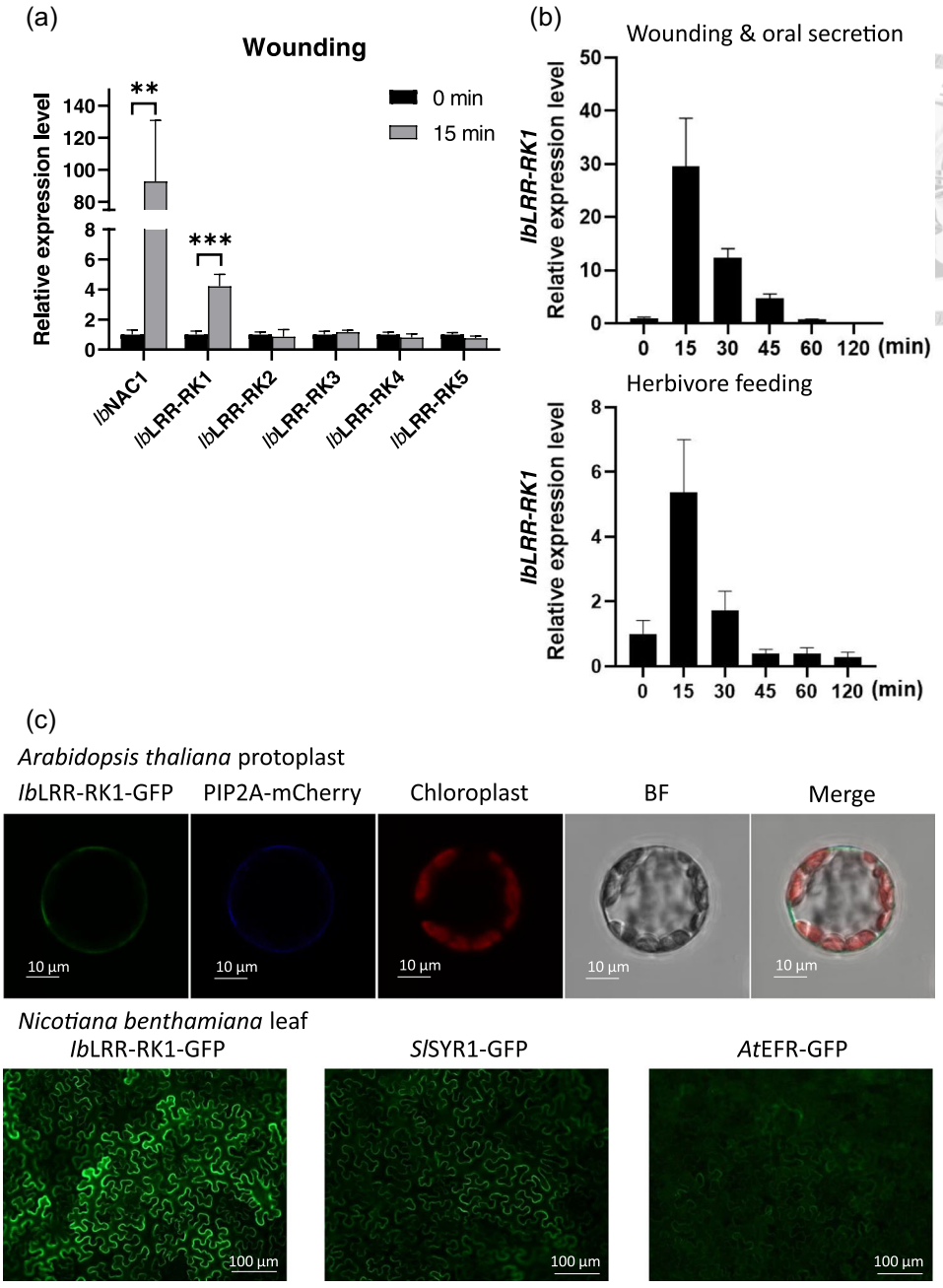

FIGURE 1 Receptor kinase *Ib*LRR-RK1 is induced by wounding and herbivory in sweet potato leaves. (a) The expression pattern of *IbLRR-RK1*–*IbLRR-RK5* receptor-like genes in response to wounding in sweet potato leaves. *IbActin1* expression was used as internal control, and *IbNAC1* was used as positive control of wounding by quantitative real-time polymerase chain reaction (RT-PCR). Bars and error bars represent mean ± SD of $n = 4$. (b) Sweet potato leaves were wounded and treated with *Spodoptera litura* larvae oral secretion, or exposed to feeding *S. litura* larvae. Expression of *Ib*LRR-RK1 was analyzed by qRT-PCR. Bars and error bars represent mean ± SD of $n = 4$. (c) Cell surface localization of the green fluorescent protein (GFP)-tagged *Ib*LRR-RK1 in transiently transformed *Arabidopsis thaliana* protoplasts or *Nicotiana benthamiana* leaf samples, observed by confocal microscope (TCS SP5 Confocal; Leica); PIP2A (plasma membrane-intrinsic protein 2A) and well-studied plasma membrane-localized receptor proteins (SYR1 from tomato and EFR from *A. thaliana* (Wang et al., 2018; Zipfel et al., 2006) were used as positive controls in *A. thaliana* and *N. benthamiana*, respectively.

in *N. benthamiana*, while the chimeric receptor SYR1-*Ib*K recognized systemin, but not *Sl*Pep6 (Figure 2e). Taken together, we demonstrated that the activation of *Ib*LRR-RK1 can trigger plant immune responses such as ROS burst, ethylene biosynthesis, and defense gene expression and identified a heterologous ligand.

3.4 | *Ib*LRR-RK1 perceives an endogenous peptide

For the molecular identification of the cognate ligand of *Ib*LRR-RK1 we took advantage of the fact that *Sl*Pep6 was functional in activating sweet potato *Ib*LRR-RK1. We hence used the sequence of *Sl*Pep6 and

doi:10.6342/NTU202302113

TABLE 1 Comparison of the full-length amino acid sequence of *Ib*LRR-RK1 with related sequences, calculation of % identity by Vector NTI.

	*It*LRR-RLK1	*Sl*PEPR1	*At*PEPR1	*At*PEPR2	*Sl*SYR1	*Sl*SYR2
*Ib*LRR-RK1	97	65	50	49	36	35
*It*LRR-RK1		64	50	49	36	35
*Sl*PEPR1			51	48	35	35
*At*PEPR1				66	36	34
*At*PEPR2					36	35
*Sl*SYR1						79

Abbreviations: At, *Arabidopsis thaliana*; Ib, *Ipomoea batatas*; It, *Ipomoea trifida*; Sl, *Solanum lycopersicum*.

TABLE 2 Comparison of the amino acid sequence of the extracellular domain of *Ib*LRR-RK1 with *At*PEPR1, *Sl*PEPR1 and *Sl*SYR1, calculation of % identity by Vector NTI.

	*Sl*PEPR1	*At*PEPR1	*Sl*SYR1
*Ib*LRR-RK1	60	48	36
*Sl*PEPR1		49	36
*At*PEPR1			36

Abbreviations: At, *Arabidopsis thaliana*; Ib, *Ipomoea batatas*; Sl, *Solanum lycopersicum*.

other Peps from the Solanaceae family as probes to search for endogenous peptides and applied scanning sequence pattern and tBlastn strategies on the sweet potato genomic resource database and the *Ipomoea* genome hub database (Supporting Information: Figure 5). Two putative Peps were selected from the *I. trifida* genomic resource database. The 23 C-terminal residues of the precursor protein *It*PROPEP1 (itf01g30920.t1) were selected according to the general length of Peps (Lori et al., 2015) and named *It*Pep1 (LSSRPPRP GLGNSGDPQTNDTSS) (Supporting Information: Figure 5b). The putative *It*Pep2 (RRGRTPPRPENLKLNLRARKHSLEDQ), containing a typical, conserved peptide motif of Peps (RRGRXP), was derived from the C-terminus of *It*PROPEP2 (itf07g21780.t1) (Supporting Information: Figure 5c). Both candidate peptides, *It*Pep1 and *It*Pep2, were synthesized and applied to *N. benthamiana* leaf discs transiently expressing *Ib*LRR-RK1. *It*Pep1, but not *It*Pep2, activated an *Ib*LRR-RK1-dependent ROS burst (Figure 3a), and neither peptide elicited a response in the SYR1-*Ib*K or p19 controls (Supporting Information: Figure 6a,b). Next, the cDNA of the *PROPEP1* gene from *I. batatas* cv. TN57 was cloned by RT-PCR using oligonucleotides deduced from *ItPROPEP1*. The CDS encompasses 378 bp and 125 deduced amino acid residues with a calculated molecular weight of 13.25 kDa, and a pI of 4.44. The putatively bioactive 23-mer peptide, *Ib*Pep1, corresponds to the C-terminus of the precursor protein and is 100% identical to the one from *It*PROPEP1 (Supporting Information: Figure 6c). As expected, the *I. batatas* PROPEP as well as the Pep amino acid sequences are more closely related to those from solanaceous plants than to those of Arabidopsis (Supporting Information: Figure 6d, Supporting Information: Table 2).

3.5 | *Ib*LRR-RK1 perceives *Ib*Pep1 with high sensitivity and specificity

Exploiting the same heterologous expression system described above we interrogated the sensitivity and the specificity of the putative ligand/receptor-pair. The dose-dependent induction of ROS by *Ib*Pep1 was clearly detectable in the subnanomolar range and the half-maximal activation of this output was estimated at 1 nM (Figure 3b). The tomato Pep (*Sl*Pep6) was 10-times less efficient in this bioassay with *Ib*LRR-RK1 (Figure 3b). In the reciprocal approach, we cloned the Pep receptor of tomato (*Sl*PEPR1, (Lori et al., 2015)), expressed it in *N. benthamiana* and compared the efficiencies of the Peps for the induction of ROS. The tomato PEPR/*Sl*Pep6 pair showed the same efficiency as the corresponding sweet potato pair, with an EC_{50} value of 1 nM. Interestingly, *Sl*PEPR1 also recognized the peptide from sweet potato, albeit with a much lower sensitivity, and an estimated EC_{50} value above 100 nM (Figure 3d).

N-terminal and C-terminal truncated versions of *Ib*Pep1 were synthesized to investigate the specificity for the predicted sweet potato peptide on *Ib*LRR-RK1 (Figure 3c). Deleting up to three N-terminal residues did not have a major impact on the perception, the loss of arginine at position 4, however, led to a severe increase of the EC_{50} value (either when deleted as in *Ib*Pep1 (5–23) or when changed to an alanine as in *Ib*Pep1 (A4)). In contrast, the C-terminus needs to be present for a sensitive perception although the last two serine residues can be replaced by alanine (*Ib*Pep1 (A22A23)).

3.6 | *Ib*PROPEP1-GFP is mainly localized with the tonoplast

We expressed *IbPROPEP1* (OP311829) as a C-terminal fusion with GFP in *N. benthamiana* and *A. thaliana* protoplasts and observed the localization of the protein by confocal microscopy. *Ib*PROPEP1-GFP not only localized with the tonoplast (Figure 4) as reported for *At*PROPEP1-YFP (Hander et al., 2019), but also aggregated into bright small globular structures, resembling bulbs (Saito et al., 2002), inside the vacuole of Arabidopsis mesophyll protoplasts. Similarly, in *N. benthamiana*, *Ib*PROPEP1-GFP mainly accumulated in the tonoplast and aggregated into several small globular structures, which

doi:10.6342/NTU202302113

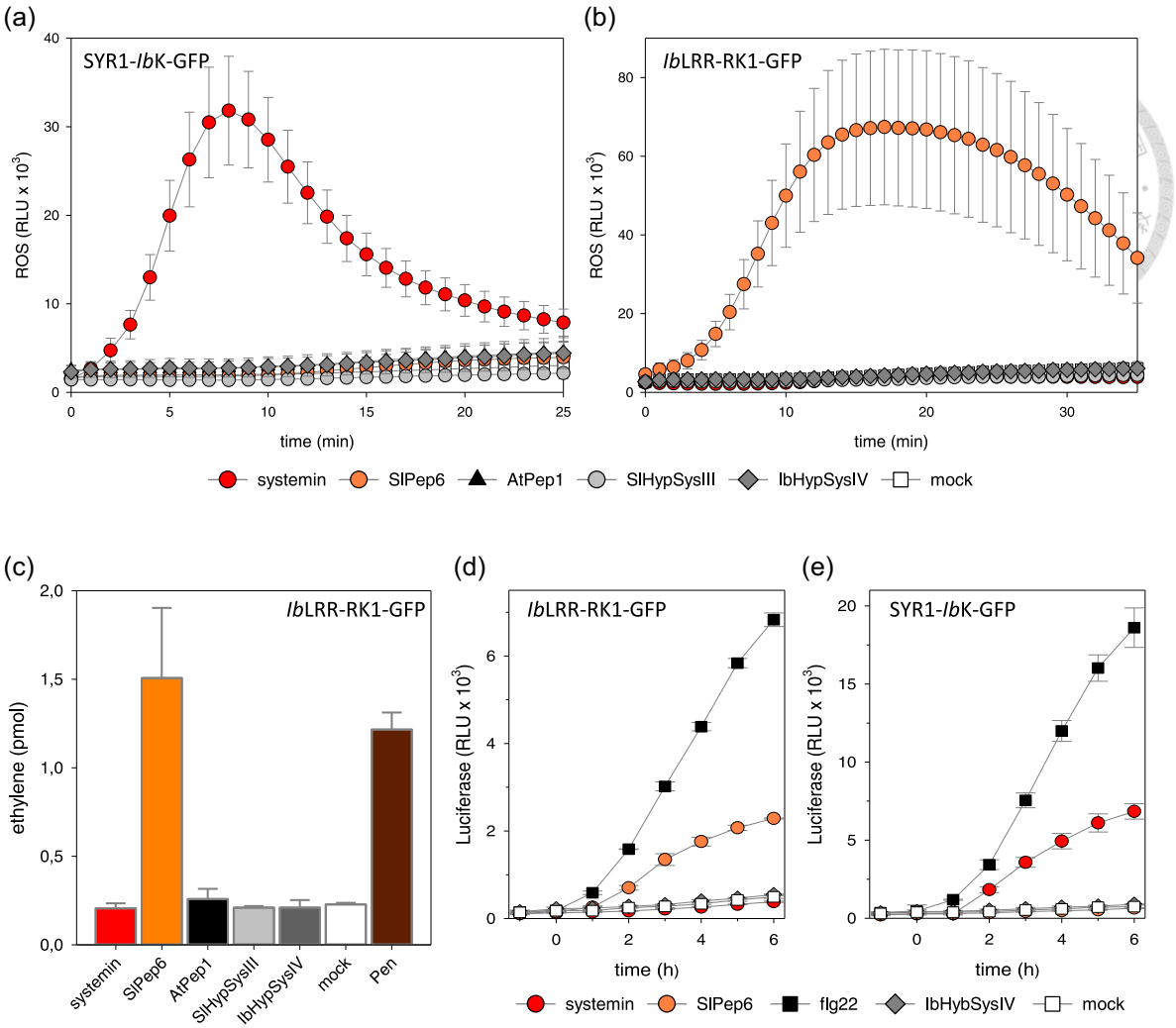

FIGURE 2 Activation of *Ib*LRR-RK1 by *Sl*Pep6 from tomato induces various immune responses. ROS burst in *Nicotiana benthamiana* leaves transformed with either SYR1-*Ib*K (a) or *Ib*LRR-RK1 (b) was induced with 1 μM systemin (red circles), *Sl*Pep6 (orange circles), *At*Pep1 (black triangles), *Sl*HypSysIII (grey circles), *Ib*HypSysIV (dark grey diamonds) or the control (BSA/NaCl, open squares). Values and error bars represent mean ± SE of $n = 4$ replicates. (c) Ethylene production in *Ib*LRR-RK1-expressing leaf discs of *N. benthamiana* was induced with the same selection of peptides at 1 μM, 90 ng/μL Pen extract (Thuerig et al., 2005) was used as a positive control. Values and error bars represent mean ± SD of $n = 3$ replicates. Mesophyll protoplasts from *Arabidopsis thaliana* Col-0 were co-transformed with either SYR1-*Ib*K (d) or *Ib*LRR-RK1 (e) and the reporter construct (pFRK1:luciferase), or with pFRK1:luciferase only (Supporting Information: Figure 4e). Induction of luminescence was monitored after treatment with either 10 nM flg22 (black squares, positive control), systemin (red circles), *Sl*Pep6 (orange circles) or *Ib*HypSysIV (dark gray diamonds) at time point 0, mock control is shown with white squares. Values and error bars represent mean ± SD of $n = 2$. [Color figure can be viewed at wileyonlinelibrary.com]

moved inside the vacuole (Supporting Information: Figure 7, Supporting Information: Movie 1).

3.7 | An *Ib*LRR-RK1-activating DAMP is present in sweet potato leaves

It has been demonstrated that PROPEPs are cleaved by wounding-activated proteases to release immunomodulatory Peps (Bartels & Boller, 2015; Hander et al., 2019). To simulate a corresponding scenario, we first prepared an extract from *I. batatas* cv. TN57 leaves and applied it on transiently *Ib*LRR-RK1-expressing *N. benthamiana* leaves. Leaf discs expressing the receptor responded to the treatment with the partially purified leaf extract with a ROS burst, which was not detectable in control leaves transformed with p19 only (Figure 5a). Next, in addition to tissue disruption to get the extract, we damaged the sweet potato leaves beforehand by squeezing them with tweezers and waiting for 10 min. This material was then harvested, in parallel to tissue from nontweezer-treated control plants. Interestingly, the elicitor activity was higher in extracts from wounded leaves in comparison to the directly extracted leaves. This activity clearly depended on the expression of *Ib*LRR-RK1

doi:10.6342/NTU202302113

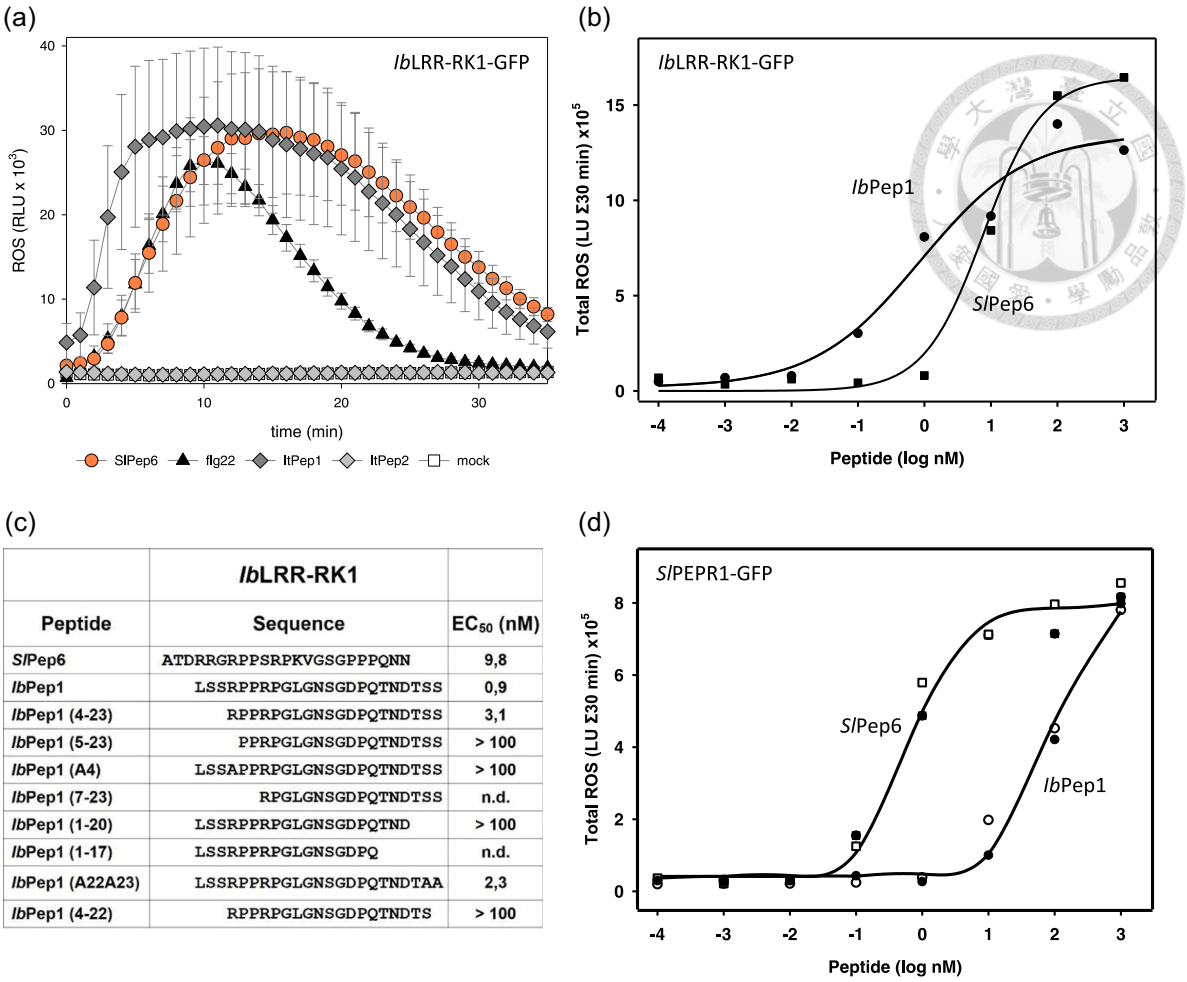

(c)

	IbLRR-RK1	
Peptide	Sequence	EC_{50} (nM)
*Sl*Pep6	ATDRRGRPPSRPKVGSGPPPQNN	9,8
*Ib*Pep1	LSSRPPRPGLGNSGDPQTNDTSS	0,9
*Ib*Pep1 (4-23)	RPPRPGLGNSGDPQTNDTSS	3,1
*Ib*Pep1 (5-23)	PPRPGLGNSGDPQTNDTSS	> 100
*Ib*Pep1 (A4)	LSSAPPRPGLGNSGDPQTNDTSS	> 100
*Ib*Pep1 (7-23)	RPGLGNSGDPQTNDTSS	n.d.
*Ib*Pep1 (1-20)	LSSRPPRPGLGNSGDPQTND	> 100
*Ib*Pep1 (1-17)	LSSRPPRPGLGNSGDPQ	n.d.
*Ib*Pep1 (A22A23)	LSSRPPRPGLGNSGDPQTNDTAA	2,3
*Ib*Pep1 (4-22)	RPPRPGLGNSGDPQTNDTS	> 100

FIGURE 3 *Ib*LRR-RK1 recognizes sweet potato *Ib*Pep1 with high sensitivity and specificity. ROS burst in *Nicotiana benthamiana* leaves transformed with p19 plus *Ib*LRR-RK1-GFP, (a) in response to 1 μM of *Sl*Pep6, *It*Pep1, *It*Pep2, 10 nM flg22 or BSA/NaCl (mock), respectively, and, (b) in response to the indicated concentrations of *Ib*Pep1 (●) and *Sl*Pep6 (■). Values and error bars in (a) represent mean ± SE of $n = 4$. (c) Sequences and specific ROS-inducing activities of various peptide derivatives of *Ib*Pep1 used in this study. EC_{50} values indicate concentrations required for induction of half-maximal ROS production in *N. benthamiana* leaves expressing *Ib*LRR-RK1-GFP. (d) Dose-response curves for *Sl*PEPR1-GFP treated with of *Ib*Pep1 (●) and *Sl*Pep6 (■), filled and open symbols correspond to independent experiments. Data in (b) and (d) correspond to the integrated ROS response over 30 min. Curve fittings and calculation of EC_{50} values were performed by nonlinear regression. [Color figure can be viewed at wileyonlinelibrary.com]

(Figure 5b). These data indicated that crude extracts of *I. batatas* leaves contain ligands for *Ib*LRR-RK1 that might accumulate upon wounding stress.

3.8 | *Ib*Pep1 and *Ib*HypSysIV activate complementary signalling cascades

We next addressed the question whether *Ib*Pep1 is involved in herbivore resistance responses in sweet potato or in other processes. Therefore, whole sweet potato plants were sprayed with 25 μM *Ib*Pep1 and analyzed for the induction of *sporamin* and other defense related genes well-known from former studies (Chen, Lin et al., 2016). For comparison, the synthetic hydroxyproline-rich glycopeptide *Ib*HypSysIV, which was shown to activate *sporamin* expression (Chen et al., 2008) was tested at 25 μM as well. The qRT-PCR analyses after 30 min and 1 h of incubation revealed HypSys-dependent transient increases of sporamin (X60930.1) (16-fold), *Ib*NAC1 (GQ280387.1) (22-fold) and *Ib*WIPK1 (HQ434622) (68-fold) transcript levels (Figure 6a), confirming the ability of HypSys peptides to rapidly trigger sporamin-related signalling cascades. In contrast, *Ib*Pep1 transiently induced *sporamin* only 3.5-fold after 30 min, while *Ib*NAC1 and *Ib*WIPK1 were induced to higher and longer-lasting expression levels compared to *Ib*HypSysIV treatment (Figure 6b). Moreover, when analyzing other defense-related genes we also found that *Ib*Pep1 and *Ib*HypSysIV treatments increased the expression of *Ib*LRR-RK1 and *Ib*CML1 (calmodulin-like protein1; OP311828) (Figure 6a,b). Further, compared to water controls and *Ib*Pep1, the application of *Ib*HypSysIV resulted in a significantly increased emission of the wound-inducible volatile DMNT (Figure 6c) (Meents et al., 2019). Scions incubated with the tomato-derived peptide

doi:10.6342/NTU202302113

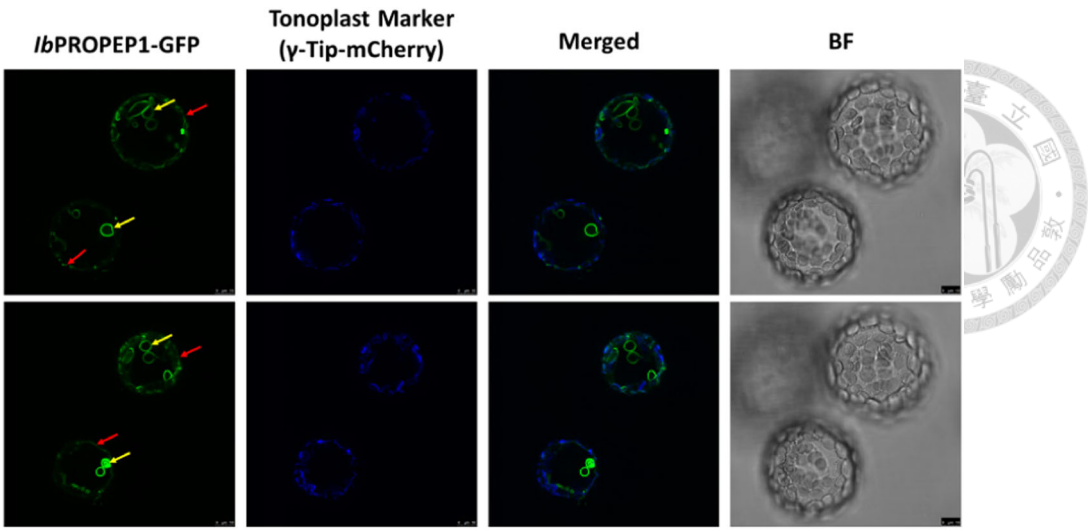

FIGURE 4 *Ib*PROPEP1 mainly localizes to the tonoplast. *Ib*PROPEP1-GFP was transiently transformed in *Arabidopsis thaliana* protoplasts, and protoplasts were observed to monitor the subcellular localization of *Ib*PROPEP1 by confocal microscopy. Partial colocalization with the tonoplast marker γ-Tip-mCherry was observed. The red arrows indicate the position of the tonoplast and the yellow arrows indicate the bulb structures. See Supporting Information: Movie 1 for the observation of moving green fluorescent protein (GFP)-labeled vesicles.
[Color figure can be viewed at wileyonlinelibrary.com]

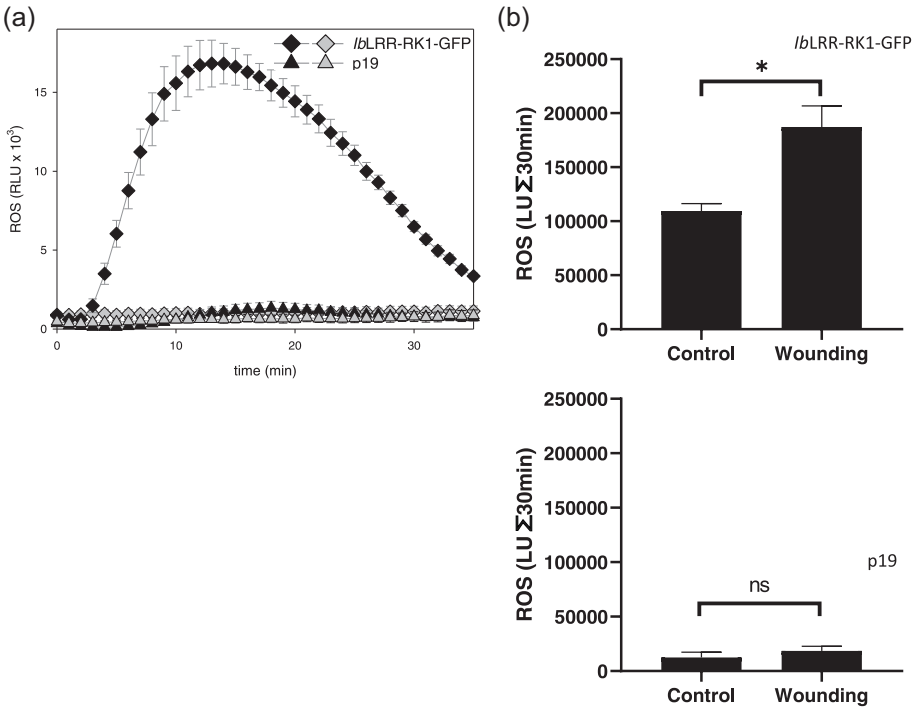

FIGURE 5 *Ib*LRR-RK1 recognizes an endogenous compound. (a) A partially purified extract from *Ipomoea batatas* leaves induces a ROS burst in *Nicotiana benthamiana* leaves expressing *Ib*LRR-RK1 (♦). The extract (black symbols, 1 µL) did not induce a response in leaf pieces transformed with p19 only (▲). Mock treatments are shown in gray symbols. Values and error bars represent mean ± SE of $n = 4$. (b) ROS burst (integrated over 30 min) in *N. benthamiana* control leaves (p19) or leaves expressing *Ib*LRR-RK1 in response to 1 µL partially purified extract from unwounded (control) or 10 min wounded sweet potato leaves. Bars and error bars represent mean ± SE of $n = 4$.

*Sl*Pep6 or an inactive scrambled peptide only displayed basal DMNT levels comparable to the control treatment, confirming thereby the functionality of the peptide application method and the (species-) specificity of the *Ib*HypSysIV elicitor.

To elucidate which role peptides play within the *Ipomoea* defense framework, local and systemic TN57 leaves were analyzed for phytohormone levels after peptide treatment. In comparison to water-treated controls, no significant differences in local and

doi:10.6342/NTU202302113

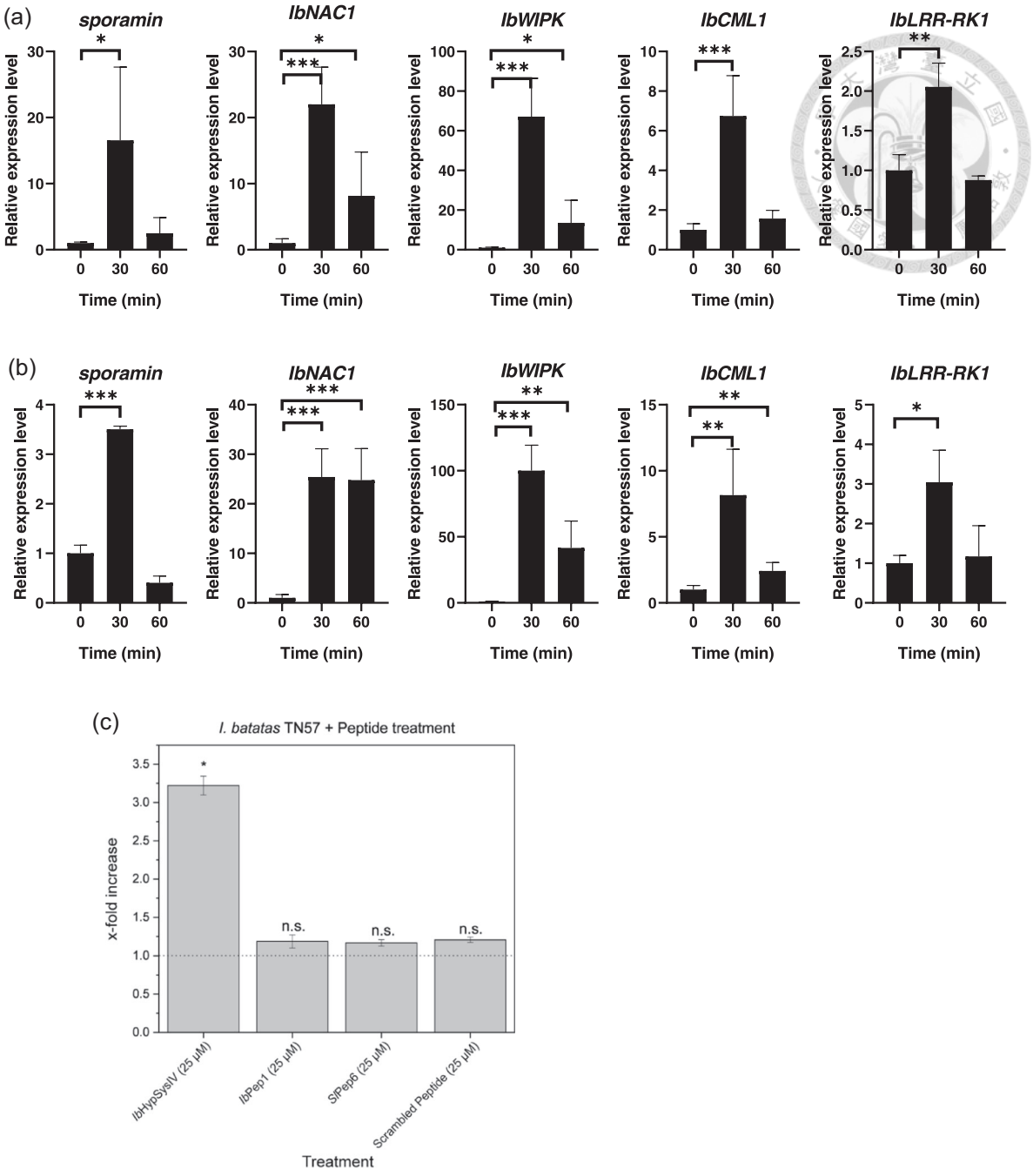

FIGURE 6 Induction of defense-related genes and volatiles in response to *Ib*Pep1 and *Ib*HypSysIV in sweet potato. Sweet potato leaves were treated with 25 µM of *Ib*HypSysIV (a) or *Ib*Pep1 (b), respectively, and tested for the expression level of herbivore defense-related genes. Expression of *sporamin*, *IbNAC1*, *IbWIPK1*, *IbCML1* and *IbLRR-RK1* were analyzed by quantitative real-time polymerase chain reaction (RT-PCR). Bars and error bars represented mean ± SE of $n = 4$. Significance levels are $^{*}p < 0.05$; $^{**}p < 0.01$; $^{***}p < 0.001$, respectively, according to one-tailed *t*-test. (c) The induced emission of (*E*)-4,8–dimethyl–nonatriene (DMNT) in *Ipomoea batatas* TN57 was evaluated after treatment of whole plants with 25 µM *Ib*HypSysIV ($n = 10$), *Ib*Pep1 ($n = 10$), *Sl*Pep6 ($n = 11$), or the scrambled peptide ($n = 7$), data are shown as fold-induction in comparison to the respective water controls. Bars represent the mean ± SE of DMNT emission. Significance levels are indicated by the asterisks (n.s. = not significant; $^{*}p < 0.05$) and are based on a Shapiro–Wilk normality test followed by a Mann–Whitney rank sum test.

systemic jasmonic acid concentrations could be observed after *Ib*HypSysIV treatment (Supporting Information: Figure 8a). Interestingly, *Ib*HypSysIV-treated leaves showed a significantly increased amount of bioactive JA-Ile, however, only locally (Supporting Information: Figure 8b). For the stress-related hormones SA and ABA, no significant differences to control treatments were detected, except for a local decrease in SA concentrations upon contact with *Ib*HypSysIV (Supporting Information: Figure 8c). Treatment with *Ib*Pep1 did neither alter jasmonate nor SA levels although low concentrations might mask possible effects. However, exposure to

doi:10.6342/NTU202302113

*Ib*Pep1 resulted in decreasing amounts of ABA, mainly observed in the local leaf (Supporting Information: Figure 8d). Although no tremendous changes in phytohormone levels were overall visible, we noted a clear tendency that for phytohormones regulated by *Ib*HypSysIV, no response would occur during exposure to *Ib*Pep1 and vice versa.

3.9 | RNAseq of *I. batatas* reveals DEGs upon *Ib*Pep1 and *Ib*HypSysIV treatment

To better understand the similarities between *Ib*Pep1 and *Ib*HypSysIV and their particular functionalities, RNAseq experiments were conducted on single leaves treated with either peptide or water (control), respectively, for 1 h (Figure 7). Overall, 29385 expressed genes were detected based on mapping onto the *I. trifida* reference genome from which 27521 were shared among all treatments including control samples. A total of 261 genes were exclusively detected upon *Ib*HypSysIV treatment, while 383 transcripts were detected only after *Ib*Pep1 treatment. An additional number of 356 common transcripts was found in both peptide treatments but not in the control (Figure 7a). Strikingly, 253 expressed genes were mapped onto the *I. trifida* genome but found only in control plants, suggesting that expression of these genes is reduced upon peptide treatments.

Further, spraying of *Ib*HypSysIV induced significant upregulation of 261 genes, whereas 294 genes were significantly downregulated, compared to water-treated control leaves (data not shown). Upon *Ib*Pep1 incubation, an even stronger response was observed with 769 genes up- and 706 downregulated (data not shown). A comparison of both peptide treatments revealed that 1923 genes were significantly differentially regulated due to these different treatments, 889 up- and 1034 downregulated, when *Ib*HypSysIV versus IbPep1 was compared (Figure 7b). These results support the idea that the two sweet potato peptides have distinct functions, which may be based on their ability to regulate different genes. To support this hypothesis, further confirmation with KEGG and GO pathway analyses and qPCR of selected genes is necessary and will be performed. All original RNAseq data are available (NCBI; accession GSE227409).

4 | DISCUSSION

Recent evidence has shown that sweet potato exhibits DAMP-mediated activation of defenses. The volatile homoterpene, DMNT, has been demonstrated to activate resistance mechanisms in leaves leading to protection against herbivore feeding (Meents & Mithofer, 2020; Meents et al., 2019). Peptide-based activation of defense reactions also has been observed in sweet potato (Chen et al., 2008). However, the biological significance and interconnection with induced resistance against insects remained unclear. This study provides evidence for the existence of a Pep/PEPR-like system in sweet potato and investigates the input- and output conditions.

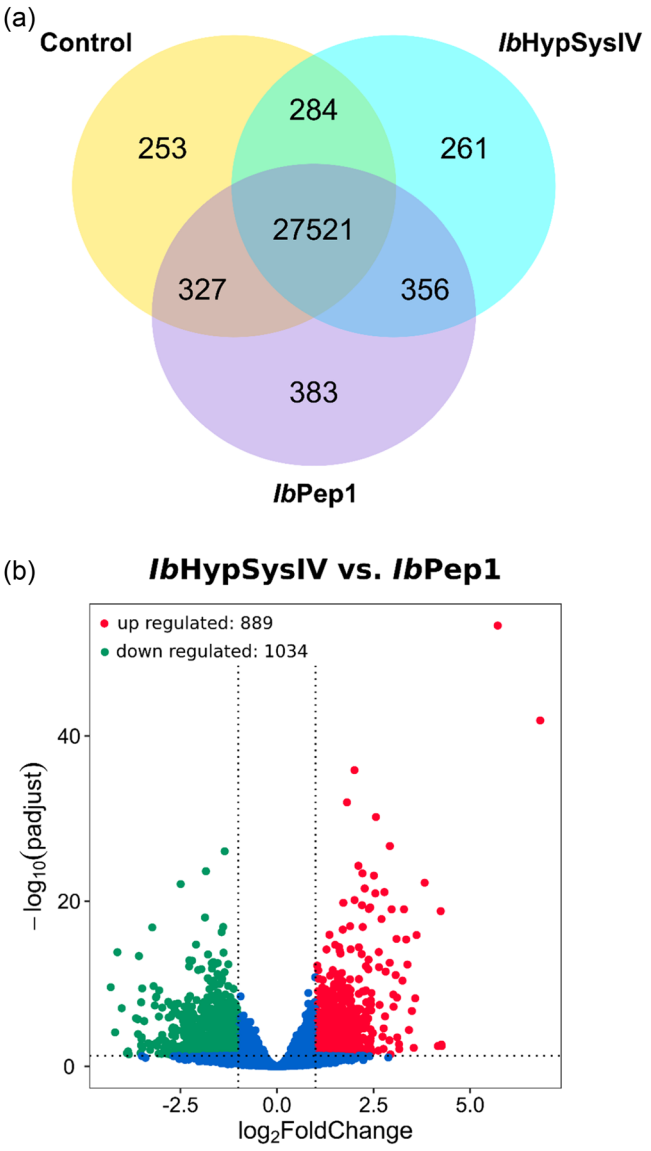

FIGURE 7 *Ib*Pep1 and *Ib*HypSysIV peptides differentially alter gene expression patterns in sweet potato leaves. (a) RNAseq data from *Ipomoea batatas* leaves, treated with 25 µM *Ib*HypSysIV, *Ib*Pep1 or ddH2O (control) for 1 h were mapped onto the *Ipomoea trifida* genome. The Venn diagram shows the numbers of identified, expressed genes in each treatment (Σ 29385 genes). Overlapping circle parts represent the shared expressed genes between the treatments. (b) Volcano plot of statistical significance (-log10 adj. $p > 1.3$, corresponds to adj. $p < 0.05$) against differentially expressed genes (DEGs, log2-fold change ≥1 and $p$adj < 0.05), by comparing both peptide treatments (25 µM each peptide, 1 h). The number of significantly upregulated genes (*Ib*HypSys vs. *Ib*Pep1) is indicated in red with the downregulated ones highlighted in green. DEGs not meeting significance thresholds are depicted in blue. [Color figure can be viewed at wileyonlinelibrary.com]

Briefly, we show that the system can be activated by a damage-amplified endogenous elicitor, provide indirect evidence that this elicitor might be *Ib*Pep1, the product of *Ib*PROPEP1 cleavage, and that it functions in parallel and complementary to a HypSys-dependent signalling pathway. Mining the sweet potato genome

doi:10.6342/NTU202302113

databases, we identified a wound- and herbivory-induced gene encoding a canonical leucine-rich repeat-containing receptor kinase, *Ib*LRR-RK1 (Figure 1a,b and Supporting Information: Figure 2). Using a chimeric receptor approach, in which we combined the cytosolic kinase domain of *Ib*LRR-RK1 with the extracellular recognition domain of *Sl*SYR1 (Supporting Information: Figure 4a), we were able to generate a functional receptor after heterologous expressions in both *N. benthamiana* and *A. thaliana* (Figure 2, Supporting Information: Figure 4c). Phylogenetic analysis suggested that *Ib*LRR-RK1 might be a member of the PEPRs. Indeed, *Sl*Pep6 from tomato, but not *At*Pep1 from *A. thaliana*, was recognized by the native *Ib*LRR-RK1, and triggered the activation of typical defense responses after expression of *Ib*LRR-RK1-GFP in both *N. benthamiana* and *A. thaliana* (Figure 2). Of note, the sweet potato peptide *Ib*HypSysIV, which is described to be involved in the wound response (Chen et al., 2008) was not recognized by *Ib*LRR-RK1.

Based on the above findings, sequences of Peps and their precursor proteins (PROPEPs) from tomato and other Solanaceae plants were used to search for the related putative peptide in the sweet potato genome. We identified a 23-amino acids long peptide ligand, *Ib*Pep1, which is derived from the C-terminus of its precursor protein *Ib*PROPEP1. *Ib*Pep1 is capable to initiate the ROS burst in transgenic *Ib*LRR-RK1-expressing *N. benthamiana* with a 10-fold-higher sensitivity in comparison to *Sl*Pep6 (Figure 3b). However, the fact that the tomato peptide was recognized by sweet potato prompted us to investigate the reciprocal scenario. Indeed, *Sl*PEPR1, the tomato receptor for *Sl*Pep6 (Lori et al., 2015) recognized *Ib*Pep1, providing here for the first time data on interfamily (Solanaceae and Convolvulaceae) compatibility of Peps.

The structure–activity characterization of the ligand of *Ib*LRR-RK1 using various synthetic *Ib*Pep1 derivatives unraveled some structural requirements for the interaction with the corresponding receptor (Figure 3c). As for other Peps, the C-terminus of the peptide is of utmost importance, since the C-terminaly truncated peptide (*Ib*Pep1(1-20)) is at least 100-fold less efficient compared to the 23-mer *Ib*Pep1 (Figure 3c). Unlike the Peps from other plant families, however, the identity of the residues at the C-terminus seems not to be as important since the replacement of the last two residues with alanine residues only marginally decreased the affinity. Peps from sweet potato share 5 of the 12 highly conserved residues with the family-specific Pep-motif of the Solanaceae (Lori et al., 2015) in the overlapping 20-mer core region (Figure 3c, Supporting Information: Figure 9a). Testing one of these highly conserved residues (*Ib*Pep1[A4]) confirmed the importance of the arginine at that position. As illustrated in a composite consensus sequence for Peps of Solanaceae and Convolvulaceae, conserved arginine and proline residues are clustered at the N-terminus of the peptides, whereas, proline and asparagine residues are conserved at the C-termini (Supporting Information: Figure 9b).

PROPEPs have been reported to distribute to distinct subcellular localizations in Arabidopsis (Bartels et al., 2013). While *At*PROPEP3 is present in the cytosol, *At*PROPEP1 and *At*PROPEP6 are positioned at the tonoplast. Our findings show that *Ib*PROPEP1-GFP is localized at the tonoplast as well (Figure 4, Supporting Information: Figure 7). In addition, *Ib*PROPEP1-GFP also appeared in vesicle-like structures attached to the tonoplast that dynamically fuse with the vacuole (Supporting Information: Movie 1). Whether these structures correspond to bulbs, which have been described as cytoplasmic projections into the vacuole, surrounded by a tonoplast-derived double membrane (Madina et al., 2018; Saito et al., 2002), or are artefacts of dimerizing GFP with which the overexpressed PROPEP is tagged (Segami et al., 2014) remains to be investigated. However, to the best of our knowledge, this localization has never been reported for other PROPEPs. We hypothesize that the purpose of *Ib*PROPEP1 enrichment in bulbs could be to store sufficient amounts of the precursor and release it rapidly after cell and vacuole injury to allow cleavage into active *Ib*Pep1. *In planta*, we demonstrated the release of a specific agonist of *Ib*LRR-RK1. Incubation of only 10 min of wounded sweet potato leaves increased the amount of the elicitor in a partially purified fraction, in comparison to nonincubated leaf material (Figure 5).

The inherent trypsin inhibitory activity of sporamin provides strong protection against herbivory in sweet potato and other, transgenic plants species expressing sporamin (Chen et al., 2006; Meents et al., 2019; Yeh, Chen, et al., 1997). Strongly induced expression of *sporamin* was detected in sweet potato leaves during pest attack and injury stress (Yeh, Lin, et al., 1997). The 18 amino acid hydroxyprolinated peptide *Ib*HypSysIV, which can be extracted from sweet potato leaves was amplifying the wounding signal and activated the expression of *sporamin* (Chen et al., 2008). In the present study, we found that spraying with either peptide, *Ib*HypSysIV or *Ib*Pep1, rapidly induced the expression of wound-induced defense response genes including *IbWIPK1*, *IbNAC1*, *sporamin* and even *IbLRR-RK1*, in sweet potato leaves (Figure 6). However, *Ib*HypSysIV treatment induced the expression of *sporamin* much more strongly than *Ib*Pep1 treatment. Previous studies have revealed that application of *At*Peps and the activation of *At*PEPR1/2 lead to increased jasmonate accumulation and induced jasmonate responses in Arabidopsis (Huffaker, 2015). We found that the application of *Ib*Pep1 did not increase the amount of jasmonates, in contrast to *Ib*HypSysIV, which induced the accumulation of JA-Ile in sweet potato leaves slightly (Supporting Information: Figure 8), suggesting that *Ib*HypSysIV may trigger the jasmonate pathway and associated responses in contrast to *Ib*Pep1. A clear discrepancy between the two peptides lies in their ability to regulate the synthesis and release of the homoterpene DMNT. This volatile danger signal is induced in sweet potato upon wounding and herbivory (Meents et al., 2019). Only treatment with *Ib*HypSysIV but neither *Ib*Pep1 nor *Sl*Pep6 nor a scrambled control peptide were able to induced DMNT, indicating the specificity of this response (Figure 6c). Overall, our study suggests that in addition to the *Ib*Pep1/*Ib*LRR-RK1 pair described here for the first time, there is another, as yet unidentified, DAMP receptor that specifically interacts with the *Ib*HypSysIV ligand in sweet potato. The latter system appears to be more active than the Pep/PEPR pair in the jasmonate pathway regulating sporamin expression. A summarizing model of both peptide-induced pathways

doi:10.6342/NTU202302113

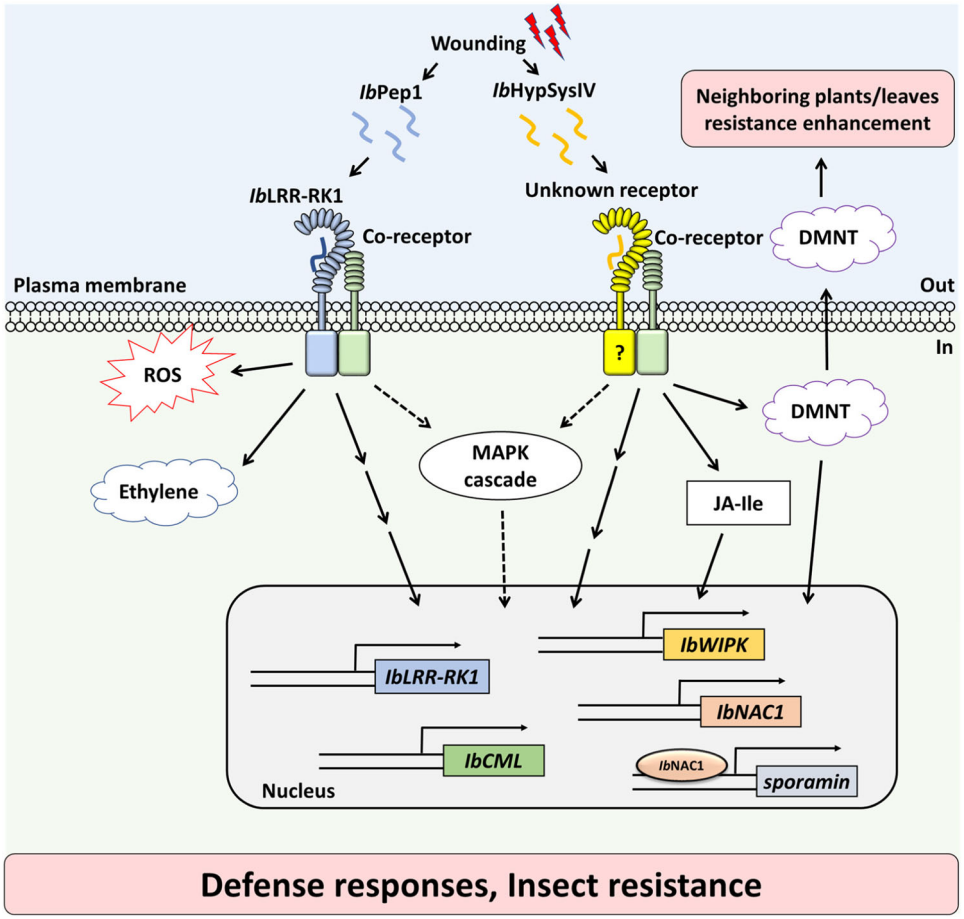

FIGURE 8 Proposed model of *Ib*Pep1 and *Ib*HypSysIV triggered resistance in sweet potato leaves. Upon wounding, peptide ligands *Ib*Pep1 and *Ib*HypSysIV are activated/induced in the treated leaf (Chen et al., 2008; Li et al., 2016). *Ib*Pep1 activates the *Ib*LRR-RK1 receptor leading to the generation of defense responses including ROS and ethylene production. Different from *Ib*Pep1, *Ib*HypSysIV induces DMNT emission as a volatile antiherbivore defense signal and the accumulation of JA-Ile (Meents et al., 2019). Both *Ib*Pep1 and *Ib*HypSysIV induce the expression of several wounding/defense-related genes such as *IbWIPK*, *IbNAC1*, *IbCML*, *IbLRR-RK1* and trypsin inhibitor gene *sporamin* (Chen, Kuo, et al., 2016; Chen, Lin, et al., 2016; Yeh, Chen, et al., 1997; Yeh, Lin, et al., 1997). In summary, *Ib*Pep1 and *Ib*HypSysIV might work in a complementary and/or parallel pathway to strengthen plant resistance against biotic threats. Dashed arrows: yet unproven pathways (here MAPK cascade).
[Color figure can be viewed at wileyonlinelibrary.com]

is shown in Figure 8. Having shown that both, *Ib*Pep1 and *Ib*HypSysIV, have a certain ability to regulate defense responses against herbivory attack and wounding, albeit with different efficacies, we have yet to define the key signalling pathway(s) regulated by *Ib*Pep1. Preliminary analyses of RNAseq data suggest that *Ib*Pep1 and *Ib*HypSysIV control partly distinct pathways, which will need to be further investigated in combination with real infestation and infection assays in the future.

5 | CONCLUSIONS

Previous studies have shown that Peps/PEPR ligand-receptor systems are widespread in plants. Here, we identified a novel peptide ligand and its corresponding receptor from sweet potato. This adds another ligand/receptor pair to the growing list of DAMP perception systems. Understanding how the downstream gene responses to different ligands are coordinated in the genetic network is a topic that needs to be addressed in the future. Although *Ib*Pep1 was not able to induce the emission of DMNT, the trypsin protease inhibitor sporamin and its TF *Ib*NAC1 were upregulated, hinting at a modular way to increase insect resistance. Peps vary widely from species to species, conserved family-specific Pep-motifs are sufficient for Pep recognition by PEPRs from different species of the same plant family (Lori et al., 2015). In our experiment, we found that the peptide ligand *Sl*Pep6 of tomato belonging to Solanaceae family did interact with *Ib*LRR-RK1 from sweet potato belonging to Convolvulaceae family and activated downstream responses. *Vice versa*, the reciprocal combination was functional as well. To our knowledge, this is the first example that a peptide ligand does not follow the rule of family-specific incompatibility of Peps but suggests the conservation of a plant order-specific peptide ligand structure in two families of Solanales, Solanaceae and Convolvulaveae.

doi:10.6342/NTU202302113

ACKNOWLEDGEMENTS

We thank Y.-R. Chen (Agricultural Biotechnology Research Center of Academia Sinica, Taiwan) and Y.-L. Chen (Department of Biotechnology and Bioindustry Sciences of National Cheng Kung University, Taiwan) for peptide analysis, S.-P. Chen (Sanming Academy of Agricultural Sciences, China) for receptor cloning, and C.-P. Cheng (Institute of Plant Biology of National Taiwan University, Taiwan) for suggestion on experimental design. We also thank M. Reichelt and A. Lehr for phytohormone measurements and experimental support, and E. Goschala for growing sweet potato plants. We are grateful to the staffs of Technology Commons in College of Life Science and the Instrumentation Center sponsored by Ministry of Science and Technology, National Taiwan University (Taiwan) for help with the confocal laser scanning microscopy (CLSM). We gratefully acknowledge the International Max Planck Research School supporting A.K.M and the National Science and Technology Council, Taiwan (110-2311-B-002-022-, 109-2311-B-002-021-, 111-2927-I-002 -501-). The research was conducted in the context of a project partially supported by the German Academic Exchange Service (DAAD; PPP Project ID 57136171). We are also grateful for financial support to G.F. by the DFG-CRC1101. Open Access funding enabled and organized by Projekt DEAL.

DATA AVAILABILITY STATEMENT

The data that support the findings of this study are available from the corresponding author upon reasonable request. All RNAseq data have been deposited in NCBI (National Center for Biotechnology Information) and are available under the accession number GSE227409.

ORCID

Hsueh-Han Lu http://orcid.org/0000-0002-7885-6541
Judith Fliegmann http://orcid.org/0000-0003-1021-8006
Ching-Shu Suen http://orcid.org/0000-0002-3096-1983
Axel Mithöfer http://orcid.org/0000-0001-5229-6913

REFERENCES

Albert, M., Jehle, A.K., Mueller, K., Eisele, C., Lipschis, M. & Felix, G. (2010) *Arabidopsis thaliana* pattern recognition receptors for bacterial Elongation Factor Tu and Flagellin can be combined to form functional chimeric receptors. *Journal of Biological Chemistry*, 285(25), 19035–19042. Available from: https://doi.org/10.1074/jbc.M110.124800

Asai, T., Tena, G., Plotnikova, J., Willmann, M.R., Chiu, W.L., Gomez-Gomez, L. et al. (2002) MAP kinase signalling cascade in Arabidopsis innate immunity. *Nature*, 415(6875), 977–983. Available from: https://doi.org/10.1038/415977a

Bartels, S. & Boller, T. (2015) Quo vadis, Pep? Plant elicitor peptides at the crossroads of immunity, stress, and development. *Journal of Experimental Botany*, 66(17), 5183–5193. Available from: https://doi.org/10.1093/jxb/erv180

Bartels, S., Lori, M., Mbengue, M., van Verk, M., Klauser, D., Hander, T. et al. (2013) The family of Peps and their precursors in Arabidopsis: differential expression and localization but similar induction of pattern-triggered immune responses. *Journal of Experimental Botany*, 64(17), 5309–5321. Available from: https://doi.org/10.1093/jxb/ert330

Beloshistov, R.E., Dreizler, K., Galiullina, R.A., Tuzhikov, A.I., Serebryakova, M.V., Reichardt, S. et al. (2018) Phytaspase-mediated precursor processing and maturation of the wound hormone systemin. *New Phytologist*, 218(3), 1167–1178. Available from: https://doi.org/10.1111/nph.14568

Binder, A., Lambert, J., Morbitzer, R., Popp, C., Ott, T. & Lahaye, T. et al. (2014) A modular plasmid assembly kit for multigene expression, gene silencing and silencing rescue in plants. *PLoS One*, 9(2), e88218. Available from: https://doi.org/10.1371/journal.pone.0088218

Böhm, H., Albert, I., Fan, L., Reinhard, A. & Nürnberger, T. (2014) Immune receptor complexes at the plant cell surface. *Current Opinion in Plant Biology*, 20, 47–54. Available from: https://doi.org/10.1016/j.pbi.2014.04.007

Boller, T. & Felix, G. (2009) A renaissance of elicitors: perception of microbe-associated molecular patterns and danger signals by pattern-recognition receptors. *Annual Review of Plant Biology*, 60, 379–406. Available from: https://doi.org/10.1146/annurev.arplant.57.032905.105346

Butenko, M.A., Wildhagen, M., Albert, M., Jehle, A., Kalbacher, H., Aalen, R.B. et al. (2014) Tools and strategies to match peptide-ligand receptor pairs. *The Plant Cell*, 26(5), 1838–1847. Available from: https://doi.org/10.1105/tpc.113.120071

Chen, H.J., Wang, S.J., Chen, C.C. & Yeh, K.W. (2006) New gene construction strategy in T-DNA vector to enhance expression level of sweet potato sporamin and insect resistance in transgenic *Brassica oleracea*. *Plant Science*, 171(3), 367–374. Available from: https://doi.org/10.1016/j.plantsci.2006.04.003

Chen, S.P., Kuo, C.H., Lu, H.H., Lo, H.S. & Yeh, K.W. (2016) The sweet potato NAC-Domain transcription factor *Ib*NAC1 is dynamically coordinated by the activator *Ib*bHLH3 and the repressor *Ib*bHLH4 to reprogram the defense mechanism against wounding. *PLoS Genetics*, 12(10), e1006397. Available from: https://doi.org/10.1371/journal.pgen.1006397

Chen, S.P., Lin, I.W., Chen, X.Y., Huang, Y.H., Chang, S.C., Lo, H.S. et al. (2016) Sweet potato NAC transcription factor, *Ib*NAC1, upregulates sporamin gene expression by binding the SWRE motif against mechanical wounding and herbivore attack. *Plant Journal*, 86(3), 234–248. Available from: https://doi.org/10.1111/tpj.13171

Chen, Y.C., Siems, W.F., Pearce, G. & Ryan, C.A. (2008) Six peptide wound signals derived from a single precursor protein in *Ipomoea batatas* leaves activate the expression of the defense gene sporamin. *Journal of Biological Chemistry*, 283(17), 11469–11476. Available from: https://doi.org/10.1074/jbc.M709002200

Chen, Y.L., Fan, K.T., Hung, S.C. & Chen, Y.R. (2020) The role of peptides cleaved from protein precursors in eliciting plant stress reactions. *New Phytologist*, 225(6), 2267–2282. Available from: https://doi.org/10.1111/nph.16241

Chien, P.S., Nam, H.G. & Chen, Y.R. (2015) A salt-regulated peptide derived from the CAP superfamily protein negatively regulates salt-stress tolerance in Arabidopsis. *Journal of Experimental Botany*, 66(17), 5301–5313. Available from: https://doi.org/10.1093/jxb/erv263

Chinchilla, D., Bauer, Z., Regenass, M., Boller, T. & Felix, G. (2006) The Arabidopsis receptor kinase FLS2 binds flg22 and determines the specificity of flagellin perception. *The Plant Cell*, 18(2), 465–476. Available from: https://doi.org/10.1105/tpc.105.036574

Curtis, M.D. & Grossniklaus, U. (2003) A gateway cloning vector set for high-throughput functional analysis of genes in planta. *Plant Physiology*, 133(2), 462–469. Available from: https://doi.org/10.1104/pp.103.027979

Hander, T., Fernández-Fernández, Á.D., Kumpf, R.P., Willems, P., Schatowitz, H., Rombaut, D. et al. (2019) Damage on plants activates Ca^{2+}-dependent metacaspases for release of immunomodulatory peptides. *Science*, 363(6433), 1301. Available from: https://doi.org/10.1126/science.aar7486

doi:10.6342/NTU202302113

Huffaker, A. (2015) Plant elicitor peptides in induced defense against insects. *Current Opinion in Insect Science*, 9, 44–50. Available from: https://doi.org/10.1016/j.cois.2015.06.003

Huffaker, A., Pearce, G. & Ryan, C.A. (2006) An endogenous peptide signal in Arabidopsis activates components of the innate immune response. *Proceedings of the National Academy of Sciences*, 103(26), 10098–10103. Available from: https://doi.org/10.1073/pnas.0603727103

Huffaker, A., Pearce, G., Veyrat, N., Erb, M., Turlings, T.C.J., Sartor, R. et al. (2013) Plant elicitor peptides are conserved signals regulating direct and indirect antiherbivore defense. *Proceedings of the National Academy of Sciences*, 110(14), 5707–5712. Available from: https://doi.org/10.1073/pnas.1214668110

Imanishi, S., KitoNakamura, K., Matsuoka, K., Morikami, A. & Nakamura, K. (1997) A major jasmonate-inducible protein of sweet potato, ipomoelin, is an ABA-independent wound-inducible protein. *Plant and Cell Physiology*, 38(6), 643–652. Available from: https://doi.org/10.1093/oxfordjournals.pcp.a029216

Klauser, D., Desurmont, G.A., Glauser, G., Vallat, A., Flury, P., Boller, T. et al. (2015) The Arabidopsis Pep-PEPR system is induced by herbivore feeding and contributes to JA-mediated plant defence against herbivory. *Journal of Experimental Botany*, 66(17), 5327–5336. Available from: https://doi.org/10.1093/jxb/erv250

Krol, E., Mentzel, T., Chinchilla, D., Boller, T., Felix, G., Kemmerling, B. et al. (2010) Perception of the Arabidopsis danger signal peptide 1 involves the pattern recognition receptor *At*PEPR1 and its close homologue *At*PEPR2. *Journal of Biological Chemistry*, 285(18), 13471–13479. Available from: https://doi.org/10.1074/jbc.M109.097394

Kunert, M., David, A., Becher, J. & Boland, W. (2009) Volatile sampling from biological sources by the closed-loop-stripping technique. *Cold Spring Harbor Protocols*, 2009(6), pdb.prot5233.

Li, Y.C., Wan, W.L., Lin, J.S., Kuo, Y.W., King, Y.C., Chen, Y.C. et al. (2016) Signal transduction and regulation of *Ib*preproHypSys in sweet potato. *Plant, Cell & Environment*, 39(7), 1576–1587. Available from: https://doi.org/10.1111/pce.12729

Lori, M., van Verk, M.C., Hander, T., Schatowitz, H., Klauser, D., Flury, P. et al. (2015) Evolutionary divergence of the plant elicitor peptides (Peps) and their receptors: interfamily incompatibility of perception but compatibility of downstream signalling. *Journal of Experimental Botany*, 66(17), 5315–5325. Available from: https://doi.org/10.1093/jxb/erv236

Madina, M.H., Zheng, H. & Germain, H. (2018) New insight into bulb dynamics in the vacuolar lumen of Arabidopsis cells. *Botany*, 96(8), 511–520. Available from: https://doi.org/10.1139/cjb-2018-0009

Meents, A.K., Chen, S.P., Reichelt, M., Lu, H.H., Bartram, S., Yeh, K.W. et al. (2019) Volatile DMNT systemically induces jasmonate-independent direct anti-herbivore defense in leaves of sweet potato (*Ipomoea batatas*) plants. *Scientific Reports*, 9, 17431. Available from: https://doi.org/10.1038/s41598-019-53946-0

Meents, A.K. & Mithöfer, A. (2020) Plant-plant communication: is there a role for volatile damage-associated molecular patterns? *Frontiers in Plant Science*, 11, 583275. Available from: https://doi.org/10.3389/fpls.2020.583275

Narváez-Vásquez, J., Pearce, G. & Ryan, C.A. (2005) The plant cell wall matrix harbors a precursor of defense signaling peptides. *Proceedings of the National Academy of Sciences*, 102(36), 12974–12977. Available from: https://doi.org/10.1073/pnas.0505248102

Nelson, B.K., Cai, X. & Nebenführ, A. (2007) A multicolored set of in *vivo* organelle markers for co-localization studies in Arabidopsis and other plants. *The Plant Journal*, 51(6), 1126–1136. Available from: https://doi.org/10.1111/j.1365-313X.2007.03212.x

Orozcocardenas, M., Mcgurl, B. & Ryan, C.A. (1993) Expression of an antisense prosystemin gene in tomato plants reduces resistance toward *Manduca Sexta* larvae. *Proceedings of the National Academy of Sciences*, 90(17), 8273–8276. Available from: https://doi.org/10.1073/pnas.90.17.8273

Pearce, G. (2011) Systemin, hydroxyproline-rich systemin and the induction of protease inhibitors. *Current Protein & Peptide Science*, 12(5), 399–408. Available from: https://doi.org/10.2174/138920311796391106

Pearce, G., Siems, W.F., Bhattacharya, R., Chen, Y.C. & Ryan, C.A. (2007) Three hydroxyproline-rich glycopeptides derived from a single petunia polyprotein precursor activate defensin I, a pathogen defense response gene. *Journal of Biological Chemistry*, 282(24), 17777–17784. Available from: https://doi.org/10.1074/jbc.M701543200

Pearce, G., Strydom, D., Johnson, S. & Ryan, C.A. (1991) A polypeptide from tomato leaves induces wound-inducible proteinase-inhibitor proteins. *Science*, 253(5022), 895–897.

Rajendran, S., Lin, I.W., Chen, M.J., Chen, C.Y. & Yeh, K.W. (2014) Differential activation of sporamin expression in response to abiotic mechanical wounding and biotic herbivore attack in the sweet potato. *BMC Plant Biology*, 14, 112. Available from: https://doi.org/10.1186/1471-2229-14-112

Ron, M. & Avni, A. (2004) The receptor for the fungal elicitor ethylene-inducing xylanase is a member of a resistance-like gene family in tomato. *The Plant Cell*, 16(6), 1604–1615. Available from: https://doi.org/10.1105/tpc.022475

Ross, A., Yamada, K., Hiruma, K., Yamashita-Yamada, M., Lu, X., Takano, Y. et al. (2014) The Arabidopsis PEPR pathway couples local and systemic plant immunity. *The EMBO Journal*, 33(1), 62–75. Available from: https://doi.org/10.1002/embj.201284303

Saito, C., Ueda, T., Abe, H., Wada, Y., Kuroiwa, T., Hisada, A. et al. (2002) A complex and mobile structure forms a distinct subregion within the continuous vacuolar membrane in young cotyledons of Arabidopsis. *The Plant Journal*, 29(3), 245–255. Available from: https://doi.org/10.1046/j.0960-7412.2001.01189.x

Segami, S., Makino, S., Miyake, A., Asaoka, M. & Maeshima, M. (2014) Dynamics of vacuoles and H^+-Pyrophosphatase visualized by monomeric Green fluorescent protein in Arabidopsis: artifactual bulbs and native intravacuolar spherical structures. *The Plant Cell*, 26(8), 3416–3434. Available from: https://doi.org/10.1105/tpc.114.127571

Thuerig, B., Felix, G., Binder, A., Boller, T. & Tamm, L. (2005) An extract of *Penicillium chrysogenum* elicits early defense-related responses and induces resistance in *Arabidopsis thaliana* independently of known signalling pathways. *Physiological and Molecular Plant Pathology*, 67(3–5), 180–193. Available from: https://doi.org/10.1016/j.pmpp.2006.01.002

Wang, L., Albert, M., Einig, E., Fürst, U., Krust, D. & Felix, G. (2016) The pattern-recognition receptor CORE of Solanaceae detects bacterial cold-shock protein. *Nature Plants*, 2(12), 16185. Available from: https://doi.org/10.1038/Nplants.2016.185

Wang, L., Einig, E., Almeida-Trapp, M., Albert, M., Fliegmann, J., Mithöfer, A. et al. (2018) The systemin receptor SYR1 enhances resistance of tomato against herbivorous insects. *Nature Plants*, 4(3), 152–156. Available from: https://doi.org/10.1038/s41477-018-0106-0

Yamaguchi, Y., Huffaker, A., Bryan, A.C., Tax, F.E. & Ryan, C.A. (2010) PEPR2 is a second receptor for the Pep1 and Pep2 peptides and contributes to defense responses in Arabidopsis. *The Plant Cell*, 22(2), 508–522. Available from: https://doi.org/10.1105/tpc.109.068874

Yeh, K.W., Chen, J.C., Lin, M.I., Chen, Y.M. & Lin, C.Y. (1997) Functional activity of sporamin from sweet potato (*Ipomoea batatas* Lam): a tuber storage protein with trypsin inhibitory activity. *Plant Molecular Biology*, 33(3), 565–570. Available from: https://doi.org/10.1023/a:1005764702510

Yeh, K.W., Lin, M.I., Tuan, S.J., Chen, Y.M., Lin, C.Y. & Kao, S.S. (1997) Sweet potato (*Ipomoea batatas*) trypsin inhibitors expressed in transgenic tobacco plants confer resistance against *Spodoptera litura*. *Plant Cell Reports*, 16(10), 696–699. Available from: https://doi.org/10.1007/s002990050304

Yoo, S.D., Cho, Y.H. & Sheen, J. (2007) Arabidopsis mesophyll protoplasts: a versatile cell system for transient gene expression analysis. *Nature*

doi:10.6342/NTU202302113

Protocols, 2(7), 1565–1572. Available from: https://doi.org/10.1038/nprot.2007.199

Zipfel, C., Kunze, G., Chinchilla, D., Caniard, A., Jones, J.D.G., Boller, T. et al. (2006) Perception of the bacterial PAMP EF-Tu by the receptor EFR restricts Agrobacterium-mediated transformation. *Cell*, 125(4), 749–760.

SUPPORTING INFORMATION

Additional supporting information can be found online in the Supporting Information section at the end of this article.

How to cite this article: Lu, H.-H., Meents, A. K., Fliegmann, J., Hwang, M.-J., Suen, C.-S., Masch, D. et al. (2023) Identification of a damage-associated molecular pattern (DAMP) receptor and its cognate peptide ligand in sweet potato (*Ipomoea batatas*). *Plant, Cell & Environment*, 46, 2558–2574. https://doi.org/10.1111/pce.14633

doi:10.6342/NTU202302113